MARMARA UNIVERSITY
INSTITUTE FOR GRADUATE STUDIES
IN PURE AND APPLIED SCIENCES

EFFECT OF ION IRRADIATION ON PROPERTIES OF DOPED $Bi_{1.5}Zn_{0.92}Nb_{1.5}O_{6.92}$ PYROCHLORES

MEHMET YUMAK

MASTER THESIS

Metallurgical and Materials Eng.

ADVISOR

Prof. Dr. A. Ayhan MERGEN

ISTANBUL, 2015

ACKNOWLEDGEMENT

I am highly thankful to my thesis advisor, Prof. Dr. Ayhan MERGEN for his sincere advice and persistent support. He recommended many useful references and attributed his insights in many theoretical issues. I am especially grateful for the time he dedicated to check my test results.

I would like to give my thanks to Marmara University Research Fund and TÜBİTAK for their financial support on this thesis.

June, 2015 **Mehmet YUMAK**

INDEX

ABSTRACT

EFFECT OF ION IRRADIATION ON PROPERTIES OF DOPED $BI_{1.5}ZN_{0.92}NB_{1.5}O_{6.92}$ PYROCHLORES

Among the ternary metallic oxides, compounds of the general formula, A2B2X6Z where A and B are cations and X and Z are anions, represent a family of pyrochlore phases. Ideal pyrochlore structure has a space group of Fd3m having eight molecules per unit cell (Z=8). Pyrochlore compounds consist of large A-site cations (radius: ~1 Å) in eightfold coordination and a network of oxygen octahedra (actually trigonal antiprisms) enclosing smaller B-site cations (radius: ~0.6 Å). In A2B2X6Z pyrochlore, while A and B cations are in 16(c) and 16(d) positions, X-anion occupies the 48f position and the Z-anion occupies the 8a position. For the ideal structure, the coordination polyhedra of the ions are : AX6Y2 , BX6 , XA2B2 , and ZA4.

In the literature, large number of pyrochlores having (3+, 4+) cations are reported compared to pyrochlores having (2+, 5+) cations because more number of (3+, 4+) ions are possible. In addition, from extensive experimental work on the synthesis and structural characterization of cubic pyrochlores, stability fields of pyrochlores have been proposed for allowable substitution into the *A* and *B* cation sites of pyrochlore based on simple measures such as the ratio of the cation size and the cation electronegativity. Pyrochlore oxides can accommodate a wide range of solid solutions between BO_2 and A_2O_3 compounds. Therefore, many different type of pyrochlore compounds can be produced by substituting variety of cations into the pyrochlore structure.

Variety of substitutions into the pyrochlore structure produce different pyrochlores with variety of interesting properties which allow them for a broad range of applications, such as high-permittivity dielectrics, as cathode and electrolyte materials in solid electrolytes, host materials for the immobilization of fission

products, catalysis, and thermal barrier coatings and fluorescence centers. The electrical properties of the pyrochlores vary from highly insulating through semiconducting to metallic behaviour. Some pyrochlores exhibit superconductivity at lower temperatures. Oxide ion conduction is also possible in pyrochlores if the compositions are tuned properly. Pyrochlore compounds are also used for immobilization nuclear wastes, especially n titanate-pyrochlores because of their chemical durability.

Recent attention has focused on bismuth based pyrochlores for their potential use in capacitor and high-frequency filter applications due to their low sintering temperature and desired properties. In bismuth based pyrochlores, the Bi^{+3} cation exist in the *A* site of pyrochlore and it has a lone pair of electrons. One of the Bi based pyrochlores is $Bi_{1.5}Zn_{0.92}Nb_{1.5}O_{6.92}$ (BZN) which are attractive materials for capacitors and wireless communications technology as microwave resonators, high frequency filter applications in multilayer structures due to their high and tunable dielectric constant, low dielectric loss, small and close to zero values of the temperature coefficient of dielectric constant, low sintering temperature and lower cost of electrode materials.

Radiation effects in a wide range of pyrochlore compositions have been investigated due to the potential application of pyrochlores. The effect of energetic ion beam (ion irradiation) on the materials depends on the ion energy, fluence and ion species. The energetic heavy ions loose their energy as they pass through the material. The ions either excite or ionize the atoms by inelastic collisions or displace atoms of the target by elastic collisions. These collisions may cause formation of defects in the microstructure like formation of columnar amorphization or formation of point defects. The strain/stress developed due to the created defects and amorphization in the structure is responsible for the modification in the different properties of the materials.

Ion beam irradiation can induce the structural disordering by mixing the cation and anion sublattices, therefore it was aimed to inevestigate effects of irradiation in pyrochlore compounds. In this study, Eu and Yb-doped $Bi_{1.5}Zn_{0.92}Nb_{1.5}O_{6.92}$ (Eu-BZN, Yb-BZN) pyrochlore compounds were synthesized by a conventional mixed oxide technique. Doping effect and single phase formation of Eu-BZN, Yb-BZN was

characterized by X-ray diffraction technique (XRD). Radiation-induced effect of 85 MeV C^{6+} ions on Eu-BZN, Yb-BZN was studied by XRD, scanning electron microscopy (SEM) and temperature dependent dielectric measurements at different fluences. XRD results revealed that the ion beam-induced structural amorphization processes in Eu-BZN and Yb-BZN structures. Our results suggested that the ion beam irradiation induced the significant change in the temprature depndent dielectric properties of Eu-BZN and Yb-BZN pyrochlores due to the increased oxygen vacancies as a result of cation and anion disordering.

June , 2015 **Mehmet YUMAK**

ÖZET

KATKILI $BI_{1.5}ZN_{0.92}NB_{1.5}O_{6.92}$ PİROKLOR MALZEMELERE İYON RADYASYONUNUN ETKİSİ

A ve B nin katyon ve X in anyon olduğu stokiyometrik piroklor formülü genellikle $A_2B_2X_7$ şeklinde yazılır. Piroklor bileşiği sekiz fold koordinasyonda büyük A-konumu katyonu (yarıçap: yaklaşık 1Å) ve daha küçük olan oksijen oktahedra ağıyla sarılmış B-konumu katyonundan (yarıçap: yaklaşık 0.6 Agstrom) oluşur. Piroklor bileşiği değişik ilginç özellikleri nedeniyle çok geniş bir uygulama alanına sahiptir. Örneğin; yüksek permitiviteye sahip dielektrikler , katı elektrotlarda katot ve elektrot malzemesi olarak , parçalanma (fizyon) ürünlerinin durağanlaştırılmasında ana malzeme olarak , katalizör ,ısı bariyeri kaplaması ve floresans merkezi olarak. İdeal stokiyometrik piroklor ($A_2B_2O_7$) Fd3m kübik uzay grubuna sahip olup, genellikle B_2O_6 oktahedra veA_2O tetrahedranın iç içe geçmiş ağ yapısı olarak tarif edilir.

Kübik piroklorun sentezi ve yapısal karakterizasyonu üzerine yapılan yoğun çalışmalar, piroklor yapısının A ve B konumuna katkılandırılacak iyonların katyon yarıçapı ve elektronegativiteleri gibi basit ölçümlerine dayanarak piroklor bileşikleri için stabilite alanları önerilmiştir . Piroklor oksitler BO_2 ile A_2O_3 arasında geniş alanda katı çözelti barındırabilir. Bu nedenle, piroklor yapısına çok farklı katyonların katkılandırılmasıyla farklı özelliklere sahip piroklor bileşikler elde edilebilir.

Son yıllarda yapılan çalışmalar bizmut bazlı piroklor bileşiklerine odaklanmış olup, bu bileşiklerde A konumunda Bi^{+3} katyonu yer almakta ve bu bileşikler kapasitör ve yüksek frekans filtre uygulamalarında potansiyel uygulama imkanına sahiptir . Bismuth tek çift elektrona sahip ve yarıçapı 1.17 Å olup, bizmut piroklor bileşiğinde A konumunda yer alan en büyük katyonlardan biridir. Bu nedenle oldukça dar bir kararlılık alanına sahiptir. Geçen son on yılda küçük katyonların katkılandırıldığı çok farklı kompleks bismuth piroklor bileşiklerinin senteziyle ilgili yürütülen deneysel çalışmalar, bu kararlılık alanını genişletmiştir. Bu malzemelerden en yoğun çalışılan malzemelerden biri $Bi_{1.5}Zn_{0.92}Nb_{1.5}O_{6.92}$ (BZN)'dir. BZN piroklor bileşiği düşük ve ayarlanabilir dielektrik sabiti, düşük dielektrik kaybı, küçük ve sıfıra yakın dilektrik

sabiti sıcaklık katsayısı, düşük sinterlenme sıcaklığı ve düşük maliyetli elektrot malzemeleriyle kullanılabilir olması özellikleri nedeniyle kapasitörlerde ve kablosuz iletişim teknolojisinde mikrodalga rezonatör olarak ve çok katlı yapılarda yüksek frekans filtre malzemesi olarak ilgi çeken malzemelerdir.

Piroklor bileşiğinin potansiyel uygulamaları nedeniyle radyasyon etkisi çok farklı piroklor bileşiklerinde detaylı olarak araştırılmıştır. Bu çalışmada, BZN olarak bilinen komleks oksit piroklorun radyasyon etkisi araştırılacaktır.

Madde üzerindeki enerjili iyon ışını (iyon ışıması) etkisi, iyon parçacıklarına, iyon enerjisine ve akıcılığına bağlıdır. Enerjili ağır iyonlar madde içinden geçerken enerjilerini kaybederler. Elastik veya elastik olmayan çarpışma ile atomu iyonize eder veya elektronunu koparırlar. Düşük enerjide elastik çarpışma baskınken, yüksek enerjide ise elastik çarpışmanın önemsiz olduğu inelastik çarpışma baskın durumdadır. Literatüre göre inelastik çarpışma nedeniyle oluşan elektronik enerji kaybı (S_e) eğer S_e elektronik enerji kaybı (S_{eth}) eşik değerinden daha düşükse noktasal/kümesel kusurlar oluşturabilir. Eğer S_e, S_{eth} den büyükse enerjili iyonlar kolonsal amorf bozunma yapabilir. Oluşan kusurlar ve amorflaşma nedeniyle meydana gelen şekil değişimi/gerilme malzemenin birçok özelliğinin modifikasyonundan sorumludur. Literatürde $BaTiO_3$ üzerindeki radyasyon ışınlama etkisi araştırılıp raporlanmıştır. $BaTiO_3$'daki amorfluk için ısıl faz geçişi ve doza bağlı sıcaklık değişimi araştırılmıştır. Jiang ve arkadaşları altın iyonu ışınlamış baryum titanatın bozunum birikimini ve iyileşmesini çalışmıştır.

Bu çalışmada, $Bi_{1.5}Zn_{0.92}Nb_{1.5}O_{6.92}$ (BZN) piroklor bileşiği Ta, Mn,ve Dy gibi farklı iyonlar doplanarak üretilecektir. Her bir katyonun çözünürlük limitleri belirlendikten sonra tek fazlı yapıya sahip katkılı BZN seramikleri farklı dozlardaki Li^{+3} iyon radyasyonuna tabi tutulacaktır. Radyasyonun farklı frekans ve sıcaklıktaki dielektrik özelliklere, değişik sıcaklıklardaki iletkenlik özelliklerine ve optik özelliklere etkisi araştırılacak, özellikler ile Li^{+3} iyon radyasyon dozu arasındaki ilişki kurulacaktır.

Haziran, 2015 **Mehmet YUMAK**

SYMBOLS

a	: Lattice Parameter (**Å**)
Å	: Angstrom (10^{-10} m)
A	: Surface Area
C	: Capacitance (coulomb/volt)
ºC	: Degree Celcius
d	: Distance of Plates
$\mathbf{d_i}$	: Relative Displacement
h	: Hour
g	: Gram
GHz	: Giga Hertz
Hz	: Hertz
k	: Dielectric Constant
K'	: Relative Dielectric Constant
K''	: Relative Loss Factor
K Hz	: Kilo Hertz
M Hz	: Mega Hertz
min	: Minute
mm	: Millimeter
MPa	: Mega Pascal (N/m^2)
$\mathbf{M_w}$	: Molecular Weight
n	: Number of Atoms
$\mathbf{N_A}$	: Avagadro's constant
P	: Polarization

ppm : Parts Per Million

q : Charge

Q : Quality Factor

tan δ : Dielectric Loss

THz : Terahertz (10^{-12} Hertz)

$\mathbf{T_m}$: Melting Temperature

V : Voltage

$\mathbf{V_b}$: Breakdown Strength

$\mathbf{W_{dry}}$: Dry Weight (gr)

$\mathbf{W_{water}}$: Weight in Water (gr)

$\mathbf{W_{wet}}$: Wet Weight (gr)

α_L : Linear Thermal Expansion Coefficient

ε : Permittivity

ε_r : Relative Permittivity

f : Resonant Peak Frequency

τ_f : Temperature Coefficient of Resonant Frequency (ppm/^{o}C)

τ_ε : Temperature Coefficient of The Permittivity

μm : Micrometer

ρ_b : Bulk Density

ρ_t : Theoretical Density

ρ_R : Relative Density

ABBREVIATIONS

Ta03 : Ta doped BZN (x=0.3)

Ta03 A : Ta doped BZN with intensity A of C^{+6} irritation

Ta03 B : Ta doped BZN with intensity B of C^{+6} irritation

Ta03 C : Ta doped BZN with intensity C of C^{+6} irritation

Ta : Ta doped BZN (x =1)

Ta A : Ta doped BZN with intensity A of C^{+6} irritation

Ta B : Ta doped BZN with intensity B of C^{+6} irritation

Ta B : Ta doped BZN with intensity B of C^{+6} irritation

Eu012 : Eu doped BZN (x =0.12)

Eu A : Eu doped BZN with intensity A of C^{+6} irritation

Eu B : Eu doped BZN with intensity B of C^{+6} irritation

Dy004 : Dy doped BZN (x =0.04)

Dy B : Dy doped BZN with intensity B of C^{+6} irritation

Dy C : Dy doped BZN with intensity C of C^{+6} irritation

Yb004 : Yb doped BZN (x =0.04)

Yb A : Yb doped BZN with intensity A of C^{+6} irritation

Yb B : Yb doped BZN with intensity B of C^{+6} irritation

BEI : Backscattered Electron Image

BZN : Bi_2O_3–ZnO–Nb_2O_5

DBS : Direct Broadcast Satellite

DF : Dissipation Factor

DR : Dielectric Resonator

EIA : Electronics Industries Association

EDS **:** Energy Dispersive Spectrometer

GPS **:** Global Positioning System

ITS **:** Intelligent Transport System

LCR **:** Inductance (L), Capacitance (C), and Resistance (R) measurement device

MIC **:** Microwave Integrated Circuits

PC **:** Personal Computer

SEI **:** Secondary Electron Image

SEM **:** Scanning Electron Microscopy

XRD **:** X-ray Diffraction

TV **:** Television

CHAPTER I

I .INTRODUCTION

Stoichiometric pyrochlore structure is usually written as $A_2B_2X_7$ where A and B are cations and X is anion. Pyrochlore compounds consist of large A-site cations (radius: ~1 Å) in eightfold coordination and a network of oxygen octahedra (actually trigonal antiprisms) and smaller B-site cations (radius: ~0.6 Å). Pyrochlore compounds exhibit a variety of interesting properties which allow them for a broad range of applications, such as high-permittivity dielectrics [1], cathode and electrolyte materials in solid electrolytes [2], host materials for the immobilization of fission products, [3, 4], catalysis, [5] and thermal barrier coatings [6-8] and fluorescence centers [9]. Ideal stoichiometric pyrochlores *(*$A_2B_2O_7$) are cubic with space group of *Fd*3*m* and often described as two interpenetrating networks of B_2O_6 octahedra and A_2O tetrahedral [10, 11].

From extensive experimental work on the synthesis and structural characterization of cubic pyrochlores, stability fields have been proposed for allowable substitution into the *A* and *B* cation sites based on simple measures such as the ratio of the cation radii size and the cation electronegativity [12]. Pyrochlore oxides can accommodate a wide range of solid solutions and different cations can be incorporated into these compounds. Therefore, by substituting variety of cations into the pyrochlore structure different pyrochlore compounds having different properties can be obtained.

Recent attention has focused on bismuth based pyrochlores, where the Bi^{+3} cation resides in the *A* site, for their potential use in capacitor and high-frequency filter applications [12]. Bismuth has a lone pair of electrons and the cation radius is 1.17 Å [13] making it one of the larger *A* cations found in the pyrochlore family and results in a relatively small region of stability in the structure field maps. In the past decade, experimental work extended this stability region, with the synthesis of numerous complex Bi pyrochlores that incorporate substitutions of small cations into both the *A* and *B* sites. The most extensively studied of these materials is $Bi_{1.5}Zn_{0.92}Nb_{1.5}O_{6.92}$ (BZN). BZN pyrochlores are attractive materials for capacitors and wireless communications technology as microwave resonators, high frequency filter applications in multilayer structures due to their high and tunable dielectric constant, low dielectric loss, small and close to zero values of the temperature coefficient of dielectric constant, low sintering temperature and lower cost of electrode materials [1, 11].

Radiation effects in a wide range of pyrochlore compositions have been extensively investigated due to the potential application of pyrochlores [14]. In the present thesis, the radiation effect on the properties of BZN pyrochlore was investigated.

The effect of energetic ion beam (ion irradiation) on the materials depends on the ion energy, fluence and ion species. The energetic heavy ions lose their energy as they pass through the material. The ions either excite or ionize the atoms by inelastic collisions or displace atoms of the target by elastic collisions. Elastic collisions are dominant in low energy regime, whereas inelastic collisions process dominates at high-energy regime where elastic collisions are insignificant. From the literature [15, 16], it is evident that electronic energy loss, S_e, due to inelastic collision is able to generate point/cluster of defects if S_e is less than the threshold value of electronic energy loss (S_{eth}). If S_e is greater than the S_{eth}, then the energetic ions can create columnar amorphization. The strain/stress developed due to the created defects and amorphization is responsible for the modification in the different properties of the materials [17, 18]. Investigations of irradiation effects on $BaTiO_3$ have been reported [19-21]. The thermal phase transitions and the temperature dependence of the dose for amorphizations in $BaTiO_3$ have been investigated [19]. Jiang et al. [21] studied damage accumulation and recovery in gold-ion-irradiated barrium titanate.

In this study, $Bi_{1.5}Zn_{0.92}Nb_{1.5}O_{6.92}$ (BZN) pyrochlore compounds were produced by doping with different cations like Eu , Dy, Ta, and Yb. After determining the solubility limits of each cations, single phase BZN ceramics were irradiated with different fluences of C^{+6} ion irradiation. The effect of irradiation on dielectric properties at different frequencies and temperatures were investigated.

Pyrochlores are of high interest in present nuclear technology as materials for disposal of nuclear wastes, due to their ability to accommodate minor actinides and an excellent resistance to radiation in the nuclear stopping regime [22]. Recently, there has been a great interest in using pyrochlore ceramics as potential host phases for the immobilization of actinides, particularly Pu. In this study, some new pyrochlore compounds were studied to investigate their possible applications in nuclear applications. In addition, swift heavy ion irradiation provides several interesting and unique aspects in understanding of damage structure and material modification. Since swift heavy irradiation affect the structure and properties of materials, dielectric properties of the doped pyrochlores were examined before and after irradiation, and a relationship were established between properties of pyrochlores and ion irradiation fluences.

CHAPTER II

GENERAL BACKGROUND

II.1. CERAMIC MATERIALS

Ceramics can be defined as solid compounds that are formed by the application of heat, and sometimes heat and pressure, comprising at least two elements provided one of them is a non-metal or a nonmetallic elemental solid. The other element(s) may be a metal(s) or another nonmetallic elemental solid(s). Ceramics normally achieved through a high-temperature heat treatment process called firing or sintering [23, 24]. Most ceramics exhibit a combination of both ionic and covalent bonding,.

Traditional ceramics' primary raw material is clay and has products that named porcelain, bricks, tiles, and, glasses and high-temperature ceramics. Consequently, a new generation of ceramic materials are evolved, which are being used in electronic, computer, communication, and related areas. [24].

Some of the general properties of ceramic materials are;

- High temperature resistance (high melting temperatures)
- High electrical resistivity (although some ceramics are superconductors)
- Broad range of thermal conductivity (many
- ceramics are good insulators)
- High hardness (many ceramics are brittle)
- Good chemical and corrosion resistance
- Low cost of raw materials
- Good appearance control through surface treatments, colorization etc."[25]

Ceramics are generally more brittle than metals and can have similar modulus of elasticity and similar strength, especially in compression. But in a tensile test they are likely to fail at a much lower applied stress. Since ceramics often have high wearresistance and hardness, most ceramic parts are formed as near net shape as possible during processing.

Ceramics are most often produced by compacting powders into a body which is then sintered at high temperatures. During sintering the body shrinks, the grains bond together and a solid material is produced. Other ceramic forming processes include: dry pressing, isostatic pressing, roll compaction, continuous tape casting, slip casting, extrusion, injection moulding, pre-sinter machining, hot-pressing, hot-isostatic pressing.

Ceramics are generally separated into the following categories: metallic oxides, glass ceramics, nitrides and carbides, glass, carbon and graphite, porcelain and ceramic fibres.

There are various classification systems of ceramic materials, which may be attributed to one of the principal category of application base system which was illustrated in Fig. II.1 [26].

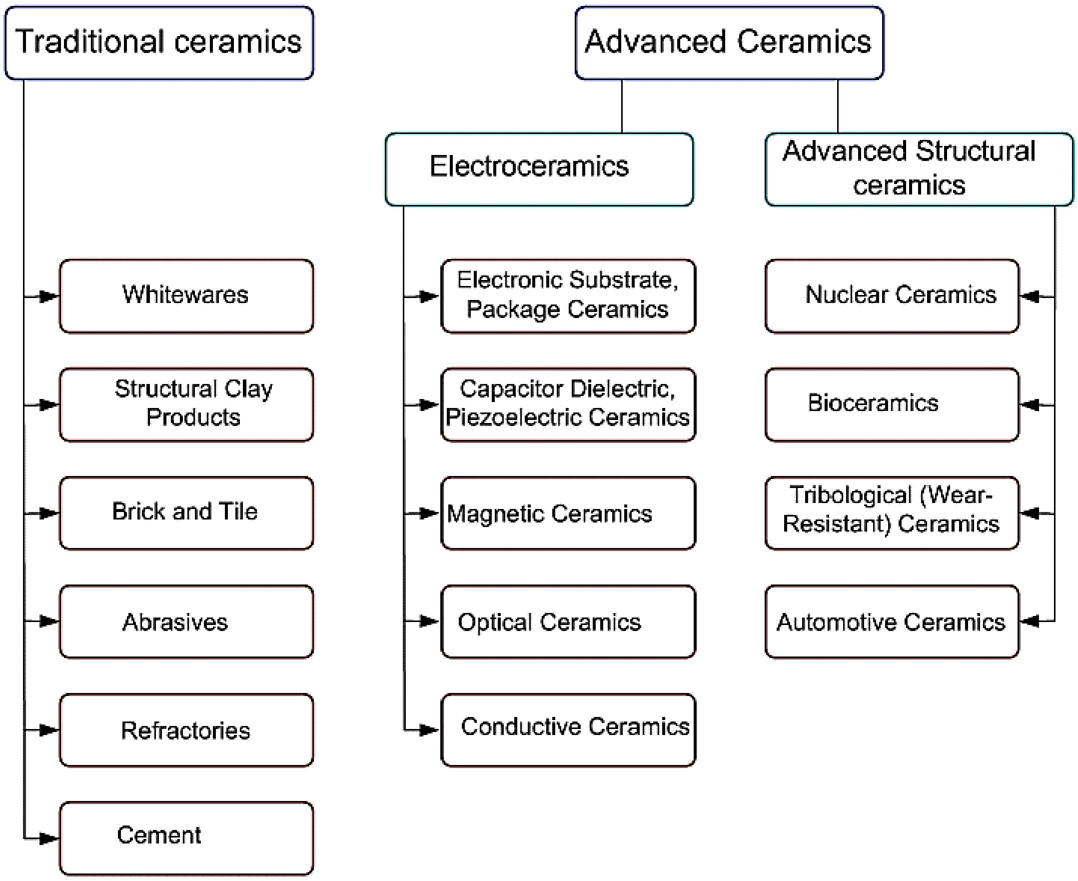

Figure II.1 Application base classification of ceramics materials.

Ceramics comprise crystallites that may vary in structure, perfection and composition as well as in size, shape and the internal stresses to which they are subjected. In addition, the interfaces between crystallites are regions in which changes in lattice orientation occur, often accompanied by differences in composition and attendant electrical effects. As a consequence it is very difficult to account precisely for the behavior of ceramics. The study of single-crystal properties of the principal components has resulted in valuable insights into the behavior of ceramics. However, the growth of single crystals is usually a difficult and time-consuming while the complexities of ceramic microstructures renders the prediction of properties of the ceramic from those of the corresponding single crystal very uncertain. Consequently, empirical observation has usually led to the establishment of new devices based on ceramics before there is more than a partial understanding of the underlying physical mechanisms [23] .

II.1.1. Crystal Structures of Ceramics

Because ceramics are composed of at least two elements, and often more, their crystal structures are generally more complex than those for metals. The atomic bonding in these materials ranges from purely ionic to totally covalent; many ceramics exhibit a combination of these two bonding types, the degree of ionic character being dependent on the electro negativities of the atoms.

For those ceramic materials for which the atomic bonding is predominantly ionic, the crystal structures may be thought of as being composed of electrically charged ions instead of atoms. The metallic ions, or cations, are positively charged, because they have given up their valence electrons to the nonmetallic ions, or anions, which are negatively charged. Two characteristics of the component ions in crystalline ceramic materials influence the crystal structure: the magnitude of the electrical charge on each of the component ions, and the relative sizes of the cations and anions [24].

Crystal structures of ceramics can be categorized in three main classes:

II.1.1.1. AX-Type Crystal Structures

Some of the common ceramic materials are those in which there are equal numbers of cations and anions. There are several different crystal structures for AX compounds; each is normally named after a common material that assumes the particular structure such as Rock Salt, Zinc Blende, Cesium Chloride, etc.

II.1.1.2. A_mX_p-Type Crystal Structures

If the charges on the cations and anions are not the same, a compound can exist with the chemical formula where *m and/or* $p \neq 1$. Some compounds that have this crystal structure include CaF_2, ZrO_2 and ThO_2.

II.1.1.3. $A_mB_nX_p$-Type Crystal Structures

It is also possible for ceramic compounds to have more than one type of cation; for two types of cations (represented by A and B), their chemical formula may be designated as $A_mB_nX_p$. Barium titanate ($BaTiO_3$) having both Ba^{2+} and Ti^{4+} cations, falls into this classification. Spinel, perovskite, calcite and pyrochlore structures are also in this group (Table II.1).

Structure	Formula	Examples
Spinel	AB_2X_4	$FeAl_2O_4$, $ZnAl_2O_4$, $MgAl_2O_4$, $CoFe_2O_4$
Calcite	ABX_3	$CaCO_3$, $MgCO_3$, $FeCO_3$, $MnCO_3$
Perovskite	ABX_3	$BaTiO_3$, $CaTiO_3$, $SrSnO_3$, $SnZrO_3$
Pyrochlore	$A_2B_2X_7$	$Bi_2Ti_2O_7$, $Am_2Zr_2O_7$, $La_2Zr_2O_7$, $Yb_2Ti_2O_7$

Table II.1 Some of the major $A_mB_nX_p$-Type Crystal Structures [27]

II.1.2. Pyrochlore

The pyrochlore structure was first determined by Von Gaertner in 1930 [REF]. The general formula of the oxide pyrochlore structure can be written as $A_2B_2O_6O$. There are four crystallographically unique atom positions and the space group is Fd3m. A common way of describing the structure is by fixing its origin on the B site, with atoms located at the following positions: A at 16d, B at 16c, O at 48f and O’ at 8b. The only internal positional variable of the pyrochlore structure is the oxygen x parameter, which characterizes the 48f oxygen atoms (Figure II.2) [10, 26]

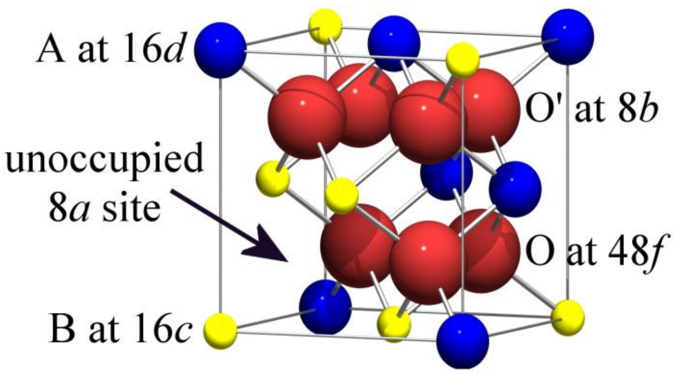

Figure II.2 Unit cell of pyrochlore. Blue spheres represent A cations, yellow B and red O.

The pyrochlore structure can thereby be considered as an ordered, defective fluorite solid solution. In CaF_2, the fluorine anions are located in the tetrahedral sites of a Ca face centered cubic array. In this description of pyrochlore, the A and B cations form the face centered cubic array, but are additionally ordered in the <110> directions such that the A cations are eight coordinated and the B cations are six coordinated with respect to oxygen. This cation ordering means that the tetrahedral anion sites are no longer crystallographically identical. In fact, there are now three distinct tetrahedral sites: the 48f, which has two A and two B nearest neighbors, the 8a, which has four B nearest neighbors and the 8b, which has four A nearest neighbors. In pyrochlore, the 8a positions are vacant. Figure II.2 depicts one eighth of the pyrochlore unit cell, which is analogous to a single fluorite unit cell. Figure II.3 depicts a full unit cell of a pyrochlore, with the anions removed in order to better view the two cationic sub lattices and the ordering along <110> directions [28].

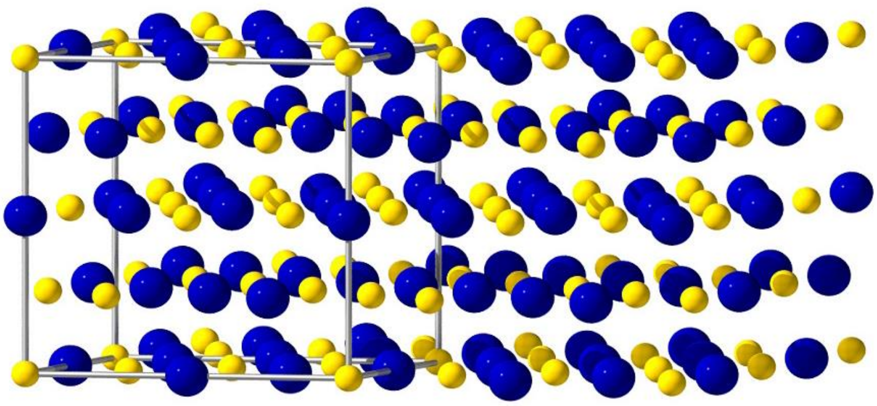

Figure II.3 The cationic sublattice of pyrochlore (anions removed).

Pyrochlore ceramics have significant scientific and technological importance due to their variety of properties. Pyrochlore ceramics that are examined in the literature have many different electrical, magnetic, dielectrical, optical and catalytic properties. Because of those properties, the application areas of pyrochlore ceramics are very wide. Some of the potential applications are; electronic sector (ferroelectric, thermistor, thick film resistors, switches, gas sensors, etc.), fuel cells (oxygen electrodes, semi-conducting electrodes, solid electrolids, high temperature electrodes etc.), heater elements and radioactive waste stabilizators. One of the other reasons of wide usage area of pyrochlore ceramics is that many elements can be easily doped into the pyrochlore without changing its structure [29].

Ceramic material forms in Bi_2O_3-ZnO-Nb_2O_5 system with a chemical formula of $Bi_{1.5}Zn_{0.92}Nb_{1.5}O_{6.92}$, (BZN) have cubic pyrochlore structure and it is non ferroelectric. But this compound has important technological dielectric properties, and this can be used as microwave dielectric material in wireless communication and multilayer ceramic capacitor. Having relatively low sintering temperature (950°C) is one of the other properties of BZN dielectric material. Low sintering temperature enables the usage of low cost silver and low palladium containing silver electrodes [1, 30, 31] .

II.2. DIELECTRIC PROPERTIES

A ***dielectric*** is an electrical insulator that may be polarized by the action of an applied electric field. When a dielectric is placed in an electric field, electric charges do not flow through the material, as in a conductor, but only slightly shift from their average equilibrium positions causing dielectric polarization. Because of dielectric polarization, positive charges are displaced along the field and negative charges shift in the opposite direction. This creates an internal electric field which partly compensates the external field inside the dielectric. If a dielectric is composed of weakly bonded molecules, those molecules not only become polarized, but also reorient so that their symmetry axis aligns to the field.

While the term "insulator" refers to a low degree of electrical conduction, the term "dielectric" is typically used to describe materials with a high polarizability. The latter is expressed by a number called the dielectric constant. A common example of a dielectric is the electrically insulating material between the metallic plates of a capacitor. The polarization of the dielectric by the applied electric field increases the capacitor's capacitance.

The study of dielectric properties is concerned with the storage and dissipation of electric and magnetic energy in materials. As a result of dipole interactions with electric fields, dielectric materials are utilized in capacitors.

II.2.1. Polarization

Polarization is the alignment of permanent or induced atomic or molecular dipole moments with an externally applied electric field. There are four types or sources of polarization: electronic, ionic, orientation and space charge. In dielectric materials; electronic, ionic, orientation and space charge polarization may contribute to the polarization mechanism. So dielectric materials ordinarily exhibit at least one of these polarization types depending on the material and also the manner of the external field application.

II.2.1.1. Electronic Polarization

Electronic polarization may be induced to one degree or another in all atoms. It results from a displacemen0t of the center of the negatively charged electron cloud relative to the positive nucleus of an atom by the electric field (Figure II.4). This polarization type is found in all dielectric materials and, of course, exists only while an electric field is present.

Figure II.4 Electronic polarization that results from the distortion of an atomic electron cloud by an electric field.

II.2.1.2. Ionic Polarization

Ionic polarization occurs only in materials that are ionic. An applied field acts to displace cations in one direction and anions in the opposite direction, which gives rise to a net dipole moment. This phenomenon is illustrated in Figure II.5. The magnitude of the dipole moment for each ion pair p_i is equal to the product of the relative displacement d_i and the charge on each ion (q), or;

$$P_i = qd_i \tag{II.1}$$

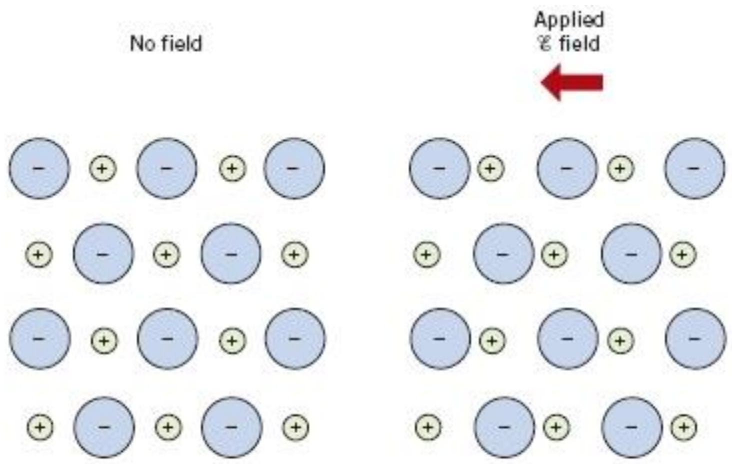

Figure II.5 Ionic polarization that results from the relative displacements of electrically charged ions in response to an electric field.

II.2.1.3. Orientation Polarization

Orientation polarization is found only in substances that possess permanent dipole moments. Polarization results from a rotation of the permanent moments into the direction of the applied field, as represented in Figure II.6. This alignment tendency is counteracted by the thermal vibrations of the atoms, such that polarization decreases with increasing temperature.

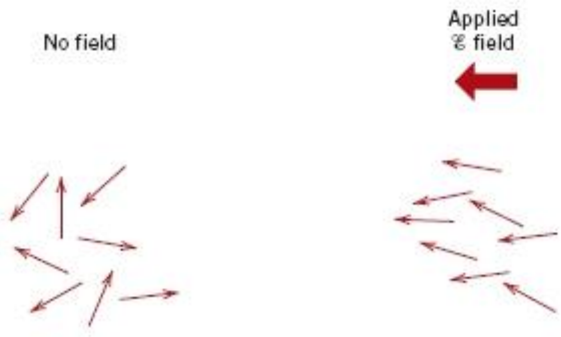

Figure II.6 Response of permanent electric dipoles (arrows) to an applied electric field, producing orientation polarization.

II.2.1.4. Space Charge Polarization

Space charge polarization is also called interfacial polarization, which is a short-range electrical conduction. A space charge develops when there is a local conduction within a dielectric. Such a local conduction stops at a barrier or an energy potential, such as grain boundaries (Figure II.7). Due to the nature of diffusion, space charge polarization occurs rather slowly. Like orientation polarization, space charge polarization is temperature dependent.

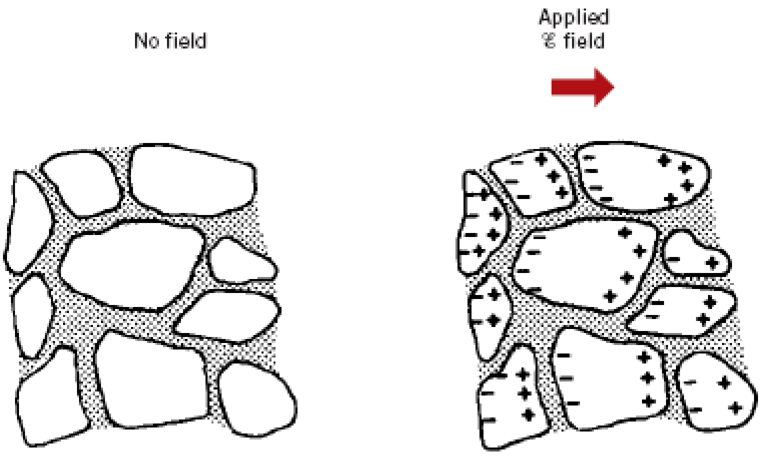

Figure II.7 Space charge polarization that results from an electric field.

The total polarization P of a substance is equal to the sum of the electronic, ionic, molecular and space charge polarizations (Pe, Pi, Pm and Ps, respectively), or

$$P = Pe + Pi + Pm + Ps \tag{II.2}$$

It is possible for one or more of these contributions to the total polarization to be either absent or negligible in magnitude relative to the others. For example, ionic polarization will not exist in covalently bonded materials in which no ions are present.

II.2.2. Dielectric Constant

One important property of a dielectric material is its permittivity. ***Permittivity*** (**ε**) is a measure of the ability of a material to be polarized by an electric field.

It is, however, easier to grasp the concept of permittivity by first discussing a closely related property, capacitance (C). Capacitance is a measure of the ability of a material to hold charge if a voltage is applied across it, and is best modeled by a dielectric layer that's sandwiched between two parallel conductive plates.

If a voltage V is applied across a capacitor of capacitance C, then the charge q that it can hold is directly proportional to the applied voltage V, with the capacitance C as the proportionality constant. Thus,

$$q = CV \tag{II.3}$$

The unit of measurement for capacitance is the farad (coulomb per volt).

The capacitance of a capacitor depends on the permittivity ε of the dielectric layer, as well as the area A of the capacitor and the separation distance d between the two conductive plates. Permittivity and capacitance are mathematically related as follows:

$$C = \varepsilon\ (A/d) \tag{II.4}$$

When the dielectric used is vacuum, then the capacitance;

$$C_o = \varepsilon_o \, (A/d) \tag{II.5}$$

where ε_o is the permittivity of vacuum (8.85 x 10^{-12} F/m).

The ***dielectric constant*** (***k***) of a material is the ratio of its permittivity ε to the permittivity of vacuum ε_o, so

$$k = \varepsilon/\varepsilon_o \tag{II.6}$$

The *dielectric constant* is therefore also known as the relative permittivity of the material. Since the dielectric constant is just a ratio of two similar quantities, it is dimensionless.

The concept of the relative dielectric constant is illustrated in Figure II.8. An electric field is applied to two flat plates of a metal such that one plate becomes positive and the other negative. The electric field causes polarization in the material in the space between the conductive plates. The relative dielectric constant compares the polarizability or charge storage capability of the material with that of a vacuum between the plates [32].

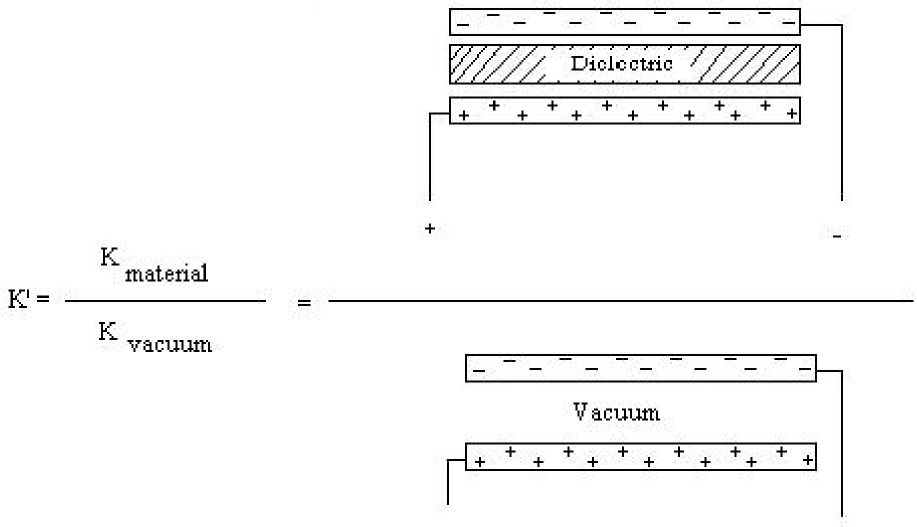

Figure II.8 Schematic illustration of the definition of relative dielectric constant K.

Given its definition, the dielectric constant of vacuum is 1. Any material is able to polarize more than vacuum, so the k of a material is always > 1. Note that the dielectric constant is also a function of frequency in some materials, e.g., polymers, primarily because polarization is affected by frequency.

The dielectric constant is affected by temperature. In fact, the effect is dependent on the source of polarization. Electronic polarization is relatively intensive to temperature, so temperature has little effect on the dielectric constant. Molecular orientation polarization is opposed by thermal agitation, so the dielectric constant goes down as the temperature increases. Ionic or atomic polarization tends to increase with temperature due to an increase in charge carriers and ion mobility. The dielectric constant is also affected by the frequency of the applied electric field or the frequency of other electromagnetic fields effecting on the material. The polarization needs time to respond to an applied field. Electronic polarization occurs very rapidly and is present even at high frequencies[33] .

A low-k dielectric is a dielectric that has a low permittivity, or low ability to polarize and hold charge. Low-k dielectrics are very good insulators for isolating signal-carrying conductors from each other. Thus, low-k dielectrics are a necessity in very dense multi-layered integrated circuit chips, wherein coupling between very close metal lines need to be suppressed to prevent a degradation in device performance.

A high-k dielectric, on the other hand, has a high permittivity. Because high-k dielectrics are good at holding charge, they are the preferred dielectric for capacitors. High-k dielectrics are also used in memory cells that store digital data in the form of charge [32].

II.2.3. Dielectric Loss

The ***dielectric loss***, (tan δ) of a material denotes quantitatively dissipation of the electrical energy due to different physical processes such as electrical conduction, dielectric relaxation, dielectric resonance and loss from non-linear processes. Origin of dielectric losses can also be considered as being related to delay between the electric field and the electric displacement vectors. The total dielectric loss is the sum of intrinsic and extrinsic losses. Intrinsic dielectric losses are the losses in the perfect crystals which depend on the crystal structure. Extrinsic losses are associated with imperfections in the crystal lattice such as impurities, microstructural defects, grain boundaries, porosity, micro cracks, order–disorder, random crystallite orientation, dislocations, vacancies, dopant atoms etc. The extrinsic losses are caused by lattice defects and therefore can be in principle eliminated or reduced to the minimum by proper material processing. The losses due to different types of defects show different frequency and temperature dependence. The crystals belonging to different symmetry groups have very different temperature and frequency dependences of dielectric loss.

Tangent δ is referred to as the *loss tangent* and is equal to K''/K', where K' is the relative dielectric constant and K'' is defined as the relative loss factor.

$$\tan\delta = \frac{K''}{K'} \tag{II.7}$$

This power loss represents a wastage of energy as well as attendant heating of the dielectric. If the rate of heat generation is faster than it can be dissipated, the dielectric will heat up, could lead to dielectric breakdown and other problems. Furthermore, as the temperature increases, the dielectric constant is liable to change as well, which for finely tuned circuits can create severe problems. Another reason for minimizing K" is related to the sharpness of the tuning circuit that would result from using the capacitor — lower losses give rise to much sharper resonance frequencies [23].

Since temperature usually tends to increase the conductivity of a ceramic exponentially, its effect on dielectric loss can be substantial. This is demonstrated in Figure II.9a, where the loss tangent is plotted as a function of temperature for different glasses that have varying resistivity. In all cases, the increased mobility of the cations results in an increase in the dielectric loss tangent. The effect of impurities, as they increase the conductivity of a ceramic, can also result in large increases in the dielectric loss. This is shown in Figure II.9b, for very pure NaCl (lower curve) and one that contains lattice impurities (top curve) [23].

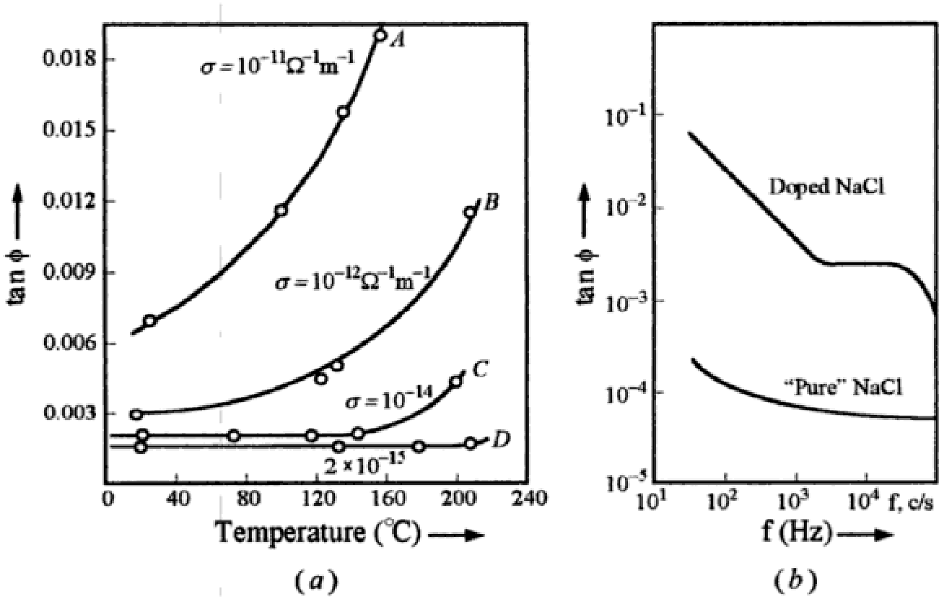

Figure II.9 (a) Variation of loss angle with temperature for alkali glasses as a function of their resistivity. **(b)** Effect of impurities and frequency on tanθ of NaCl.

Dielectric properties of several different materials are given in Table II.2. Some of these materials are used for capacitors, while others may be present in oscillators or other devices where dielectric losses may affect circuit performance. The dielectric constant and the dissipation factor are given at two frequencies, 60 Hz and 1 MHz. The righthand column of Table II.2 gives the approximate breakdown voltage of the material. This would be for thin layers where voids and impurities in the dielectrics are not a factor. Breakdown usually destroys a capacitor, so capacitors must be designed with a substantial safety factor. It can be seen that most materials have dielectric constants between one and ten. One exception is barium titanate with a dielectric constant greater than 1000. It also has relatively high losses which keep it from being more widely used than it is [34].

Material	ϵ_r 60 Hz	ϵ_r 10^6 Hz	DF 60 Hz	DF 10^6 Hz	V_b V/mil
Air	1.000585	1.000585	-	-	75
Aluminum oxide	-	8.80	-	0.00033	300
Barium titanate	1250	1143	0.056	0.0105	50
Carbon tetrachloride	2.17	2.17	0.007	<0.00004	-
Castor oil	3.7	3.7	-	-	300
Glass, soda-borosilicate	-	4.84	-	0.0036	-
Heavy Soderon	3.39	3.39	0.0168	0.0283	-
Lucite	3.3	3.3	-	-	500
Mica, glass bonded	-	7.39	-	0.0013	1600
Mica, glass, titanium dioxide	-	9.0	-	0.0026	-
Mica, ruby	5.4	5.4	0.005	0.0003	-
Mylar	2.5	2.5	-	-	5000
Nylon	3.88	3.33	0.014	0.026	-
Paraffin	2.25	2.25	-	-	250
Plexiglas	3.4	2.76	0.06	0.014	-
Polycarbonate	2.7	2.7	-	-	7000
Polyethylene	2.26	2.26	<0.0002	<0.0002	4500
Polypropylene	2.25	2.25	<0.0005	<0.0005	9600
Polystyrene	2.56	2.56	<0.00005	0.00007	500
Polysulfone	3.1	3.1	-	-	8000
Polytetrafluoroethylene(teflon)	2.1	2.1	<0.0005	<0.0002	1500
Polyvinyl chloride (PVC)	3.2	2.88	0.0115	0.016	
Quartz	3.78	3.78	0.0009	0.0001	500
Tantalum oxide	2.0	-	-	-	100
Transformer oil	2.2	-	-	-	250
Vaseline	2.16	2.16	0.0004	<0.0001	-

Table II.2 Relative Permittivity (Dielectric Constant) ε_r, Dissipation Factor (Dielectric Loss) *DF* and Breakdown Strength V_b of selected materials[35] .

II.2.4. Temperature Coefficient of Resonant Frequency

The ***temperature coefficient of resonant frequency*** τ_f is the parameter which indicates the thermal stability of the resonator. The τ_f indicates how much the resonant frequency drifts with changing temperature. The electronic device with microwave resonators requires τ_f values as close to zero as possible. Microwave circuits will normally have some low characteristics τ_f, so the resonator components which go into them are required to compensate for the inherent drift. For this reason, the τ_f values of resonators required are typically non-zero but with some low finite value. The origin of τ_f is related to linear expansion coefficient α_L which affects the resonator dimensions and its dielectric constant variation with temperature. Mathematically the relationship is:

$$\tau_f = -\alpha_L - \frac{\tau_\varepsilon}{2} \qquad \text{(II.8)}$$

Where τ_ε is the *temperature coefficient of the permittivity* and α_L is the *linear thermal expansion coefficient* of the dielectric material which is usually positive. In practice, Equation (II.8) is valid for 100% electric energy storage in the sample and the thermal expansion of the metal cavity enclosing the dielectric resonance (*DR*) is negligible. For an ideal resonator the temperature coefficient of resonant frequency (τ_f) should be near to zero. Hence from Equation (II.8) for a zero τ_f, the τ_ε should have twice the value of α_L and should be negative. Since resonators are used in communication systems, temperature restability is an important factor and should be close to zero. For most of the electronic ceramic materials, α_L is about +10 ppm/°C indicating the significant influence of τ_ε on τ_f [36].

Experimentally τ_f is measured by following the drift in the resonant peak frequency f as the temperature is slowly varied. In order to measure τ_f, DR is kept end shorted between two copper plates under Courtney setup. This is then kept inside a temperature - controlled oven. The E-field probe is kept near the DR in such a way to get resonance. The mode is identified and the setup is then slowly heated (~1°C/min) in the range 25–80°C. The probe of the thermocouple is kept just inside the oven so that it does not disturb the resonant frequency. Shift of the resonant frequency as a result of heating in the reflection mode is noted using network analyzer when the temperature is steady. The variation of resonant frequency is plotted as a function of temperature. The τ_f is calculated from the slope of the curve using equation:

$$\tau_f = \frac{f_{80} - f_{25}}{f_{25}(80 - 25)} \tag{II.9}$$

The τ_f is expressed as parts per million per degree Celsius (ppm/°C) The τ_f can also be measured by the cavity method used for measuring the quality factor. The thermal expansion of the cavity during heating limits the accuracy of the method. However, use of a cavity made of invar can minimize the inaccuracy. The τ_f is related to thermal expansion and relative permittivity by the Equation (II.8). The temperature coefficient of dielectric constant τ_ε is of considerable interest to users of dielectric substrates. This can be obtained by the parallel plate capacitor method using an LCR meter at low frequency (e.g., 1 MHz) and heating the sample. From the ε_r noted at different temperatures the τ_ε can be obtained. At microwave frequency, one can obtain τ_ε from the value of τ_f and α_L and using Equation (II.8) [36].

II.3. MICROWAVE CERAMICS

Wireless technologies have already penetrated many aspects of modern life and the trend is set to continue. This has in turn been a strong stimulant to the development of specially tailored microwave dielectrics. Figure II.10 gives an indication of specific technologies and of the corresponding frequency bands.

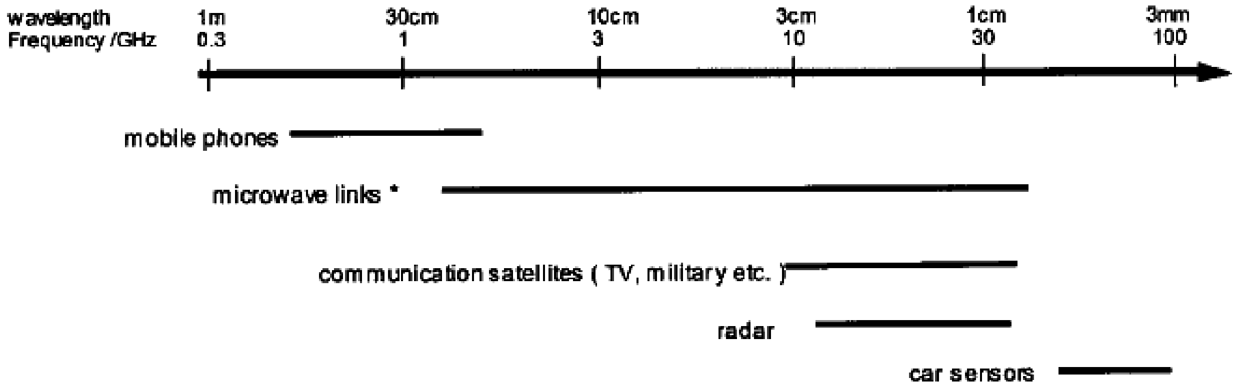

Figure II.10 Frequency bands covered by the various wireless technologies

(* includes '*Bluetooth*'; Harald Blatand (Bluetooth) was a famous King of Denmark who is known for encouraging communication between people)

Oxide ceramics are critical elements in these microwave circuits, and a full understanding of their crystal chemistry is fundamental to future development. Properties of microwave ceramics critically depend on several parameters, such as purity of starting materials, calcination temperature and duration, shaping method and sintering temperature and durations. Design of the heating/cooling schedule requires knowledge of formation mechanism of various phases in multicomponent systems. The starting powders must be sintered to high density to get optimum electrical properties. Figures II.11-12 show typical examples of the effect of calcination and sintering temperatures and time on the density and microwave dielectric properties of $Ba(Sm_{1/2}Nb_{1/2})O_3$ ceramics.

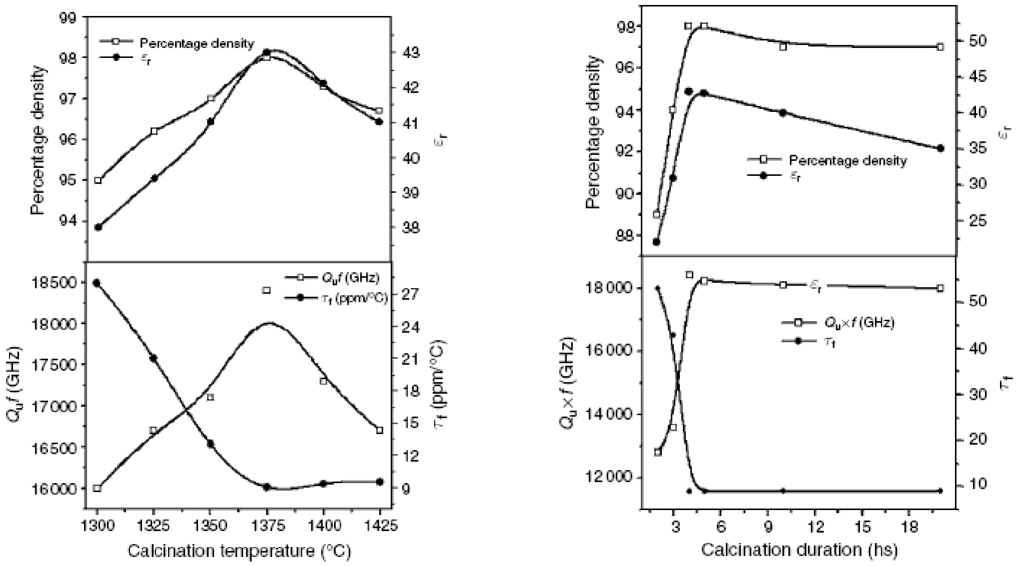

a **b**

Figure II.11 The variation of the relative density, ε_r, $Q\times f$ and τ_f of $Ba(Sm_{1/2}Nb_{1/2})O_3$ ceramic versus **a)** calcination temperature **b)** calcination duration at 1375°C [35].

The microwave ceramics are usually optimized for the best density for which the ε_r and $Q\times f$ are normally the best. Powders prepared by solid state methods require a higher sintering temperature as compared to those prepared by chemical methods. However, the sintering temperature can be lowered by using sintering aids. High $Q\times f$ can be achieved only in ceramics with fine grains and/or homogeneous microstructures. The ceramics with discontinuous and excess grain growth exhibit poor performance. Incomplete densification is mainly due to discontinuous grain growth. Due to rapid and discontinuous grain growth, porosity is trapped in. If the distance from these trapped pores to the path of the fast material transport or grain boundaries is large, the rate of material transport to close the pores will be limited. The materials will be porous and the dielectric and mechanical properties will be poor. Densification can be promoted by the use of additives. [35, 36]

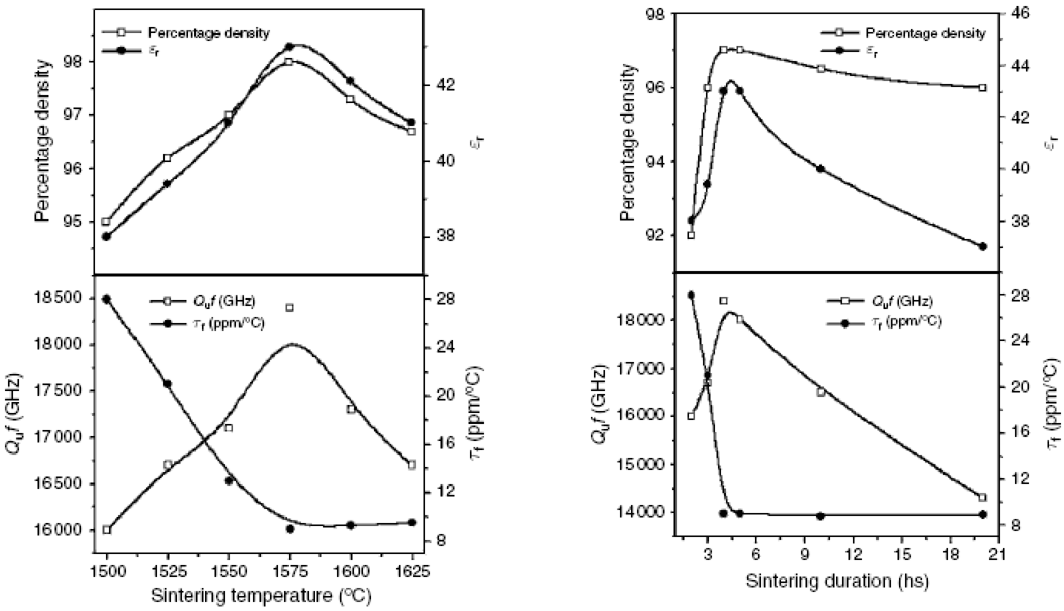

a **b**

Figure II.12 The variation of the relative density, ε_r, $Q\times f$ and τ_f of $Ba(Sm_{1/2}Nb_{1/2})O_3$ ceramic versus **a)** sintering temperature **b)** sintering duration at 1575°C [35]

II.3.1. Effects of Additives on Microwave Ceramics

Additives aid fabrication by allowing densification to occur at lower temperatures in shorter times or by inhibiting discontinuous grain growth and allowing pore elimination to proceed to completion. Use of these additives is for most part empirical, and experimental verification of their role is impossible usually limited to the grain boundaries. At least two theories were advanced to explain the effect of these additives.

II.3.1.1. Liquid phase assistance

Additive with a lower melting point is used for densification by melting and coating the ceramic particles, rapid dissolution and transfer of the base material to fill the interparticle spaces, which leads to enhanced densification. The additive has to be fairly soluble in the base ceramic and several wt % of the additive is necessary to provide sufficient liquid phase to coat all the powder particles.

II.3.1.2. Solid solution effect

Addition of a solute with a different valency enhances bulk material transport due to the introduction of vacancies in the ceramic. These vacancies render the diffusion coefficient extrinsic by making thermal vacancy concentration insignificant up to a certain temperature. If added in sufficient quantity, it can significantly alter the rate of material transport through the solid phase.

Sintering aids affect ceramics in many ways by changing the density, microstructure, defect structure and possibly crystal structure. These changes brought about by the sintering aids affect the resulting dielectric properties. The density, ε_r, Q and τ_f are all affected by the additives. A higher relative density results in a higher ε_r. The selection of proper additives, their optimum quantity and optimum processing conditions are effective in enhancing the quality factor [36].

II.3.2. Capacitors

When a voltage is applied across a capacitor, one plate becomes positively charged, the other negatively charged, with the corresponding electric field directed from the positive to the negative.

Each of the materials in Table II.2 has its own advantages and disadvantages when used in a capacitor. The ideal dielectric would have a high dielectric constant, like barium titanate, a low dielectric loss, like polystyrene, a high breakdown voltage, like mylar, a low cost, like aluminum oxide, and be easily fabricated into capacitors. It would also be perfectly stable, so the capacitance would not vary with temperature or voltage. No such dielectric has been discovered so we must apply engineering judgment in each situation, and select the capacitor type that will meet all the requirements and at least cost [34].

Capacitors used for ac must be unpolarized so they can handle full voltage reversals. They also need to have a lower dielectric loss than capacitors used as dc filter capacitors. One important application of ac capacitors is in tuning electronic equipment. These capacitors must have high stability with time and temperature, so the tuned frequency does not drift beyond some specified amount.

Ceramic capacitors are made with one of a large number of ceramic materials, which include aluminum oxide, barium titanate, and porcelain. These are very widely used as bypass capacitors that are capacitors employed to conduct an alternating current around a component or group of components. The older style is a single layer of dielectric separating two conducting plates and packaged in a small disc. The newer style is the monolithic, which appears in a rectangular package. It consists of alternating layers of ceramic material and printed electrodes which are sintered together to form the final package. The self resonant frequency is on the order of 15 MHz for the 0.01 μF size, for a total lead length of 0.5 inch, and on the order of 165 MHz for the 0.0001 μF=100 pF size. Ceramic capacitors are classified into Class 1 ($\varepsilon_r < 600$) and Class 2 ($\varepsilon_r > 600$) by the Electronics Industries Association (EIA). Class 1 ceramic capacitors tend to be larger than their Class 2 counterparts, and have better stability values with changes in temperature, voltage, or frequency. The best Class 1 capacitor, with nearly constant characteristic, will be labeled 'C0G' using EIA designators, but is often referred to as 'NP0' which stands for 'negative-positive-zero' (temperature coefficient) [34].

II.3.3. Dielectric Resonators

A ***dielectric resonator*** is an electromagnetic component that exhibits resonance with useful properties for a narrow range of frequencies. The resonance is similar to that of a circular hollow metallic waveguide except for the boundary being defined by a large change in permittivity rather than by a conductor. Dielectric resonators (DR) generally consist of a puck of ceramic that has a high permittivity and a low dissipation factor. The resonant frequency is determined by the overall physical dimensions of the puck and the permittivity of the material and its immediate surroundings. The key properties required for a DR are high *quality factor* (Q), high *relative permittivity* (ε_r) and near zero *temperature coefficient of resonant frequency*

(τ_f). An optimal DR that satisfies these three properties simultaneously is difficult to achieve in a particular material. [35, 36]

In the early microwave systems, bulk metallic cavities were used as resonators, but were huge and not integrated with microwave integrated circuits (MICs). On the other hand, stripline resonators have a poor quality factor and poor temperature stability resulting in the instability of the circuit. Hence the importance of DRs, which are easily integrated with MICs with low loss and with thermally stable frequency, especially at mm wavelengths. Most of the microwave-based device systems are located in the frequency range 300MHz–300GHz as shown in Figure II.13. Technological improvements in DRs have contributed to considerable advancements in modern wireless communications [36].

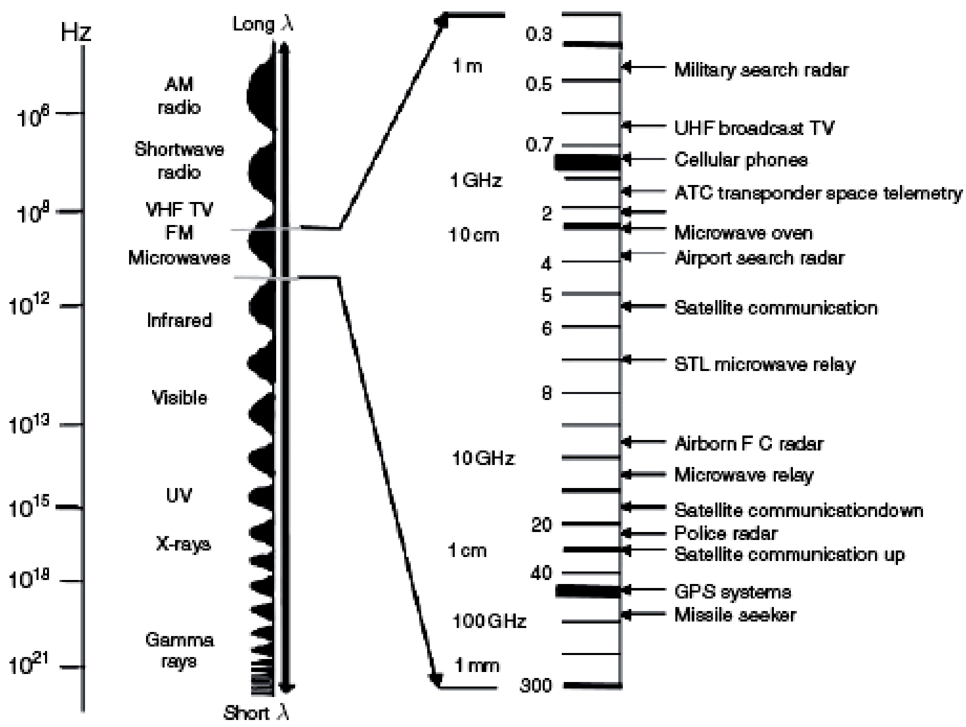

Figure II.13 Microwave spectrum and applications

Ceramic DRs have the advantage of being more miniaturized as compared to traditional microwave cavities, and have a significantly higher quality factor. DRs have replaced cavity resonators in most microwave and millimeter-wave applications for reasons of cost, dimension, mass, stability, efficiency, tenability, ruggedness and ease of use. In addition, the temperature variation of the resonant frequency of DRs can be engineered to a desired value to meet circuit designer's requirements. Functioning as important components in communication circuits, DRs can create and filter frequencies in oscillators, amplifiers and tuners. In order to respond to the requirement for increased channel capacity in ground-based cellular and satellite communications, new devices with superior performance must be developed. The system performance is closely related to material properties. In microwave communications, DR filters are used to discriminate between wanted and unwanted signal frequencies from the transmitted and received signals. The desired frequency is extracted and detected to maintain a strong signal-to-noise ratio. For clarity, it is also critical that the wanted signal frequencies are not affected by seasonal temperature changes [35, 36].

The low permittivity ceramics are used for millimeter-wave communication and also as substrates for microwave integrated circuits. The medium ε_r ceramics with permittivity in the range 25–50 are used for satellite communications and in cell phone base stations. The high ε_r materials are used in mobile phones, where miniaturization of the device is very important. For millimeter-wave and substrate application, a temperature-stable low permittivity and high Q (low loss) materials are required for high speed signal transmission with minimum attenuation [30]. High permittivity dielectrics are good at holding charge, they are the preferred dielectric for capacitors. High permittivity dielectrics are also used in memory cells that store digital data in the form of charge [32].

II.4. BZN CERAMICS

In recent years, many researchers have focused on the application of high-frequency dielectrics, such as Ba–Nd–Ti–O system and Bi–Zn–Nb–O system [27, 37]. Bismuth-based pyrochlore exhibit well-known high-frequency dielectric with useful properties for multilayer capacitor. As a member of the pyrochlore family of compound, bismuth zinc niobate is a typical high frequency dielectrics with high permittivity and low dielectric loss, and can be applied as various devices, such as temperature-stable multilayer ceramics capacitor and microwave resonator and filter [38, 39]. Bismuth zinc niobate system was reported for the first time by the Chinese researcher in 1974 while recognition widely worldwide began in the 1990s. Much work has been performed on improving dielectric properties, especially enhancing permittivity and reducing dielectric loss [40-42].

Ternary oxides in the Bi_2O_3–ZnO–Nb_2O_5 (BZN) system exhibit high dielectric constants, relatively low dielectric losses, and compositionally tunable temperature coefficients of capacitance [1]. Apart from the high dielectric constant and low loss, these systems possess a field-dependent permittivity, which makes them potential materials for the present day frequency and phase agile devices. Such properties, combined with sintering temperatures of less than 950°C, render these materials attractive candidates for capacitor and high frequency filter applications in multilayer structures cofired with silver electrodes [43, 44] .

However, it is also important that dielectric materials for these applications posses a low dielectric loss or high quality factor, as well as a temperature-independent dielectric behavior. The ferroelectric materials have intrinsically high losses in the microwave regions below their Curie temperature and hence they are temperature-dependent materials. Consequently the development of new tunable materials with low loss rather than ferroelectrics is becoming important. BZN based pyrochlore system has proved to have significant voltage tunability, with a high dielectric constant and low loss [45].

BZN pyrochlore compound has a high dielectric constant (~121) and low quality factor (Q×f ~ 487 GHz) at high frequency levels of 2.27 GHz [46]. BZN pyrochlore also indicates dielectric relaxation between 100 and 400 K at 1.8 GHz peaking around 230 K. Dielectric relaxation may occur near room temperature at THz level frequencies [47]. Dielectric relaxation at microwave frequencies could occur due to substitutional point defects in BZN [47] or due to polarization of the pyrochlore crystal lattice associated with off-center displacement of bismuth and zinc cations on the A sites, linked to off-center displacement of oxygens [13].

CHAPTER III

THE STUDY

III.1. PRODUCTION OF DOPED $Bi_{1.5}Zn_{0.92}Nb_{1.5}O_{6.92}$ PYROCHLORES

Doped $Bi_{1.5}Zn_{0.92}Nb_{1.5}O_{6.92}$ (BZN) pyrochlore compositions were synthesized by conventional powder processing technique. The general flow diagram for the production of doped BZN pyrochlore is given in Figure III.1. The starting materials were reagent grade oxide powders of Bi_2O_3 (99,9% purity Acros), ZnO (99% purity Sigma-Aldrich) and Nb_2O_5 (99.9% purity Alfa Aesar). For doping, oxides of Ta, Eu, Dy and Yb (99.9% purity Ta_2O_5, Eu_2O_3,; Dy_2O_3,; Yb_2O_3) were used as additives. The dopants were introduced into the BZN structure considering the $Bi_{1.5-x}Eu_xZn_{0.92}Nb_{1.5}O_{6.92}$ (where x=0.12), $Bi_{1.5-x}Dy_xZn_{0.92}Nb_{1.5}O_{6.92}$ (where x=0.04), $Bi_{1.5}Zn_{0.92}Nb_{1.5-x}Ta_xO_{6.92}$ (x=0.3 and 1.0) and $(Bi_{1.5-x/3}Zn_{0.46-x}Yb_x)(Zn_{0.46}Nb_{1.5})O_{6.92}$ (where x= 0.04) compositions.

In Table III.1, the ionic radius of Bi, Zn and Nb cations in BZN pyrochlore structure are given together with ionic radius of dopant elements made into the BZN. Considering the ionic radius of the dopant elements, it can be concluded that while Eu and Dy cations can be inserted into the Bi site (or A site of pyrochlore), Ta can be inserted into the Nb-site (or B site of pyrochlore). Yb ion can replace the Zn ions in the A-site of pyrochlore. Zn ions in the BZN pyrochlore share the positions between A and B-site of pyrochlores.

Cation	Coordination number	Ionic radius (A)	Oxide	Element Type
Bi +3	8	1,17	Bi_2O_3	Start elements
Zn +2	8	0,9	ZnO	
Zn +2	6	0,74	ZnO	
Nb +5	6	0,64	Nb_2O_5	
Ta +5	8	0,64	Ta_2O_5	Precious element
Eu +3	8	1,07	Eu_2O_3	Rare earth elements
Dy +3	8	1,03	Dy_2O_3	
Yb +3	8	0,99	Yb_2O_3	

Table III.1 $Bi_{1.5}Zn_{0.46})(Zn_{0.46}Nb_{1.5})O_{6.92}$ structure cations and their properties.

Stoichiometric mixtures of Bi, Zn and Nb oxides and required amount of aditive oxides were ball milled in a polypropylene container for 15h in ethanol using 10 mm diameter zirconia balls. After drying the slurry at 100°C for 24h, the powders were calcined in a closed alumina crucible at 800 °C for 4h. Calcination process was performed at such a low temperature of 800 °C to prevent the evaporation of Bi_2O_3 since it has relatively low melting temperature (825 °C). For detecting possible evaporation during calcination, powders were weighed before and after calcination to record the weight loss amounts. Calcined powders were milled in an agate mortar and they were pressed into pellets with 10 mm in diameter and 1,5-2 mm in thickness at 2MPa by using a uniaxial press. Then the pellets were sintered between 1000-1050°C for 4h in a high temperature furnace (Figure III.2) in a tightly closed alumina crucible with a heating and cooling rates of 250°C/h. The weight of the pellets were recorded before and after the sintering to observe the possible weight losses.

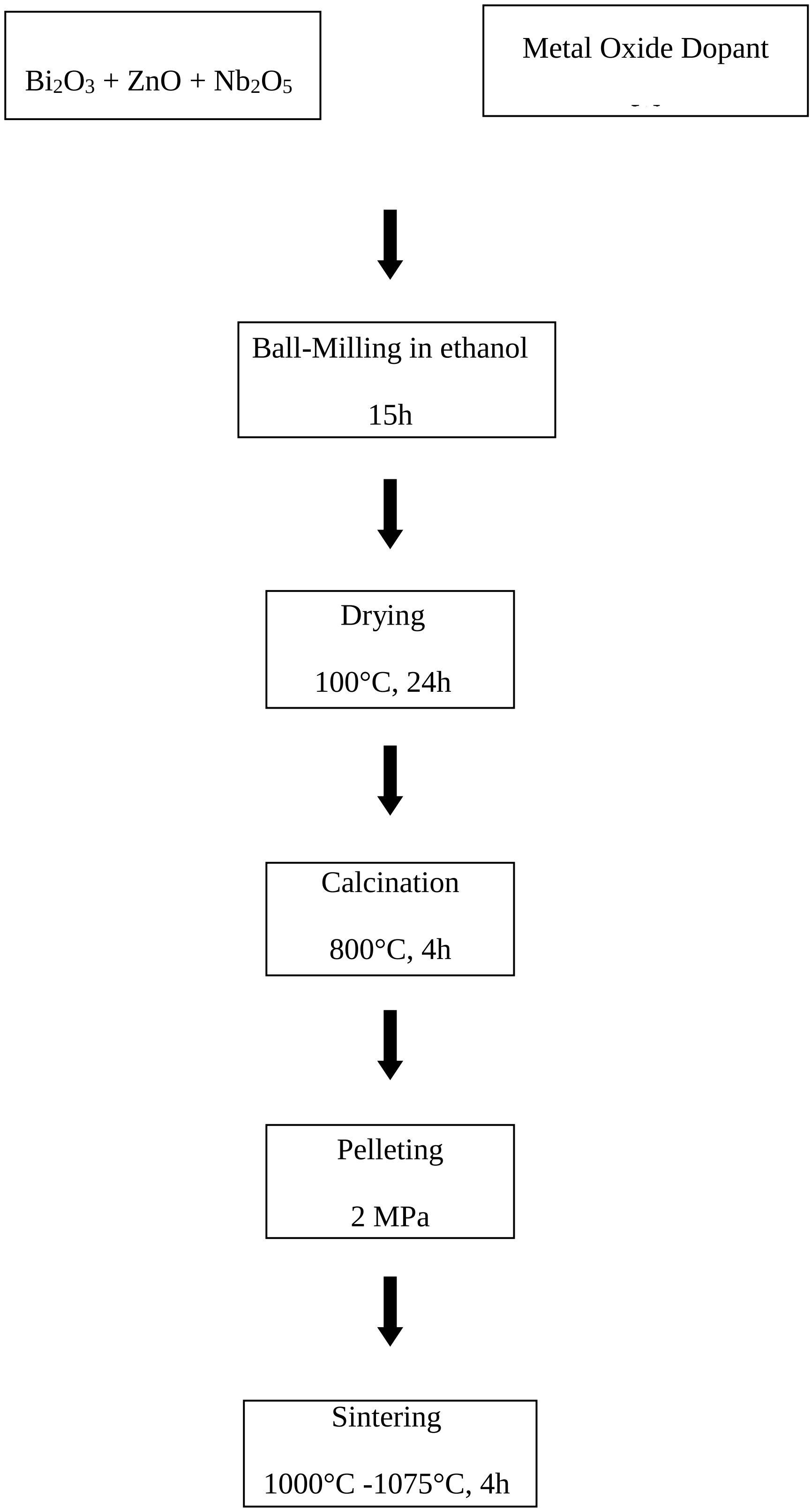

Figure III.1 Flowchart of doped BZN pyrochlore production.

Figure III.2 High-temperature furnace used in calcination and sintering

III.2. X-RAY DIFFRACTION ANALYSIS

The sintered pellets were ground into powder in an agate mortar for X-ray diffraction (XRD) analysis. Powders were placed on a glass sample holder. X-ray diffraction analysis was performed using Rigaku X-ray Diffractometer (Figure III.3) with Ni filtered Cu Kα radiation between 10-70° at a scan rate of 1°/minute. For computer based examination, MDI Jade 6.5 software was used.

To determine the lattice parameters of single phase BZN pyrochlore, low scanning rates (0.25°/minute) were used during XRD examination.

Figure III.3 X-Ray Diffractometer (Rigaku).

III.3. SCANNING ELECTRON MICROSCOPY INVESTIGATION

The microstructures of sintered specimens were examined using a scanning electron microscope (SEM, JEOL 5910LV) equipped with energy dispersive spectrometer (EDS, Oxford-Inca-7274) (Figure III.4). Fracture surfaces and also the surface of the pellets were examined to investigate the second phases. Before the SEM investigation, to increase the surface conductivity, specimens were coated with Au by using Polaron Range Sputter Coater-SC7620 for 3-5 minutes (Figure III.5). SEM examination was performed at 20kV and with secondary electron imaging (SEI) and backscattered electron imaging (BEI) techniques. EDS was used for compositional analysis of phases.

Figure III.4 Scanning electron microscope (JEOL 5910LV)

Figure III.5 SEM coating device (Polaron Range Sputter Coater - SC7620)

III.4. DENSITY MEASUREMENTS

First of all, to increase the precision of density measurements, pellets were ground to get rid of any burr on the surface by using a SiC grinding papers with 1200 grade. To remove the impurities on the surface, pellets were washed with distilled water. Then the height and diameter of the pellets were measured by using a digital caliper.

The densities of the samples were measured by Archimedes method. Firstly, dry weight (W_{dry}) of the samples was measured and then the samples were kept in a boiling distilled water for 5 minutes. After cooling the samples, their weights in water (W_{water}) were also measured by density measurement apparatus (Figure III.6). Afterwards, samples were taken out of water and their wet weight (W_{wet}) were measured in air.

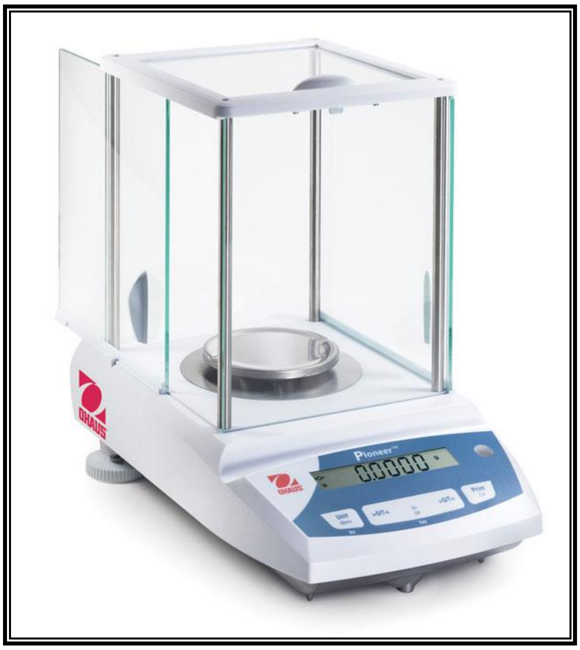

Figure III.6 Density measurement apparatus (Ohaus Pioneer)

The bulk densities (ρ_b) were found by using the Equation III.1:

$$\rho_b = \frac{W_{dry}}{V} = \frac{W_{dry}}{W_{dry} - W_{water}} \tag{III.1}$$

The theoretical densities (ρ_t) were also found by using the Equation III.2:

$$\rho_t = \frac{n \times M_w}{a^3 \times N_A} \tag{III.2}$$

where;

n = number of atoms

M_w = molecular weight of each cation or anion

a = lattice parameter (found by XRD)

N_A = Avagadro’s constant (6.023 x 10^{23})

By using both bulk and theoretical densities, relative densities (ρ_R) were calculated with following equation:

$$\rho_R = \frac{\rho_b}{\rho_t} \times 100 \qquad \text{(III.3)}$$

III.5 IRRADIATION OF DOPED $Bi_{1.5}Zn_{0.46})(Zn_{0.46}Nb_{1.5})O_{6.92}$ PYROCHLORES

Eu, Dy, Ta and Yb doped $Bi_{1.5}Zn_{0.92}Nb_{1.5}O_{6.92}$ pyrochlore put under fluence of C^{6+} irradiation. 3 different dose of irradiation was applied in the irradiation studies. Irradiation level was labeled as A, C and B which were 1 x 10^{11}, 1 x 10^{12} and 1 x 10^{13}. Dielectric properties of the doped pyrochlore ceramic pellets were measured before and after irradiation and effect of irradiation on the dielectric properties of doped BZN pyrochlore were determined. In addition, FTIR analysis of the irradiated samples were also performed.

Sample	Sample Code
Eu doped BZN	Eu Unirradiated Eu A Eu B
Dy doped BZN	Dy1 Unirradiated Dy1 A Dy1 B Dy1 C
Ta doped BZN (With concentration 0.3)	Ta0.3 Unirradiated Ta0.3 A Ta0.3 B Ta0.3 C
Ta doped BZN (With concentration 1.0	Ta1.0 Unirradiated Ta1.0 A Ta1.0 B Ta1.0 C
Yb doped BZN	Yb Unirradiated Yb A Yb B

Fluence amount of C^{6+} ions	
Fluence A	1 x 10^{11}
Fluence B	1 x 10^{13}
Fluence C	1 x 10^{12}

Table III.2 Irradiation dose levels of Eu, Dy, Ta and Yb doped pyrochlore ceramics.

III.V DIELECTRIC MEASUREMENTS OF DOPED $(Bi_{1.5}Zn_{0.46})(Zn_{0.46}Nb_{1.5})O_{6.92}$ PYROCHLORES

$Bi_{1.5}Zn_{0.92}Nb_{1.5}O_{6.92}$ pyrochlore composition was doped with Eu, Dy, Ta and Yb to produce single phase pyrochlores which had high densities (min. %97-98 relative density). Dielectric properties were measured after sintering and the surface of the pellets were coated with gold before measurement. Thermal evaporating method was used for gold coating with Boc Edwards Auto 500 System (Figure III.7). Pyrochlore pellets were placed inside mask having 5 mm diameter and pure gold (99.995) was used for coating process. After coating, low resistant wire (50 ohm) was used to make contact with the surface of the pellets using silver paint. Then samples were placed on top of lam with silver paint to prevent electric contact during vacuum and heating process. A setup consisting of an LCR meter, temperature controller, small chamber, and vacuum pump was used (Figure III.8). Each substrate was individually placed inside the small vacuum chamber with a heater contacted to substrate. At the beginning of dielectric measurement, pressure decreased below 10^{-2} torr and substrate was heated to 200°C to establish silver paint well contact to the sample and to remove the solvent which could cause electrical noises. Then the sample was cooled to room temperature.

When vacuum reached above 10^{-3}torr, dielectric measurement was started. Dielectric measurement was measured as a function of temperature and frequency. Temperature was changed from room temperature to 40°C and then increased to 200°C with 20°C interval. In every temperature step, frequency was also changed from 1kHz to 30kHz with 1 kHz interval and from 30kHz to 2MHz with 25kHz interval. The data were recorded separately, then were used to monitor dielectric constant and dielectric loss changes with respect to frequency and temperature.

Figure III.7 Thermal eveperator (Boc Edwards Auto 500 System).

Figure III.8 Dielectric measurement setup: Chamber, temperature and heater controller, LCR meter, Computer and Unique program.

The dielectric constant was calculated using the following formula:

$$k = C_p . d / A . \varepsilon_o \qquad \text{(III.4)}$$

where k = Dielectric constant

C_p = Capacitance

d = Distance between the electrods

A = Area of electrods

ε_o = permittivity of vacuum (8.85 x 10^{-12} F/m)

CHAPTER IV

RESULTS AND DISCUSSION

IV.1 Eu DOPED BZN

Since Eu cation has a similar radius with Bi (radius of Eu: 1.07 Å, radius of Bi: 1.17 Å), Eu was used as a replacement of Bi in the $Bi_{1.5}Zn_{0.92}Nb_{1.5}O_{6.92}$ (BZN) structure. Considering $Bi_{1.5-x}Eu_xZn_{0.92}Nb_{1.5}O_{6.92}$ composition, Eu content was selected as x=0.12 depending on the previous study [48] and $Bi_{1.38}Eu_{0.12}Zn_{0.92}Nb_{1.5}O_{6.92}$ composition was produced. XRD analysis revealed that the doping content of x=0.12, gave only single phase BZN structure and no any other phases were detected (Figure IV.1). This result indicates that the added Eu was dissolved in the Bi site of BZN pyrochlore.

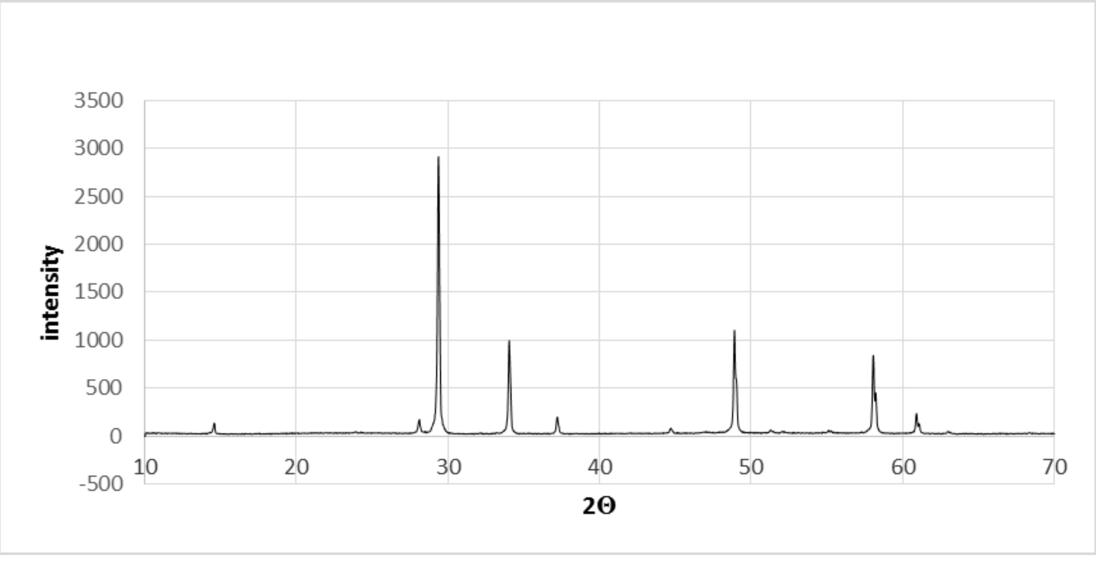

Figure IV.1 XRD pattern of $Bi_{1.5-x}Eu_xZn_{0.92}Nb_{1.5}O_{6.92}$ where x=0.12 giving $Bi_{1.38}Eu_{0.12}Zn_{0.92}Nb_{1.5}O_{6.92}$ composition sintered at 1050 °C for 4h.

IV.2 Dy DOPED BZN

The ionic radius of Dy (1.03 Å) is similar to ionic radius of Bi (1.17 Å) and therefore Dy was doped into the Bi site or A site of BZN pyrochlore using the $Bi_{1.5-x}Dy_xZn_{0.92}Nb_{1.5}O_{6.92}$ composition. Dy doping content was x=0.04 regarding the previous work (REF) and $Bi_{1.46}Dy_{0.04}Zn_{0.92}Nb_{1.5}O_{6.92}$ composition was produced. XRD analysis resulted in single phase pyrochlore structure revealing that doped Dy cation was dissolved in the BZN structure (Figure IV.2).

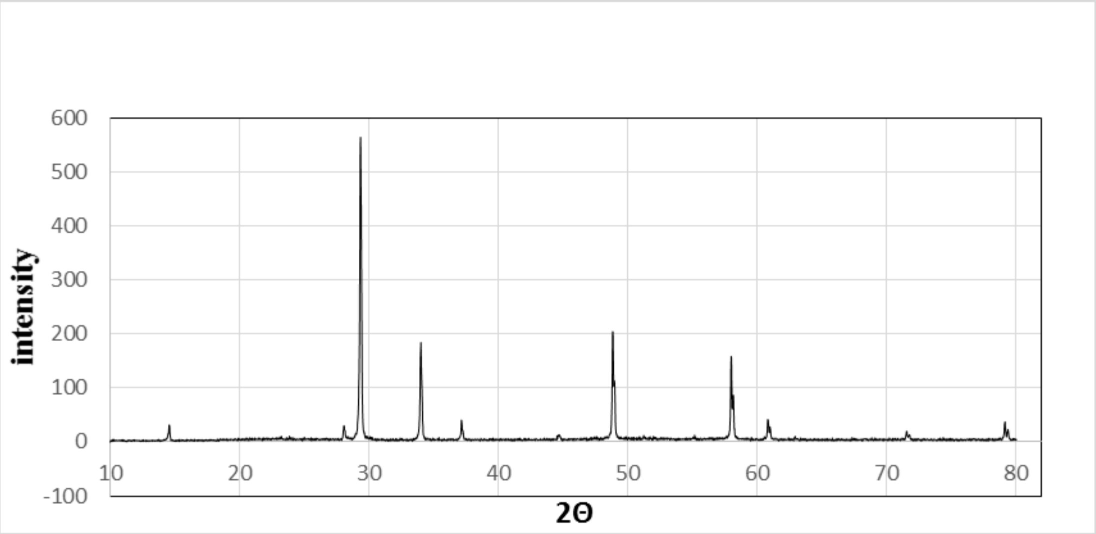

Figure IV.2 XRD pattern of $Bi_{1.5-x}Dy_xZn_{0.92}Nb_{1.5}O_{6.92}$ where x=0.04 giving $Bi_{1.46}Dy_{0.04}Zn_{0.92}Nb_{1.5}O_{6.92}$ composition sintered at 1025 °C for 4h.

The microstructure of Dy doped BZN ceramic was also investigated using SEM which confirmed the XRD results showing only single phase microstructure (Figure IV.2). The microstructure revealed that the BZN grains were nearly equiaxed and contained very small amount of porosity. EDS results indicated that the composition of BZN grains were very near to theoretical pyrochlore composition containing also Dy (Figure IV.2).

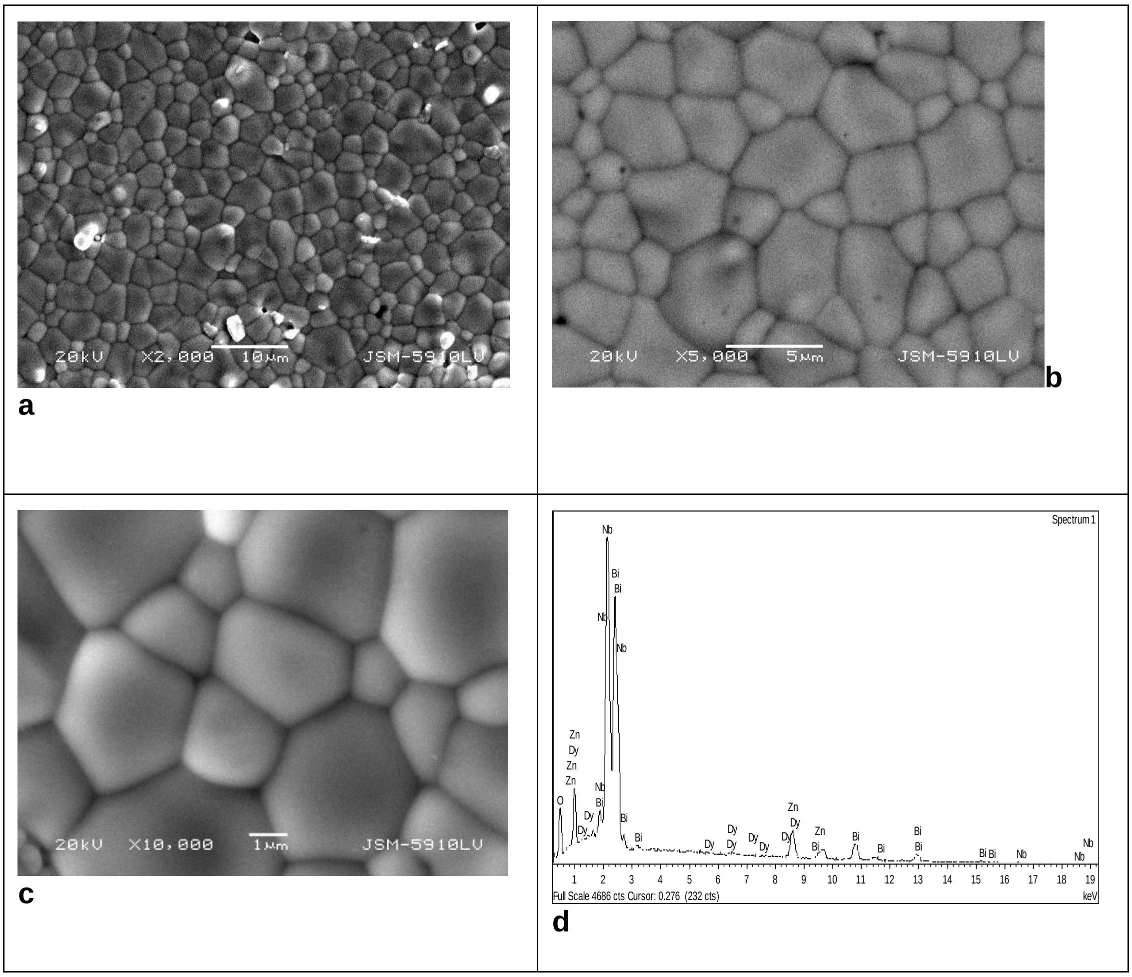

Figure IV.3: SEM micrographs and EDS analysis of $Bi_{1.43}Dy_{0.07}Zn_{0.92}Nb_{1.5}O_{6.92}$ pyrochlore composition (x=0.04) **a)** BEI at ×2.000, **b)** BEI at ×2.000, **c)** BEI at ×5.000 d) EDS analysis from pyrochlore grains.

IV.3 Ta DOPED BZN

Since Ta cation has identical radius with Nb cation (Ta: 0.64 Å and Nb: 0.64 Å), Ta cation was used to replace the Nb cation in the BZN structure using the $Bi_{1.5}Zn_{0.92}Nb_{1.5-x}Ta_xO_{6.92}$ composition. Ta content was determined as x=0.3 and x=1.0 considering the previous study[49]. XRD analysis of Ta doped samples (x=0.3 and 1.0) revealed only single phase structure (Figure IV.4).No any second phase was detected in the XRD. This result showed that Ta can form a solid solution with BZN. In addition, Ta doped sample with x=0.3 was also examined with SEM which revealed only pyrochlore grains with high density (Figure IV.5).EDS results also showed that the compositions were near to the theoretical values.

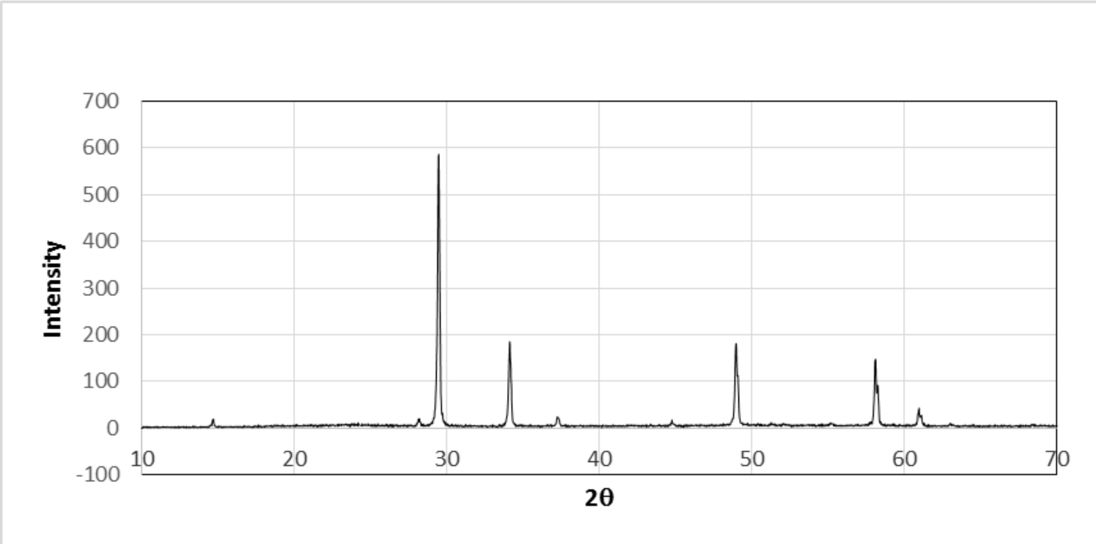

Figure IV.4: XRD pattern of $Bi_{1.5}Zn_{0.92}Ta_xNb_{1.5-x}O_{6.92}$ sample with composition of x=0.3 sintered at 1025°C for 4 h.

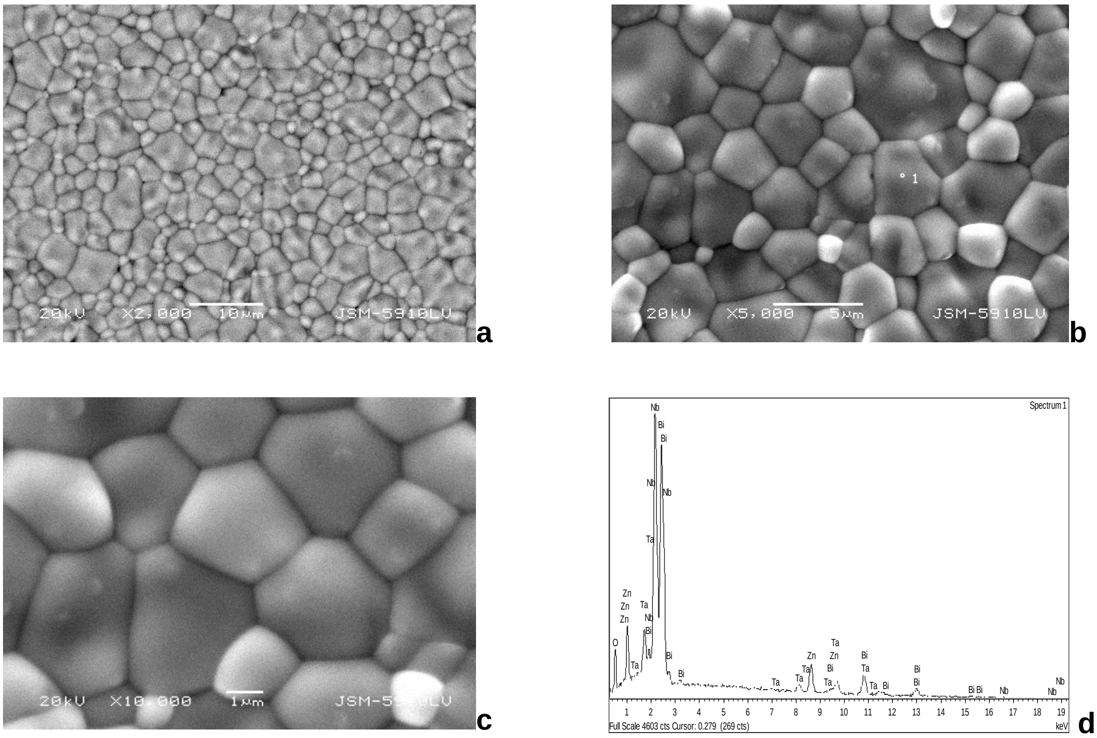

Figure IV.5 : SEM micrographs and EDS analysis of $Bi_{1.5}Zn_{0.92}Nb_{1.5-x}Ta_xO_{6.92}$ composition with x=0.3 ($Bi_{1.5}Zn_{0.92}Nb_{1.2}Ta_{0.2}O_{6.92}$) which was sintered at 1025°C for 4 hours **a)** BEI at ×2.000, **b)** SEI at ×5.000, **c)** SEI at ×10.000 and **d)** EDS result from BZN grains.

IV.4 Yb DOPED BZN

Since the ionic radius of Yb element (0.985 Å) is near to the ionic radius of Zn cation (0.90 Å) in the A-site of pyrochlore, Yb was doped into the A site of BZN pyrochlore replacing the Zn cation with the composition of $(Bi_{1.5-x/3}Zn_{0.46-x}Yb_x)(Zn_{0.46}Nb_{1.5})O_{6.92}$. Yb doping content was selected as x=0.04 regarding the previous study[50]. XRD analysis revealed only sing phase structure and no any other phase was detected (Figure IV.6). However, SEM results of the same sample examined in the XRD (x=0.04) indicated some second phases in the microstructure (Figure IV.7). EDS analysis taken from BZN pyrochlore grains were identical with theoretical values showing also Yb content.

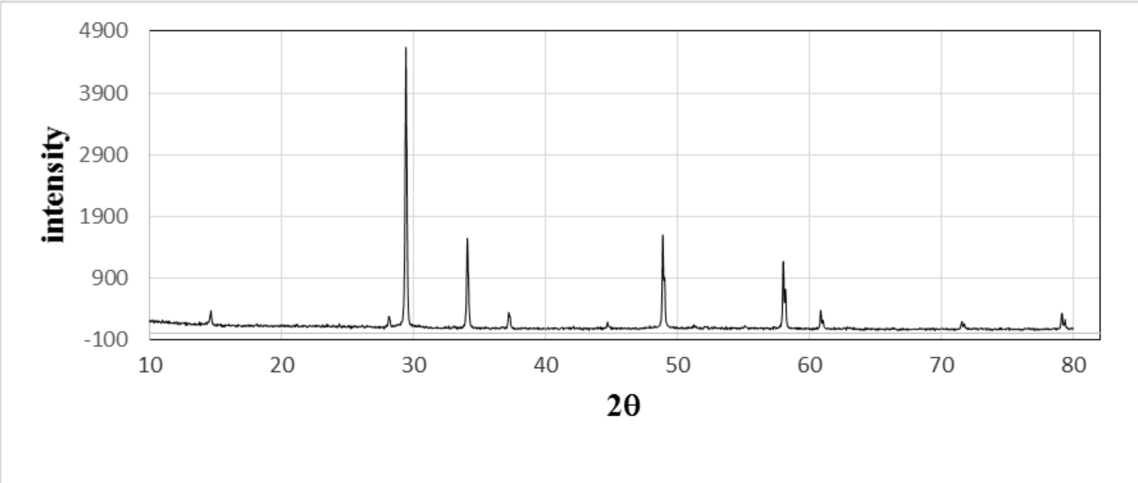

Figure IV.6 : XRD pattern of $(Bi_{1.5-x/3}Zn_{0.46-x}Yb_x)(Zn_{0.46}Nb_{1.5})O_{6.92}$ with composition x =0.04 $(Bi_{1.486}Zn_{0.42}Yb_{0.04})(Zn_{0.46}Nb_{1.5})O_{6.92})$ sintered at 1050°C for 4h.

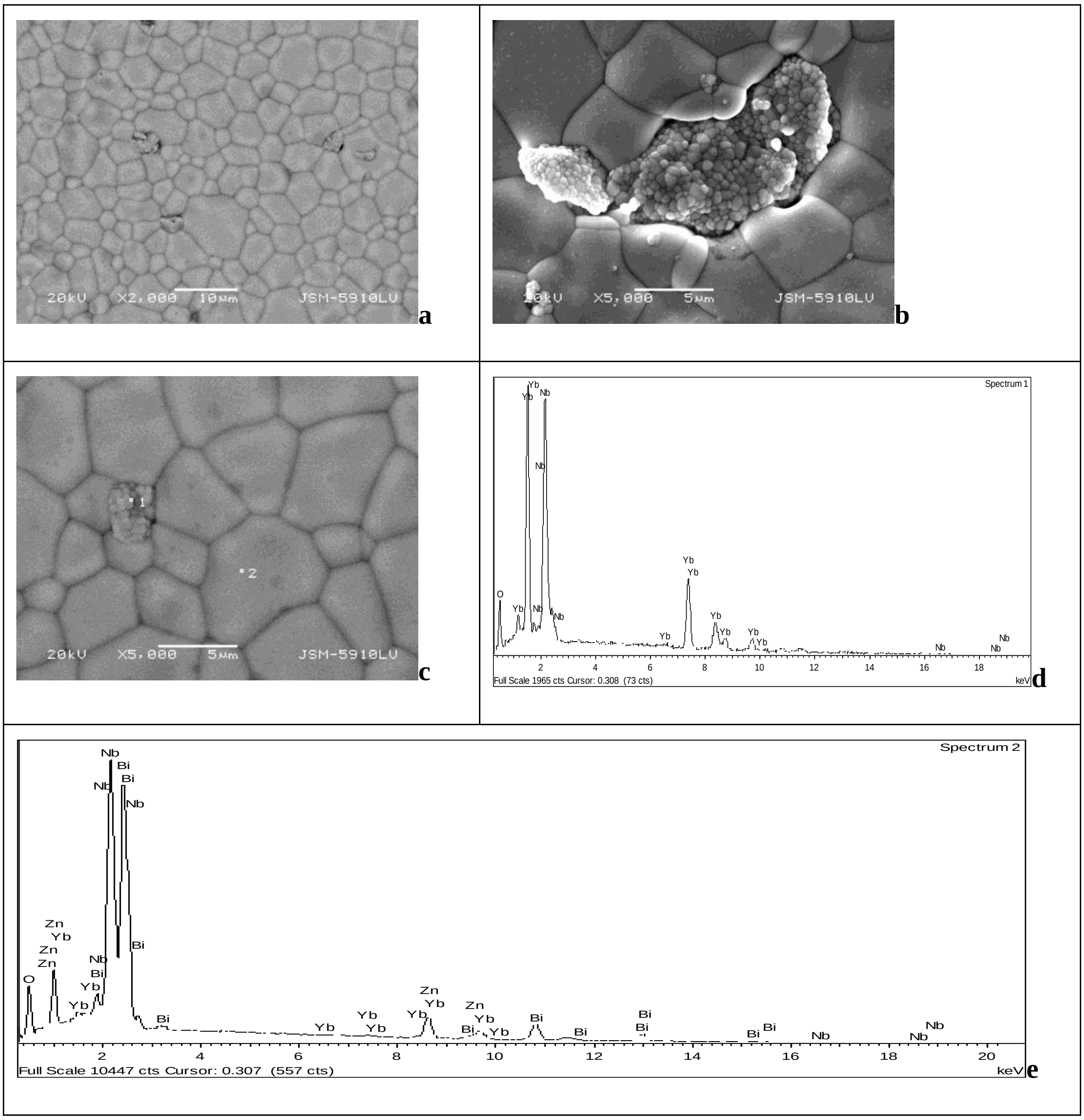

Figure IV.7 : SEM micrographs and EDS analysis of $(Bi_{1.5-x/3}Zn_{0.46-x}Yb_x)(Zn_{0.46}Nb_{1.5})O_{6.92}$ composition with x=0.04 which was sintered at 1050°C for 4 hours (**a)** BEI a ×2.000 multiplication, **b)** SEI at ×5.000 multiplication, **c)** BEI at ×5.000, d) EDS analysis from BZN pyrochlore grains and e) EDS analysis from second phase.

IV.5 DENSITIES AND LATTICE PARAMETERS OF DOPED $(BI_{1.5}ZN_{0.46})(ZN_{0.46}NB_{1.5})O_{6.92}$ PYROCHLORES

After calcining the doped BZN powders, they were made pellets and sintered between 1025-1050°C for 4 hours depending on the type of additives. Considering the theoretical density of $Bi_{1.5}Zn_{0.92}Nb_{1.5}O_{6.92}$ pyrochlore as 7.111 g/cm^3 [51], it was determined that the sintered pellets had a relative density above 99%. Lattice parameter of $Bi_{1.5}Zn_{0.92}Nb_{1.5}O_{6.92}$ pyrochlore is 10.5616 A° [52] .The lattice parameter of doped BZN pyrochlores are given in Table IV.1 **.**

	Cation	**Composition**	**Structure**	**Lattice Parameters (Å)**
Replacement for **Bi**	**Eu**	x = 0,12	Tek Faz	10.5392
	Dy	x = 0,04	Tek Faz	10.5445
Replacement for **Nb**	**Ta**	x = 0,3	Tek Faz	10,5426
		x = 1.0	Tek Faz	10.5473
Replacement for **Zn**	**Yb**	x = 0,04	Tek Faz	10.5381

Table IV.1 Lattice parameters of doped $(Bi_{1.5}Zn_{0.46})(Zn_{0.46}Nb_{1.5})O_{6.92}$ pyrochlores ceramics.

IV.7.1 IRRADIATED Eu DOPED BZN

IV.7.1.1 Dielectric Results

Dielectric values of Eu doped BZN radiated with 10^{11} +6C influence (called as Eu A) varied from 75 to 87 with respect to temperature and frequency. At room temperature dielectric values changed from 78 to 84 for frequency range from 1 kHz to 2 MHz. While temperature was increased dielectric values were decreased within frequency range of 1 kHz to 2 Mhz and dielectric values decreased to the lowest values at 200°C which were between 75 to 79 (Figure IV.1a, Table IV.2).

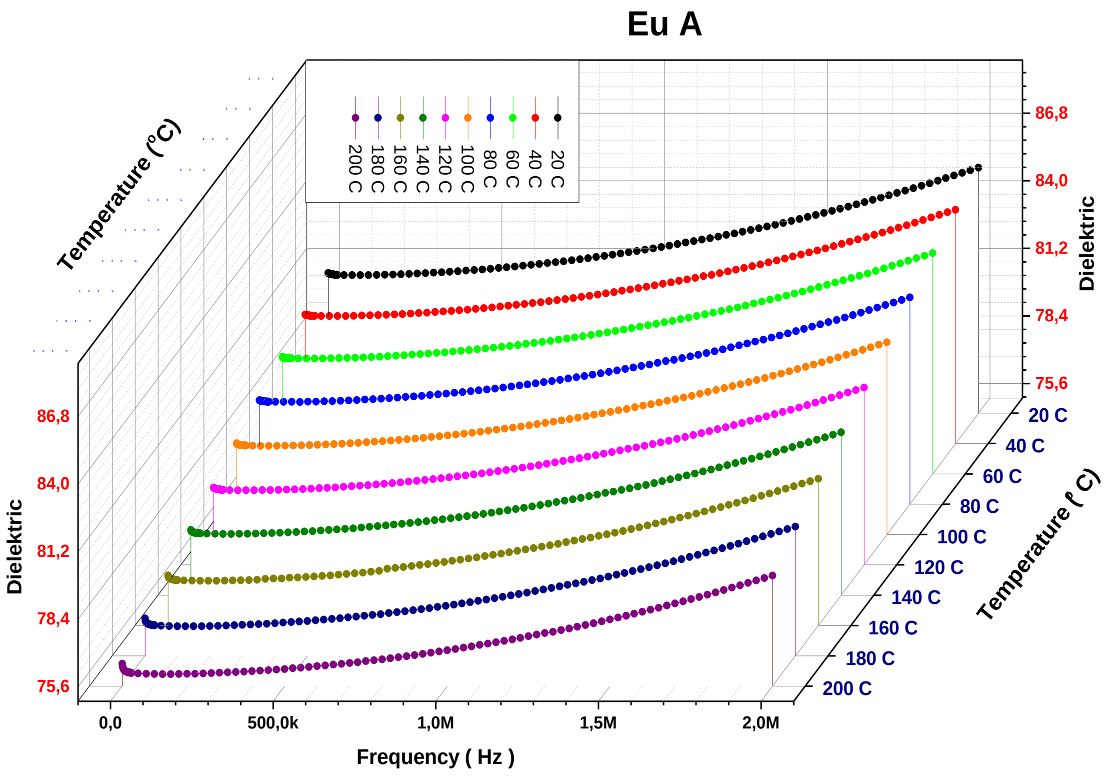

Figure IV.1a Variation of dielectric constant with temperature and frequency for Eu A (Eu doped BZN radiated with 10^{11} +6C influence)

Dielectric values of Eu doped BZN radiated with 10^{13} +6C influence (called as Eu B) varied from 78 to 87 with respect to temperature and frequency. At room temperature dielectric values changed from 82 to 86 for frequency range from 1 kHz to 2 MHz. While temperature was increased dielectric values were decreased within frequency range of 1 kHz to 2 Mhz and dielectric values decreased to the lowest values at 200°C which were between 78 to 82 (Figure IV.1b, Table IV.2).

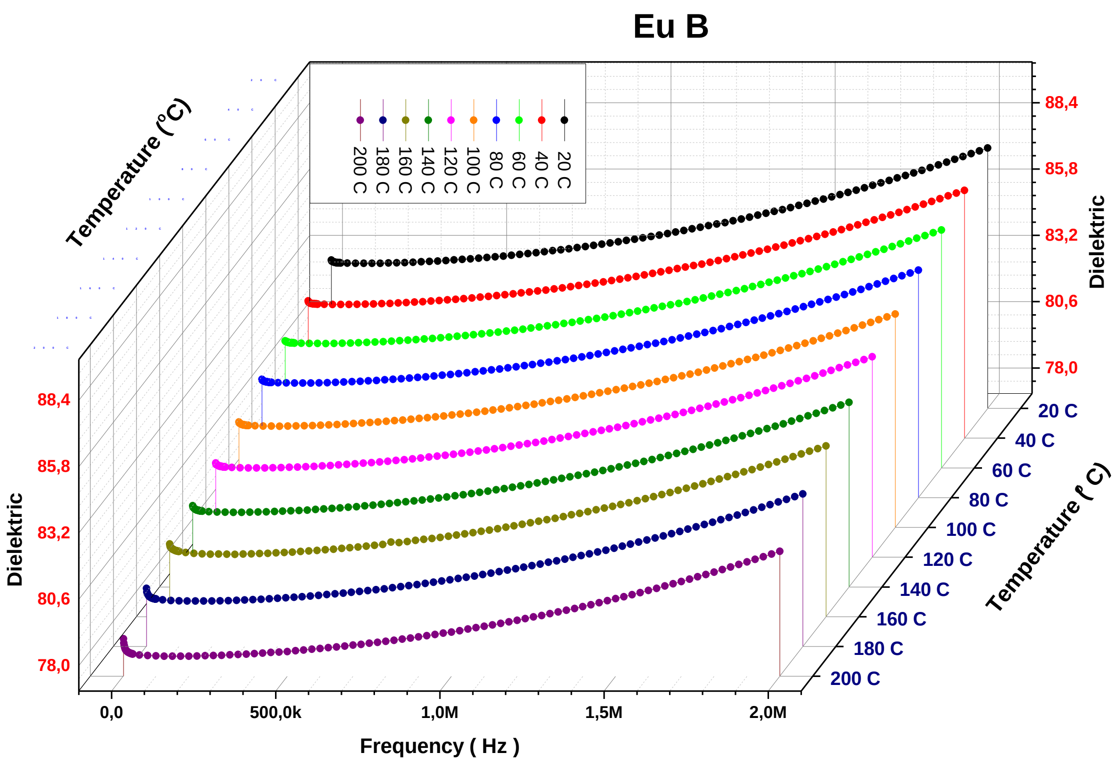

Figure IV.1b Variation of dielectric constant with temperature and frequency for Eu B (Eu doped BZN radiated with 10^{13} +6C influence)

While at low frequency range of 1 kHz-125 kHz, the dielectric values of both samples, Eu A and Eu B, decreased at all temperatures of 20-200°C, they were started to increase at 125 kHz and continued to increased with frequency until 2 MHz (Figure IV.1c).

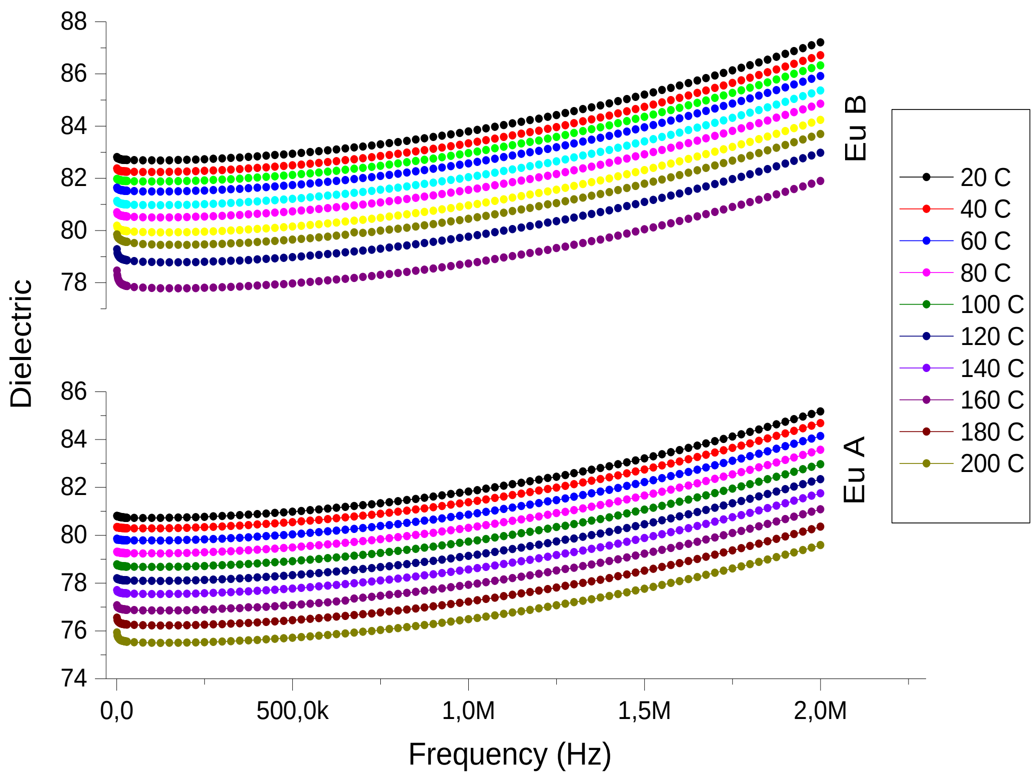

Figure IV.1c Variation of dielectric constant with frequency and temperature of Eu doped BZN irradiated with 10^{11} +6C and 10^{13} +6C fluences (Eu A and Eu B).

Dielectric changes Eu doped BZN after C^{+6} irradiation			
	1 KHz – 75 KHz Eu A **1 KHz – 125 KKz Eu B**		
	40 °C	**120 °C**	**200 °C**
Eu A	**80.34 – 80.28**	**78.20 – 78.09**	**75.93 – 75.51**
Eu B	**82.37 – 82.24**	**80.70 – 80.50**	**78.47 – 77.78**
	75 KHz – 2 MHz Eu A **125 KHz – 2 MHz Eu B**		
	40 °C	**120 °C**	**200 °C**
Eu A	**80.28 – 84.69**	**78.09 - 82.34**	**75.51 – 79.58**
Eu B	**82.24 – 86.72**	**80.50 – 84.86**	**77.78 – 81.90**

Table IV.2 Dielectric constant values of Eu doped BZN irradiated with 10^{11} +6C (Eu A) and 10^{13} +6C (Eu B) fluences at different frequencies and temperatures.

IV.7.1.2 Dielectric Loss Results

Dielectric loss values of Eu A is varied from 3.23 to 66.34 (x 10^{-4}) with respect to temperature and frequency changes. At room temperature dielectric loss values varied from 3.23 to 57.35 (x 10^{-4}) for frequency range 1kHz to 2 MHz. At 200°C, dielectric loss values decreased from 35.29 to 8.54 (x 10^{-4}) and from 8.54 to 66.34 (x 10^{-4}) when frequency increased from 1 kHz to 100 kHz and from 100 kHz and 2 MHz, respectively (Figure IV.2a, Table IV.3).

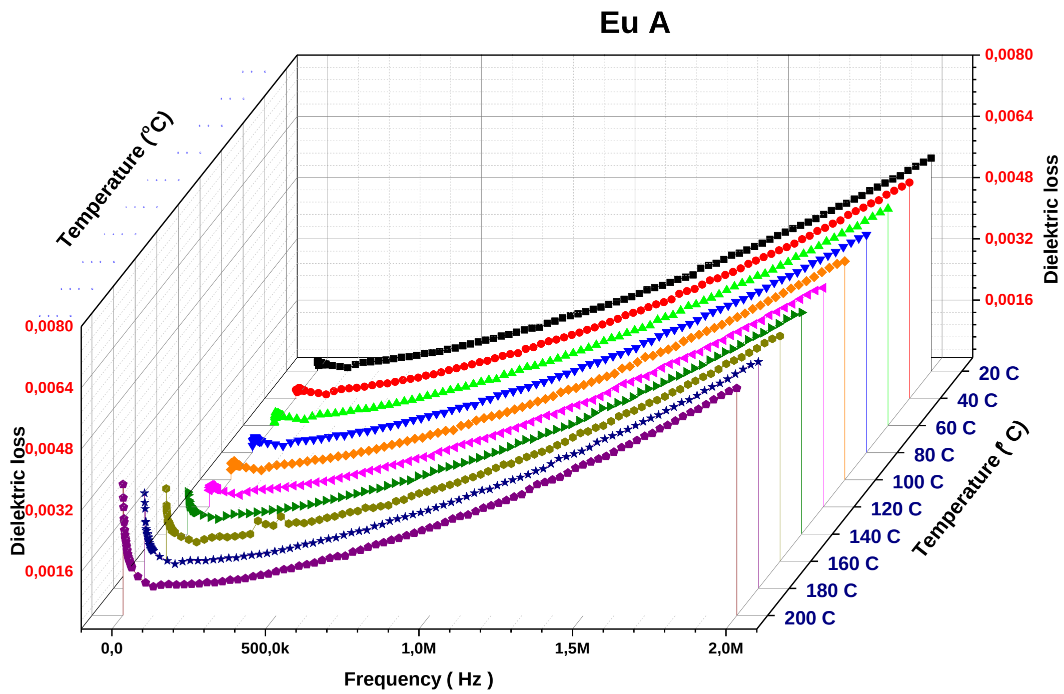

Figure IV.2a Variation of dielectric loss with frequency and temperature of Eu doped BZN irradiated with 10^{11} +6C (Eu A).

Dielectric loss values of Eu B changed from 5.93 to 66.63 (x 10^{-4}) with respect to temperature and frequency. At room temperature, dielectric lost values varied from 5.93 to 59.85 (x 10^{-4}) when frequency increased from 1 kHz to 2 MHz. However, at 200°C dielectric loss values decreased from 55.75 to 14.56 (x 10^{-4}) and increased from 14.56 to 66.63 (x 10^{-4}) when frequency increased from 1 kHz to 100 kHz and 100 kHz to 2 MHz, respectively (Figure IV.2b, Table IV.3).

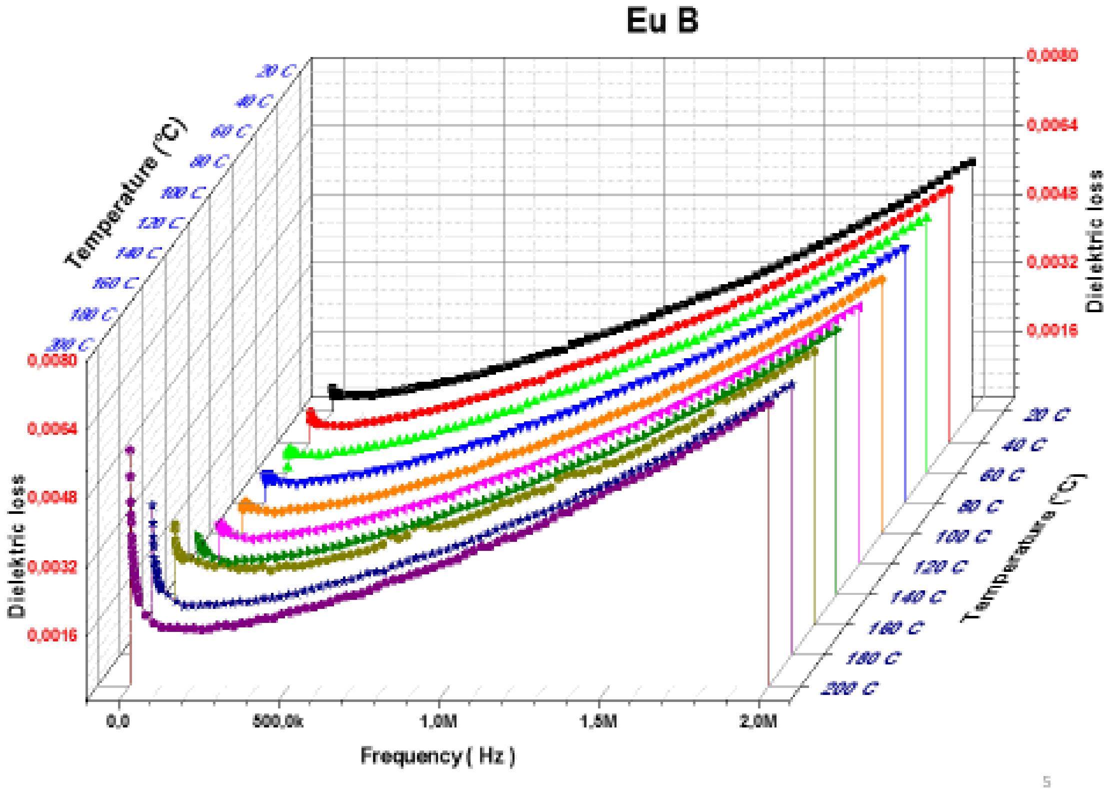

Figure IV.2b Variation of dielectric loss with frequency and temperature of Eu doped BZN irradiated with 10^{13} +6C (Eu B).

Dielectric loss measurement of both Eu A and Eu B indicated that loss value initially decreased until 100 kHz between 20-200°C and then the loss values started to increase with frequency (Figure IV.2c).

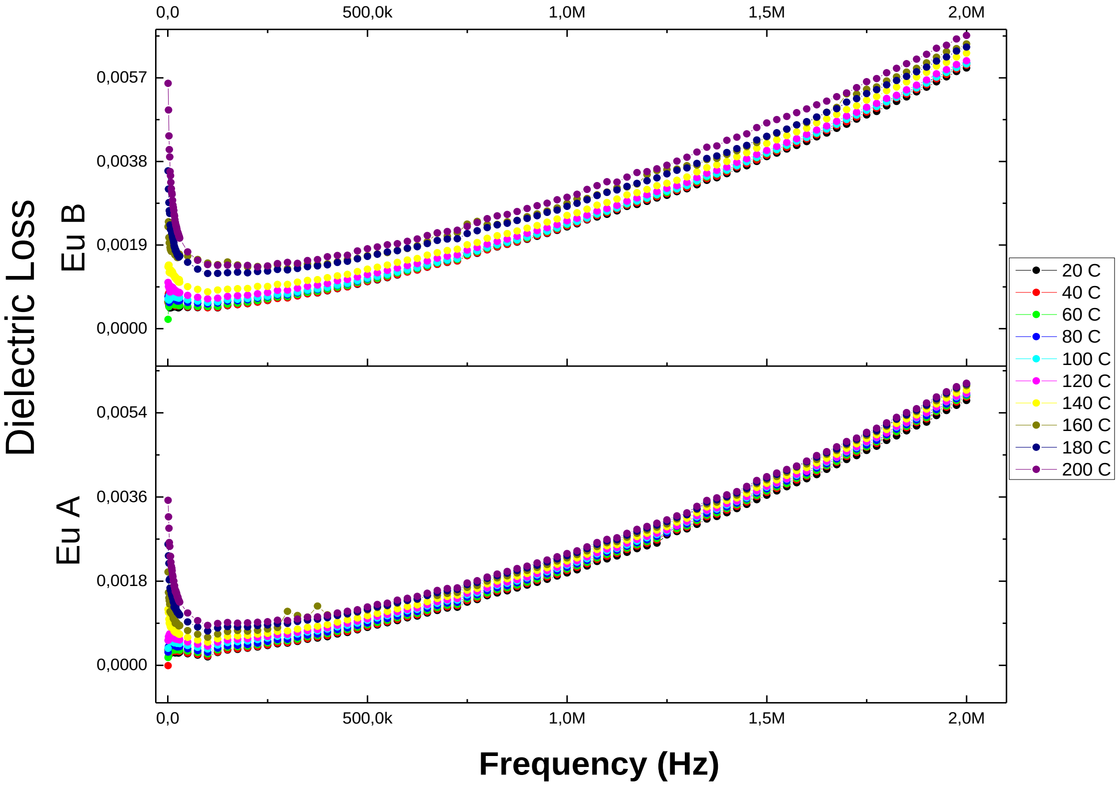

Figure IV.2c Variation of dielectric loss with frequency and temperature of Eu doped BZN irradiated with 10^{11} +6C and 10^{13} +6C (Eu A and Eu B).

Dielectric loss changes Eu dopet BZN after C^{+6} irradiation			
	1 KHz – 100 KHz (X 10^{-4})		
	40 ºC	120 ºC	200 ºC
Eu A	**3.23 – 1.99**	**5.33 – 4.09**	**35.29- 8.54**
Eu B	**5.93 – 4.75**	**10.51 – 6.77**	**55.75 – 14.56**
	100 KHz – 2 MHz (X 10^{-4})		
	40 ºC	120 ºC	200 ºC
Eu A	**1.99 – 57.35**	**4,09 – 58.2**	**8.54 – 60.34**
Eu B	**4.75 – 59.85**	**6.77 – 60.87**	**14.56 - 66.63**

Table IV.3 Dielectric loss values of Eu doped BZN irradiated with 10^{11} +6C (Eu A) and 10^{13} +6C (Eu B) fluences at different frequencies and temperatures.

IV.7.2 IRRADIATE Dy DOPED BZN

IV.7.2.1 Dielectric Results

Dielectric values of Dy doped BZN radiated with 10^{13} +6C influence (called as Dy B) varied from 118 to 106 with respect to temperature and frequency. At room temperature dielectric values increased from 118 to 124 for frequency range from 1 kHz to 2 MHz. With increasing the temperature, dielectric values decreased between 1 kHz-2 MHz. For example, dielectric value of 118 at 40°C at 125 kHz decreased to 106 at 200°C at 125 kHz. However, at each temperature value, the dielectric value increased with frequency like dielectric value increased from 107 at 1 kHz at 200°C to 112 at 2 MHz at 200°C (Figure IV.3a, Table IV.4).

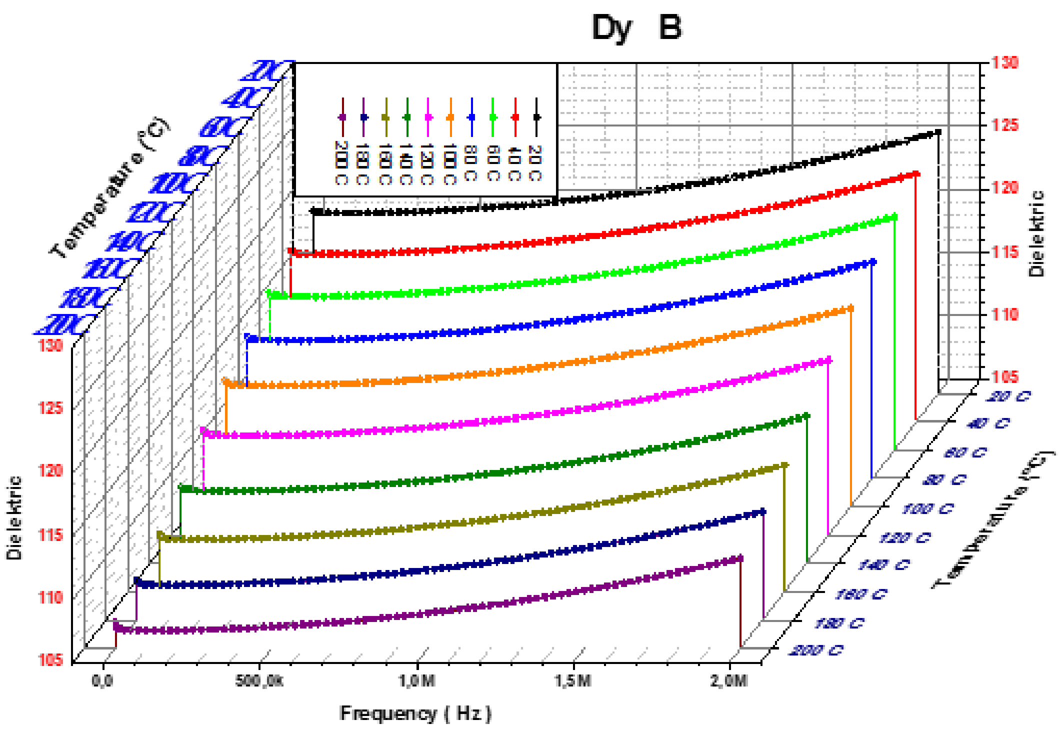

Figure IV.3a Variation of dielectric constant with frequency and temperature of Dy doped BZN irradiated with 10^{13} +6C (Dy B).

Dielectric constant values of Dy C varied between 63 – 62 with respect to temperature and frequency. At room temperature, dielectric value increased from 63 to 67 when frequency increased from 1 kHz to 2 MHz. Through temperature increase dielectric value decreased within this frequency range and it has reached the lowest value at 200°C which was 59-62 at 1 kHz and 2 MHz.

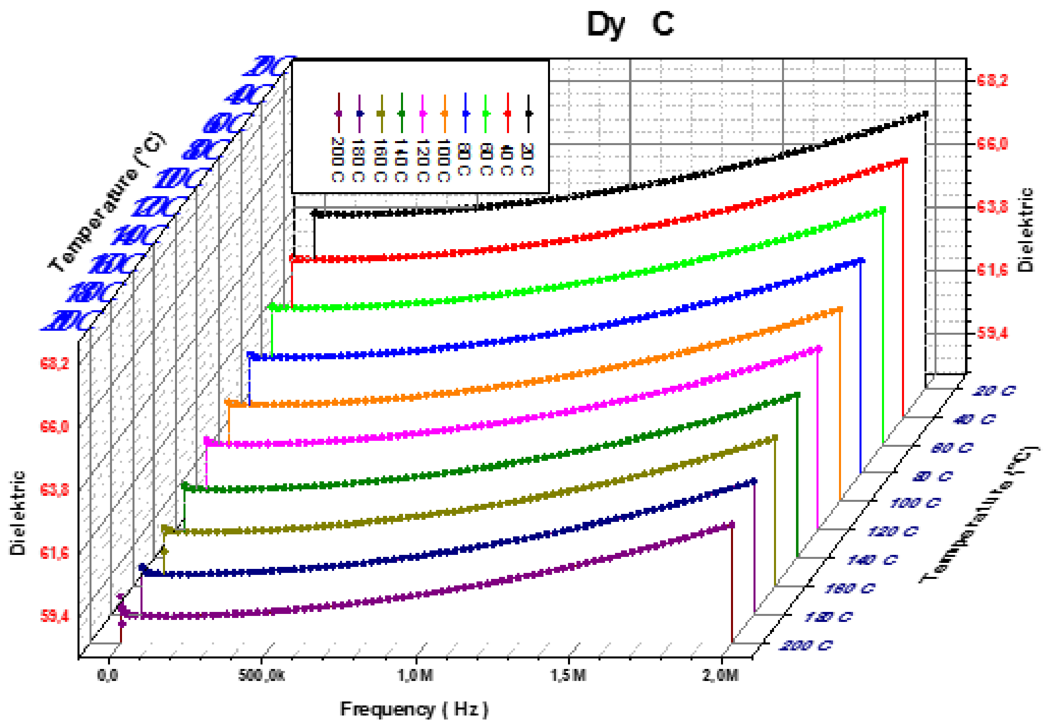

Figure IV.3b Variation of dielectric constant with frequency and temperature of Dy doped BZN irradiated with 10^{12} +6C (Dy C).

Dielectric measurement results also showed that dielectric values of both Dy B and Dy C samples were nearly stable with frequency between 1 kHz -125 kHz for the temperature range of 20-200°C. Nevertheless, dielectric constant values started to increase when frequency rised from 125 kHz to 2 MHz for the temperature range of 20-200°C (Figure 3c and Table IV.4).

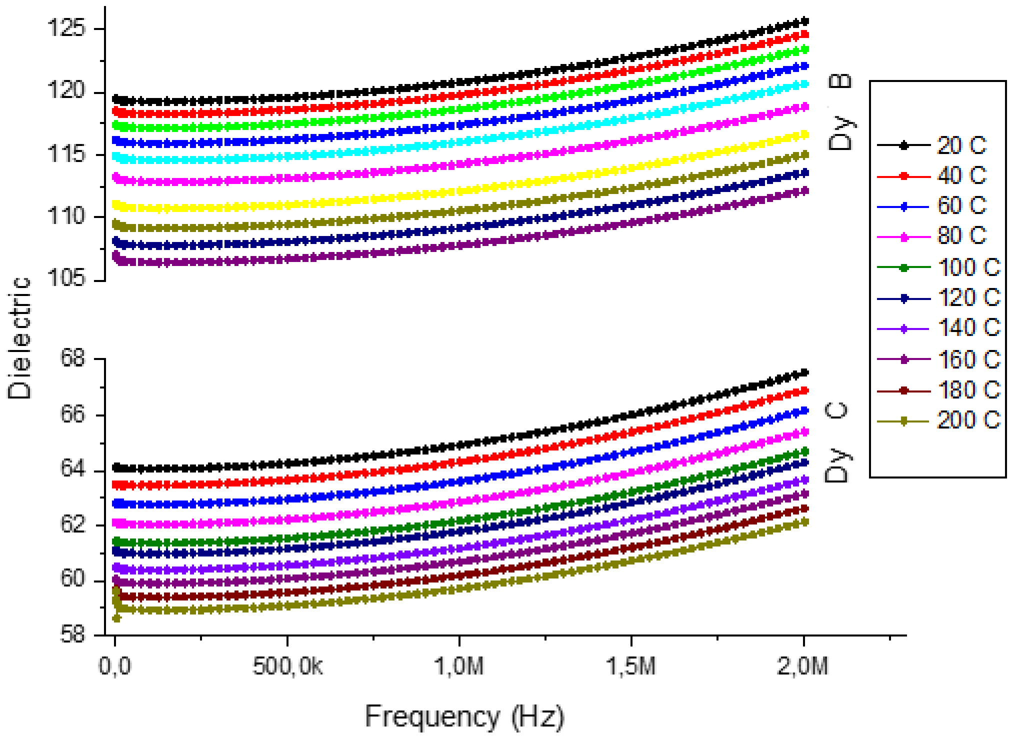

Figure IV.3c Variation of dielectric constant with frequency and temperature of Dy doped BZN irradiated with 10^{12} +6C and 10^{13} +6C (Dy C and Dy B).

Dielectric changes Dy dopet BZN after C^{+6} irradiation			
	1 KHz – 125 KHz		
	40 °C	120 °C	200 °C
Dy B	118.53 – 118.28	113.26 – 112.86	107.07 – 106.42
Dy C	63.51 – 63.47	61.10 – 60.99	59.62 – 58.94
	125 KHz – 2 MHz		
	40 °C	120 °C	200 °C
Dy B	118.28 – 124.63	112.86 – 118.85	106.42 – 112.16
Dy C	63.47 – 66.92	60.99 – 64.30	58.94 – 62.14

Table IV.4 Dielectric constant values of Dy doped BZN irradiated with 10^{12} +6C (Dy C) and 10^{13} +6C (Dy B) fluences at different frequencies and temperatures.

IV.7.2.2 Dielectric Loss Results

Dielectric loss values of Dy B samples varied from 4.54 – 61.85 (x 10^{-4}) with respect to temperature and frequency. At room temperature dielectric loss values increased from 4.54 – 63.71 (x 10^{-4}) for frequency values of 10 kHz to 2 MHz. At 200°C, dielectric loss values of Dy B samples rised from 56.61 to 61.85 (x 10^{-4}) when increasing the frequency from 10 kHz to 2 MHz. Dielectric loss values between 1-10 kHz were not used since these values were not stable possibly due to measurement errors. At room temperature, dielectric losses continuously increased with frequency up to 2 MHz but above room temperature values this continuity was not observed. For example, at 200°C for the frequency range of 10 kHz to 100 kHz dielectric loss dramatically decreased from 56,61 to 9.00 (x 10^{-4}) while the loss values increased from 9.00 to 61.85 (x 10^{-4}) for the frequency range of 100 kHz to 2 MHz (Figure 4a and Table IV.5).

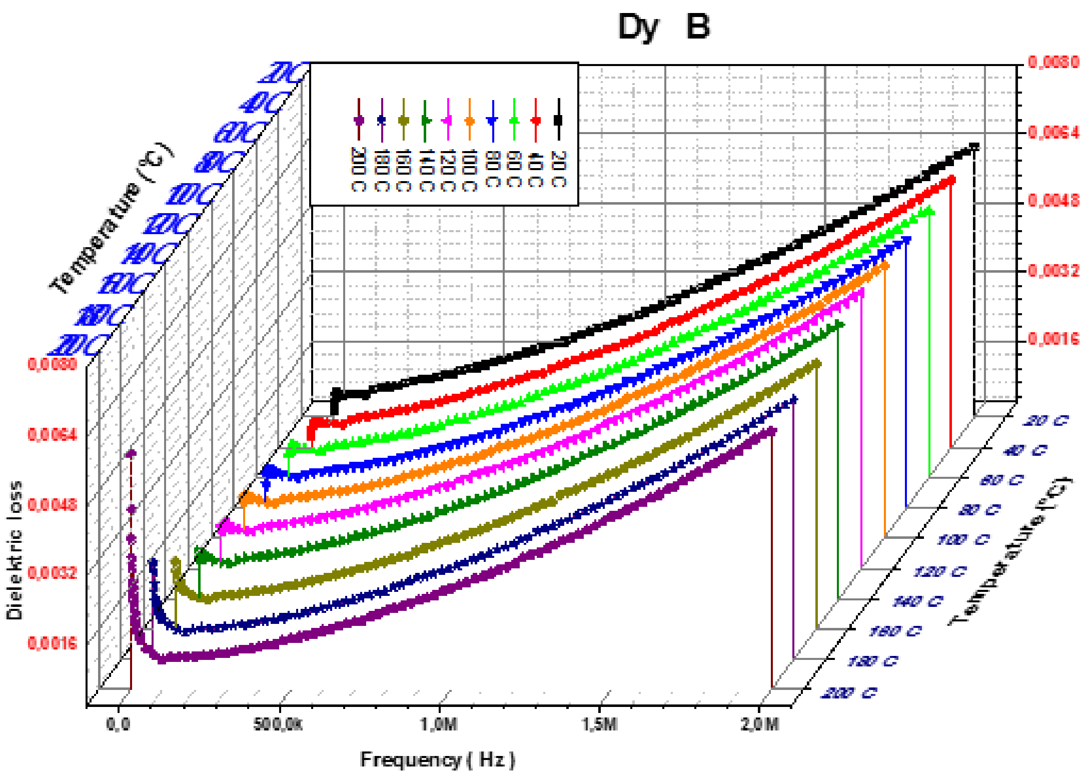

Figure IV.4a Variation of dielectric loss with frequency and temperature of Dy doped BZN irradiated with 10^{13} +6C (Dy B).

Dielectric loss values of Dy C samples changed from 4.89 – 59.61 (x 10^{-4}) with respect to temperature and frequency changes. While at room temperature dielectric loss values increased from 4.89 – 60.15 (x 10^{-4}) for frequency values of 10 kHz to 2 MHz, loss values increased from 38.39 to 59.61 (x 10^{-4}) for higher frequency range of 10 kHz to 2 MHz. At room temperature, although dielectric loss values initially decreased from 4.89 – 3.40 (x 10^{-4}) with respect to frequency between 10 kHz to 100 kHz, these values increased from 3.40 to 60.15 (x 10^{-4}) between 100 kHz - 2 MHz. At 200°C, dielectric loss values firstly decreased from 39.39 to 10.89 (x 10^{-4}) and then increased from 10.89 to 59.61 (x 10^{-4}) when increasing the frequency from 100 kHz to 2 MHz (Figure IV.4b and Table IV.5).

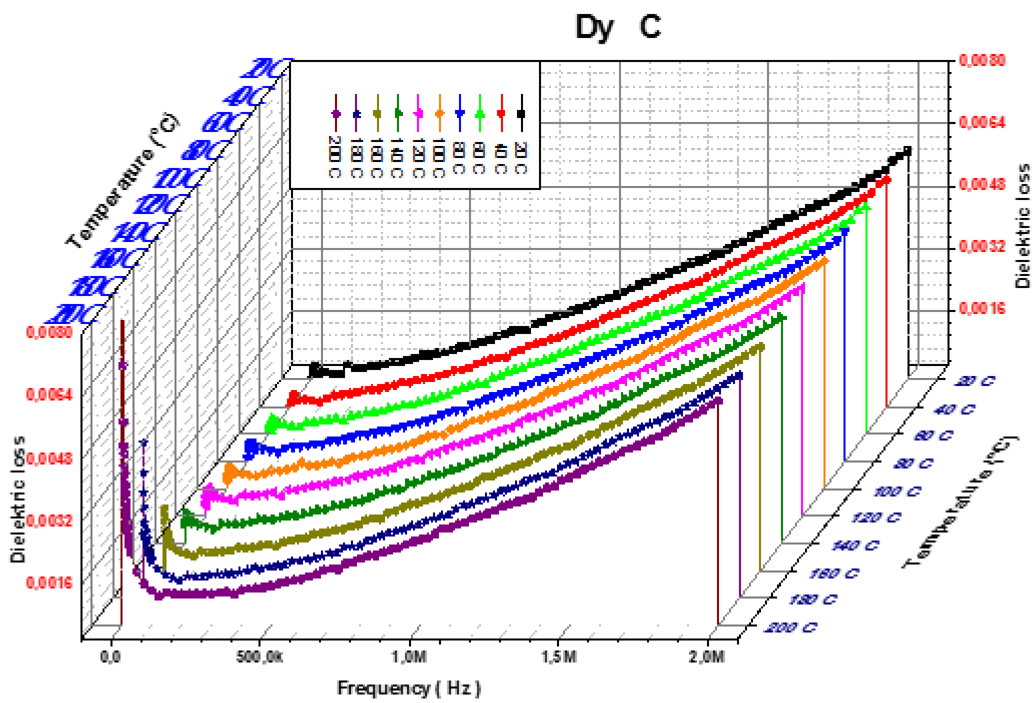

Figure IV.4b Variation of dielectric loss with frequency and temperature of Dy doped BZN irradiated with 10^{12} +6C (Dy C).

Dielectric loss measurement of both Dy B and Dy C indicated that loss values decreased at low frequencies between 10 kHz -100 kHz for the temperature range 20-200°C and then the loss values started to increase with frequency between 100 kHz-2 MHz (Figure IV.4c).

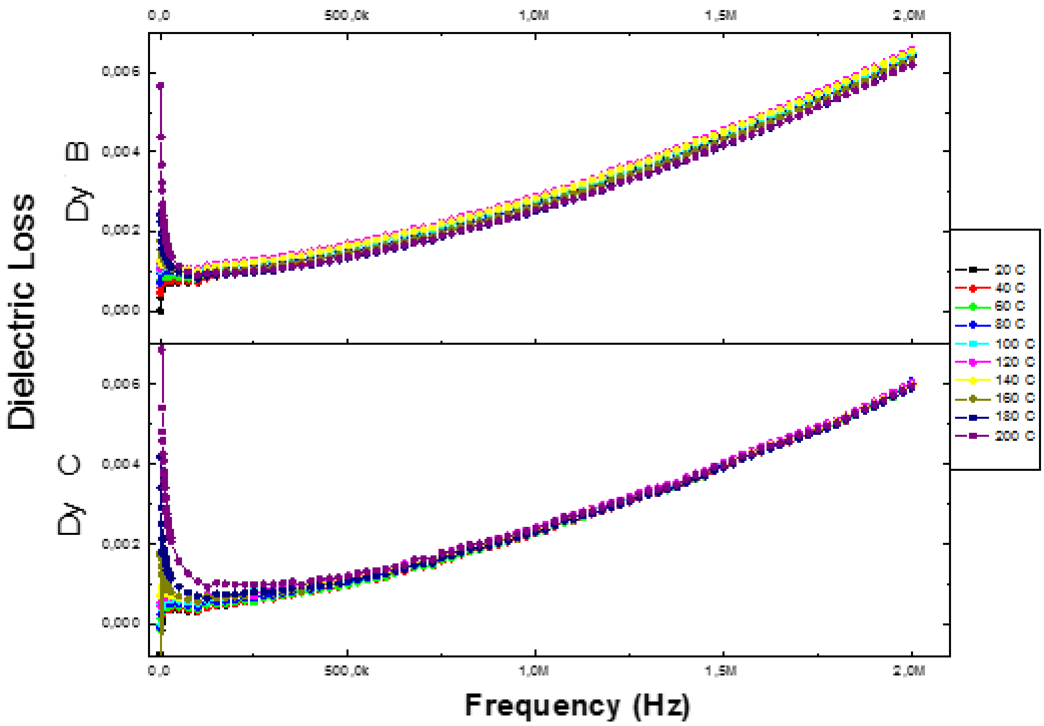

Figure IV.4c Variation of dielectric loss with frequency and temperature of Dy doped BZN irradiated with 10^{12} +6C and 10^{13} +6C (Dy C and Dy B).

Dielectric loss changes Dy dopet BZN after C^{+6} irradiation			
	10 KHz – 100 KHz (X 10^{-4})		
	40 ^{o}C	120 ^{o}C	200 ^{o}C
Dy B	4.54 – 7.31	10.67 – 10.51	56.61 – 9.00
Dy C	4.89 – 3.40	8.26 – 6.01	38.39 – 10.89
	100 KHz – 2 MHz (X 10^{-4})		
	40 ^{o}C	120 ^{o}C	200 ^{o}C
Dy B	7.31 – 63.71	10.51 – 65.77	9.00 – 61.85
Dy C	3.40 – 60.15	6.01 – 60.42	10.89 -59.61

Table IV.5 Dielectric loss values of Dy doped BZN irradiated with 10^{12} +6C (Dy C) and 10^{13} +6C (Dy B) fluences at different frequencies and temperatures.

IV.7.3 IRRADIATED Ta (X=0.3) DOPED BZN

IV.7.3.1 Dielectric Results

Dielectric constant values of Ta 03 A varied from 118 to 124 with respect to temperature and frequency changes. At room temperature dielectric values increased from 118 to 124 when frequency increased from 1 kHz to 2 MHz. With temperature increase dielectric constant value decreased to 111 and 117 at 200°C at 125 kHz and 2 MHz (Figure IV.5a and Table IV.6).

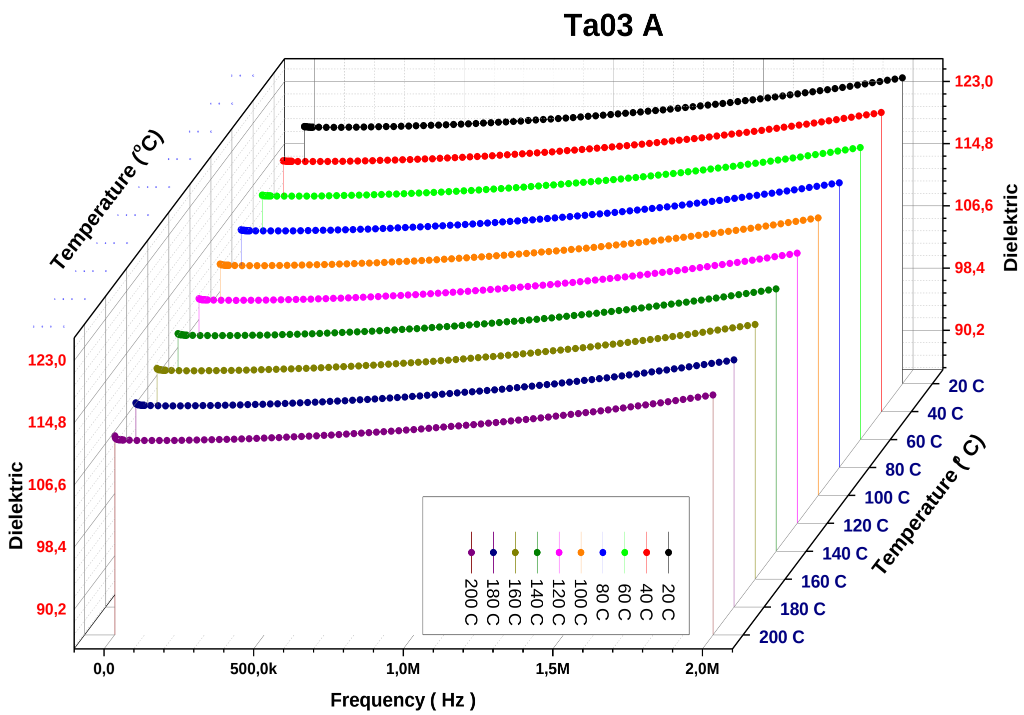

Figure IV.5a Variation of dielectric constant of Ta doped BZN irradiated with 10^{11} +6C (Ta A) with frequency and temperature

Dielectric values of Ta 03 B varied between 85 and 92 with respect to temperature and frequency. At room temperature dielectric constant increased from 92 to 97 when increasing the frequency from 1 kHz to 2 MHz. Increasing the temperature to 200°C decreased the dielectric value to 85 and 89 at 125 kHz and 2 MHz (Figure IV.5b and Table IV.6).

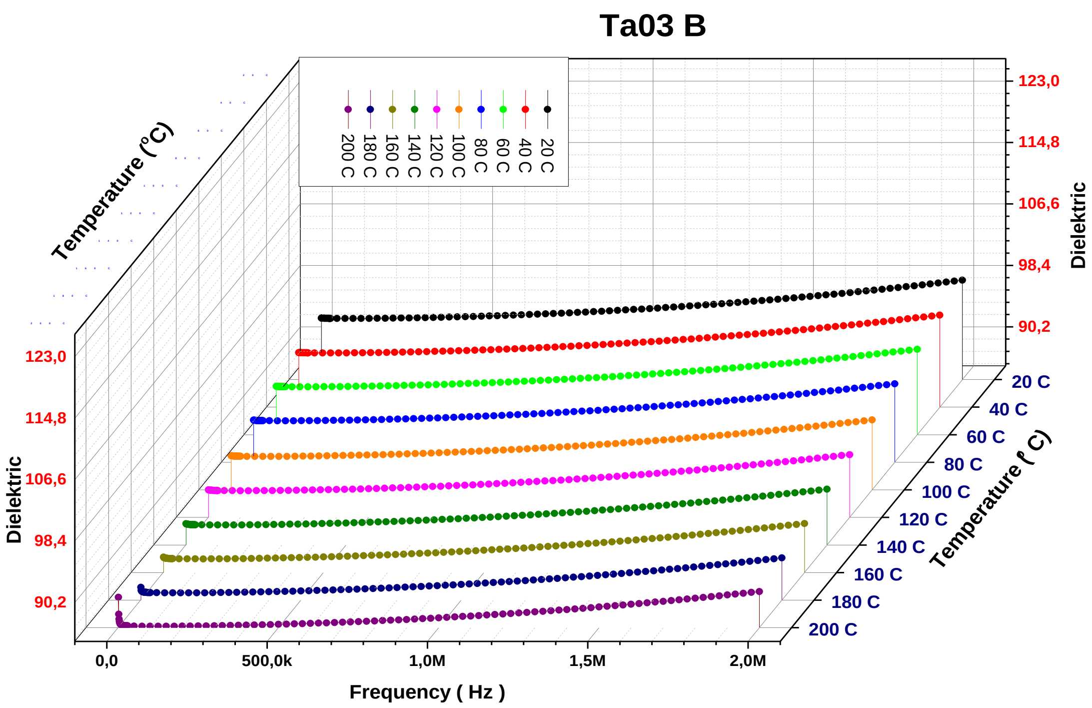

Figure IV.5b Variation of dielectric constant of Ta doped BZN irradiated with 10^{13} +6C (Ta B) with frequency and temperature

Dielectric constant values of Ta 03 C varied between 91 and 103 with respect to temperature and frequency. At room temperature dielectric constant increased from 98 to 104 when frequency increased from 1 kHz to 2 MHz. However, with temperature increase, dielectric constant decreased like at 1 kHz, decreasing from 98 at 40°C to 92 at 200°C o at 2 MHz, decreasing from 98 at 40°C to 97 at 200°C (Figure IV.5c and Table IV.6).

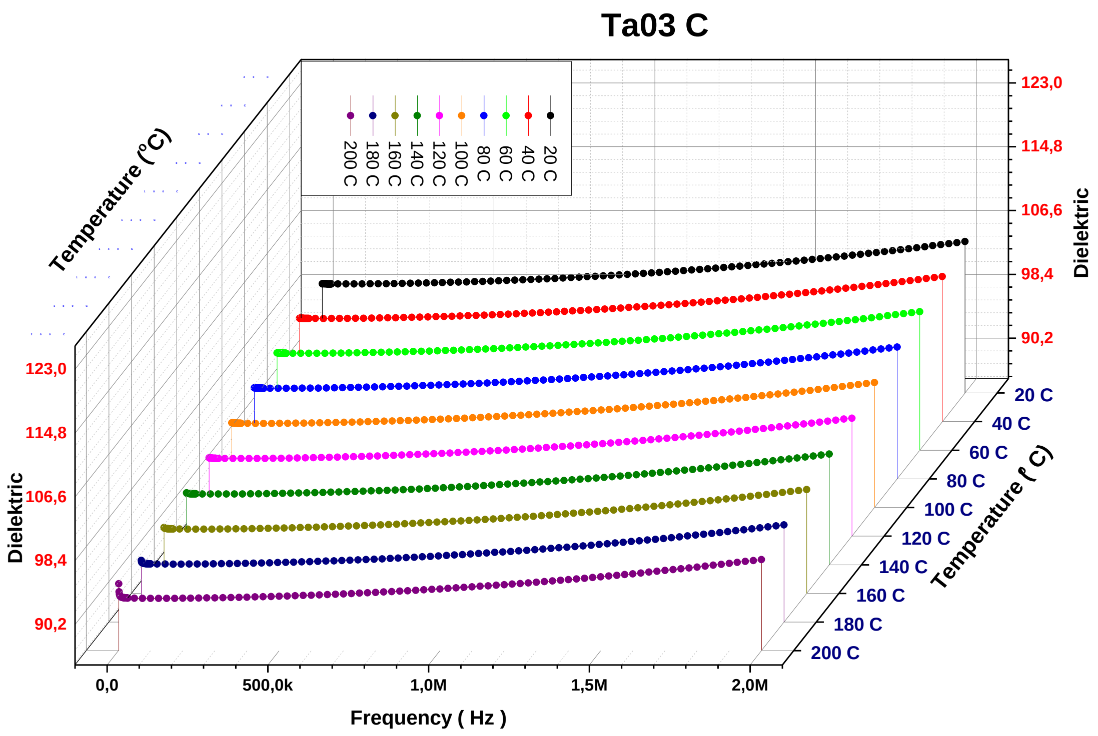

Figure IV.5c Variation of dielectric constant of Ta doped BZN irradiated with 10^{12} +6C (Ta C) with frequency and temperature

Dielectric measurements of Ta doped BZN samples indicated that although the dielectric constant values of Ta 03 A, Ta 03 B, and Ta 03 C samples did not change considerably with frequency at low frequency region between 1 kHz and 125 kHz for the temperature range of 20-200°C, the values increased with frequency above 125 kHz until 2 MHz**)** (Figure IV.5d and Table IV.6).

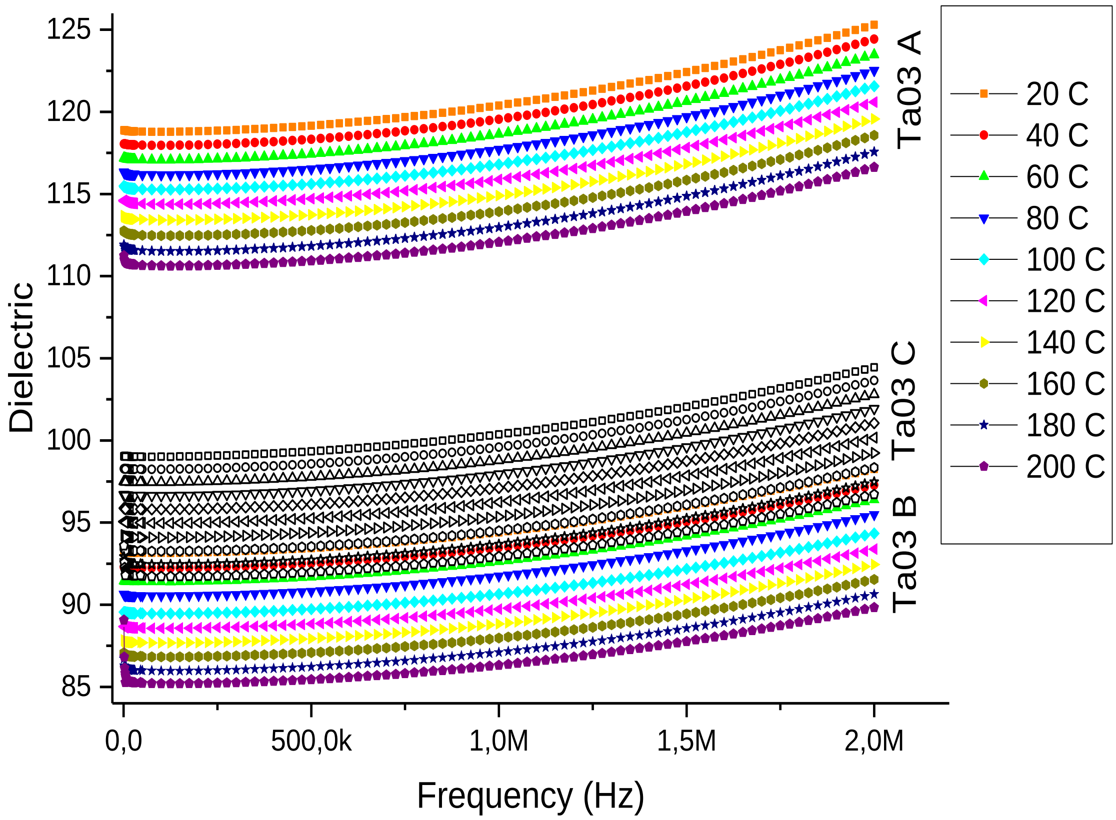

Figure IV.5d Variation of dielectric constant with frequency and temperature of Ta doped BZN irradiated with 10^{11} +6C, 10^{13} +6C and 10^{12} +6C (Ta A, Ta B and Ta C).

Dielectric changes Ta(x=0.3) doped BZN after C^{+6} irradiation			
	1 KHz – 125 KHz		
	40 °C	120 °C	200 °C
Ta A	118.05 – 117.96	114.61 – 114.38	111.24 – 110.62
Ta B	92.28 – 92.23	88.69 – 88.56	89.07 – 85.19
Ta C	98.28 – 98.24	95.07 – 94.97	93.60 – 91.72
	125 KHz – 2 MHz		
	40 °C	120 °C	200 °C
Ta A	117.96 – 124.43	114.38 – 120.59	110.62 – 116.63
Ta B	92.23 – 97.28	88.56 – 93.38	85.19 – 89.83
Ta C	98.24 – 103.64	94.97 – 100.16	91.72 – 96.72

Table IV.6 Dielectric constant values of Ta doped BZN irradiated with 10^{11} +6C (Ta A), 10^{13} +6C (Ta B) and 10^{12} +6C (Ta C) fluences at different frequencies and temperatures.

IV.7.3.2 Dielectric Loss Results

Dielectric loss values of Ta 03 A increased from 4.22 to 62.69 (x 10^{-4}) with respect to temperature and frequency. While at room temperature, dielectric loss values increased from 4.22 to 59.33 (x 10^{-4}), at 200°C dielectric loss values increased from 19.83 to 62.69 (x 10^{-4}) when frequency increased from 1 kHz to 2 MHz. However, when the loss values were examined in detail it can be seen that the dielectric loss values decreased from 4.22 to 3.56 (x 10^{-4}) at lower frequency range between 1 kHz-100 kHz at room temperature but loss values increased with frequency above 100 kHz until 2 MHz from 3.56 to 59.33 (x 10^{-4}). Identical behavior was also observed above room temperature up to 200°C (Figure IV.6a and Table IV.7).

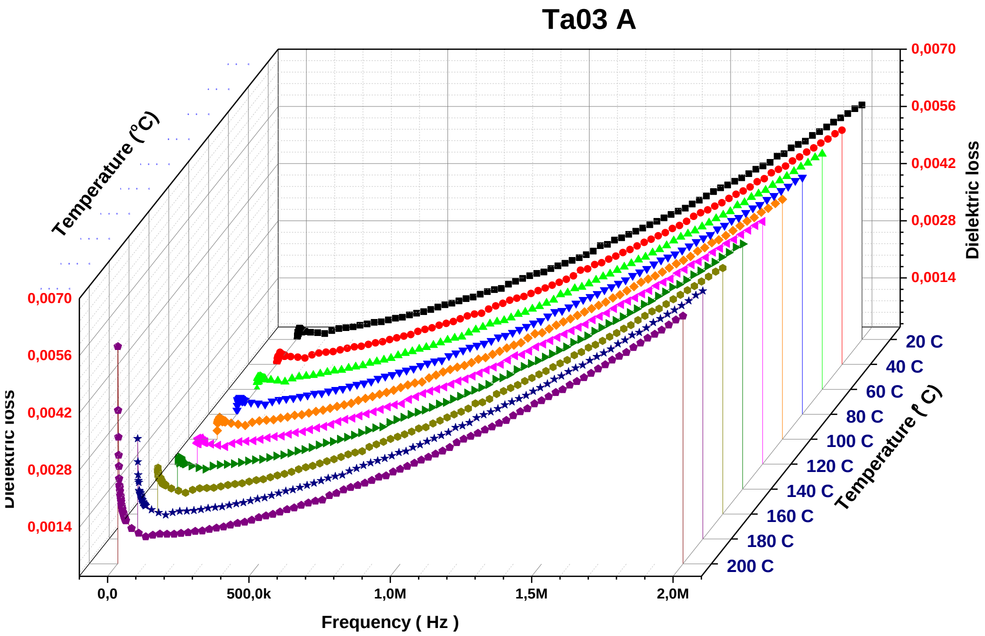

Figure IV.6a Variation of dielectric loss of Ta doped BZN irradiated with 10^{11} +6C (Ta A) with frequency and temperature

Dielectric loss values of Ta 03 B increased from 3.38 to 62.89 (x 10^{-4}) with respect to temperature and frequency. While at room temperature, dielectric loss values increased from 3.38 to 58.66 (x 10^{-4}), at 200°C dielectric loss values decreased from 195.95 to 62.89 (x 10^{-4}) when frequency increased from 1 kHz to 2 MHz. However, when the loss values were examined in detail it can be seen that the dielectric loss values decreased from 3.38 to 2.74 (x 10^{-4}) at lower frequency range between 1 kHz-100 kHz at room temperature but loss values increased with frequency above 100 kHz until 2 MHz from 2.74 to 58.66 (x 10^{-4}). Identical behavior was also observed above room temperature up to 200°C (Figure IV.6b and Table IV.7).

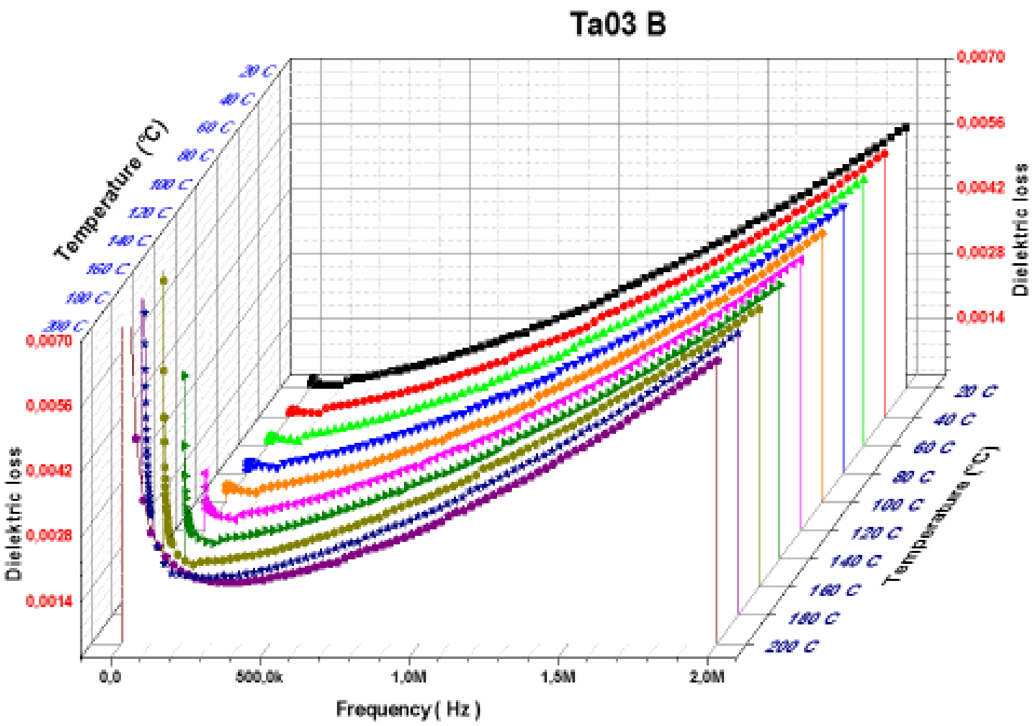

Figure IV.6b Variation of dielectric loss of Ta doped BZN irradiated with 10^{13} +6C (Ta B) with frequency and temperature

Dielectric loss values of Ta 03 C increased from 2.95 to 60.61 (x 10^{-4}) with respect to temperature and frequency. While at room temperature, dielectric loss values increased from 2.95 to 57.59 (x 10^{-4}), at 200°C dielectric loss values decreased from 70.33 to 60.61 (x 10^{-4}) when frequency increased from 1 kHz to 2 MHz. However, when the loss values were examined in detail it can be seen that the dielectric loss values decreased from 2.95 to 1.6 (x 10^{-4}) at lower frequency range between 1 kHz-100 kHz at room temperature but loss values increased with frequency above 100 kHz until 2 MHz from 1.6 to 57.59 (x 10^{-4}). Identical behavior was also observed above room temperature up to 200°C (Figure IV.6b and Table IV.7).

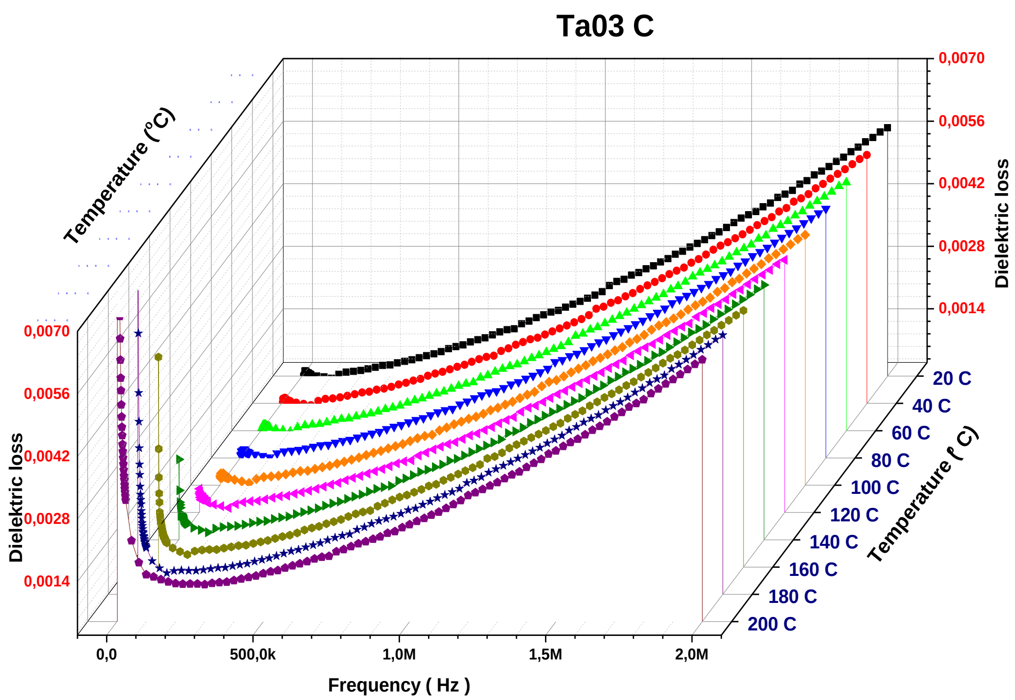

Figure IV.6c Variation of dielectric loss of Ta doped BZN irradiated with 10^{12} +6C (Ta C) with frequency and temperature

Dielectric loss measurement of Ta 03 samples showed that the dielectric loss values of Ta 03 A, Ta 03 B, and Ta 03 C decreased at low frequency range between 1 kHz - 100 kHz interval for the temperature range between 20-200°C. However, when frequency increased above 100 kHz, the loss values started to increase with frequency until 2 MHz (Figure IV.6d and Table IV.7).

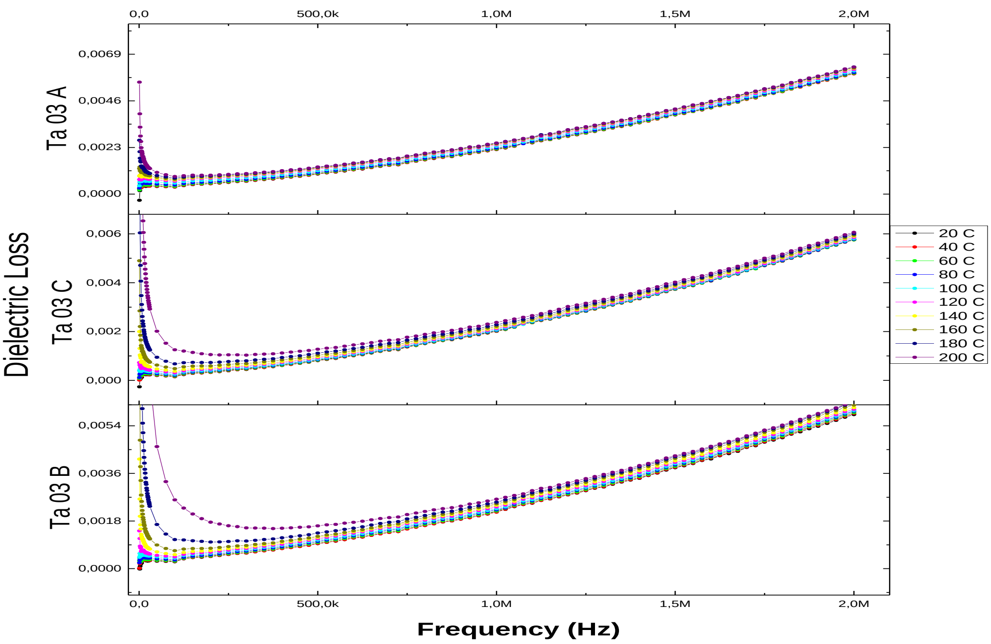

Figure IV.6d Variation of dielectric loss with frequency and temperature of Ta doped BZN irradiated with 10^{11} +6C, 10^{13} +6C and 10^{12} +6C (Ta A, Ta B and Ta C).

Dielectric loss changes Ta(x=0.3) dopet BZN after C^{+6} irradiation			
	10 KHz – 100 KHz (X 10^{-4})		
	40 °C	120 °C	200 °C
Ta A	4.22 – 3.56	7.92 – 6.29	19.83 -8.68
Ta B	3.38 – 2.74	6.89 – 4.41	195.95 – 25.99
Ta C	2.95 – 1.6	5.33 – 3.04	70.33 – 12.53
	100 KHz – 2 MHz (X 10^{-4})		
	40 °C	120 °C	200 °C
Ta A	3.56 – 59.33	6.29 – 61.39	8.68 – 62.69
Ta B	2.74 – 58.66	4.41 – 60.17	25.99 – 62.89
Ta C	1.6 – 57.59	3.04 – 58.51	12.53 – 60.61

Table IV.7 Dielectric loss values of Ta doped BZN irradiated with 10^{11} +6C (Ta A), 10^{13} +6C (Ta B) and 10^{12} +6C (Ta C) fluences at different frequencies and temperatures.

IV.7.4 IRRADIATED Ta (X=1.0) DOPED BZN

IV.7.4.1 Dielectric Results

Dielectric constant values of Ta A increased from 79 to 80 with respect to temperature and frequency changes. At room temperature dielectric values increased from 79 to 84 when frequency increased from 1 kHz to 2 MHz. With temperature increase dielectric constant values were 79 and 80 at 200°C at 125 kHz and 2 MHz (Figure IV.7a and Table IV.7).

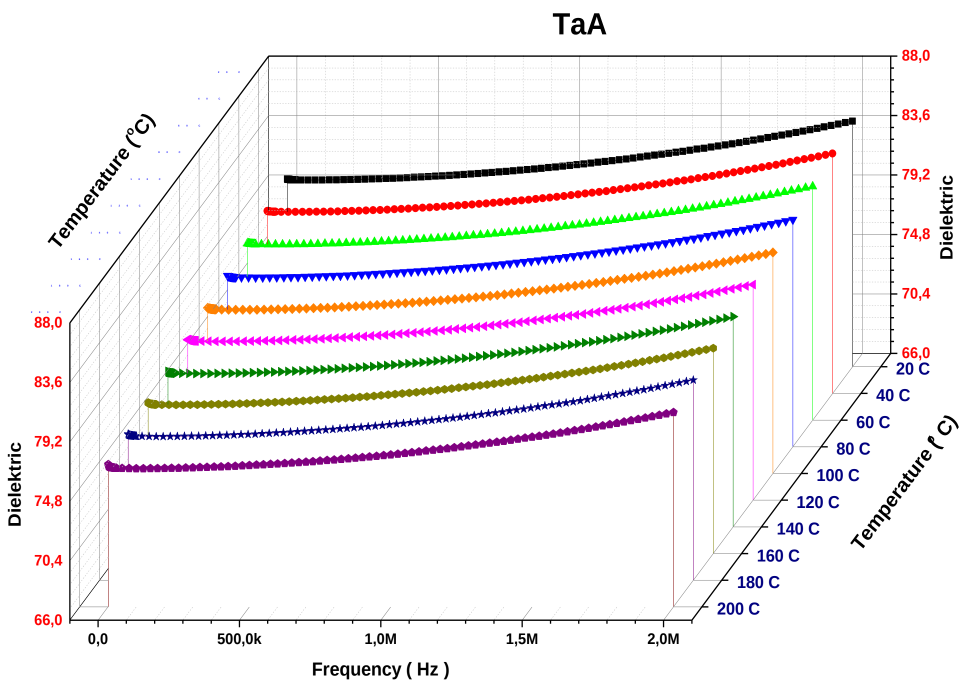

Figure IV.7a Variation of dielectric constant of Ta doped BZN irradiated with 10^{11} +6C (Ta A) with frequency and temperature

Dielectric constant values of Ta B increased from 70 to 71 with respect to temperature and frequency changes. At room temperature dielectric values increased from 71 to 75 when frequency increased from 1 kHz to 2 MHz. With temperature increase dielectric constant values decreased to 67 and 71 at 200°C at 125 kHz and 2 MHz (Figure IV.7b and Table IV.7).

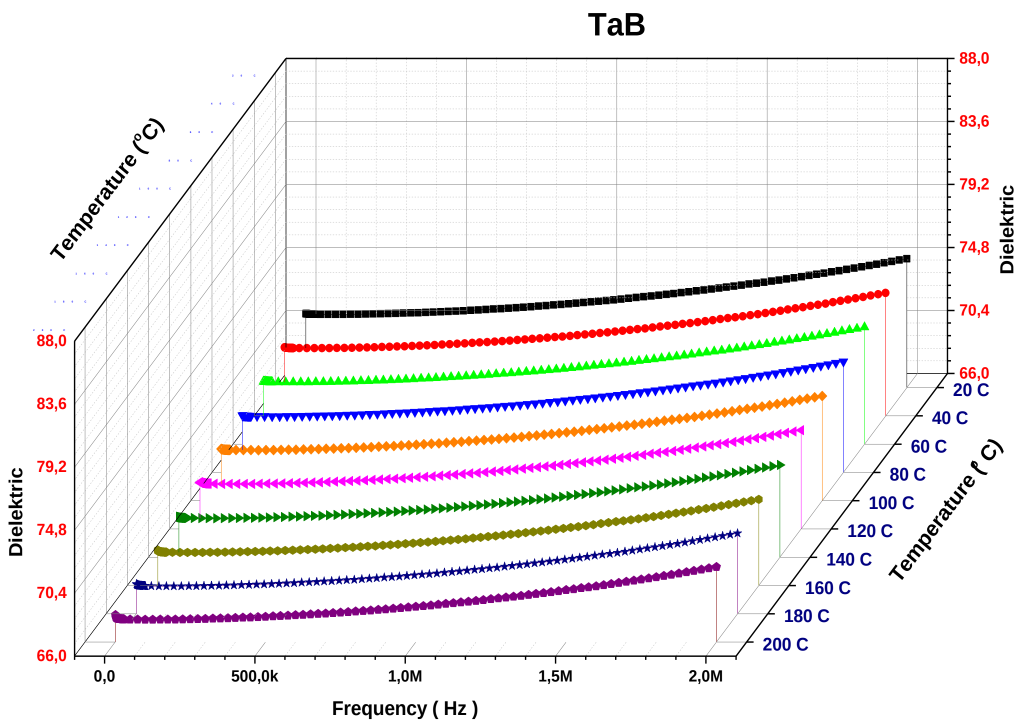

Figure IV.7b Variation of dielectric constant of Ta doped BZN irradiated with 10^{13} +6C (Ta B) with frequency and temperature

Dielectric constant values of Ta C had identical values of 75 at room temperature at 1 kHz and at 200°C at 2 MHz. At room temperature dielectric values increased from 75 to 79 when frequency increased from 1 kHz to 2 MHz. With temperature increase dielectric constant values decreased to 71 at 125 kHz but at same temperature when increasing the frequency to 2MHz, the dielectric constant reached to 75 again (Figure IV.7b and Table IV.8).

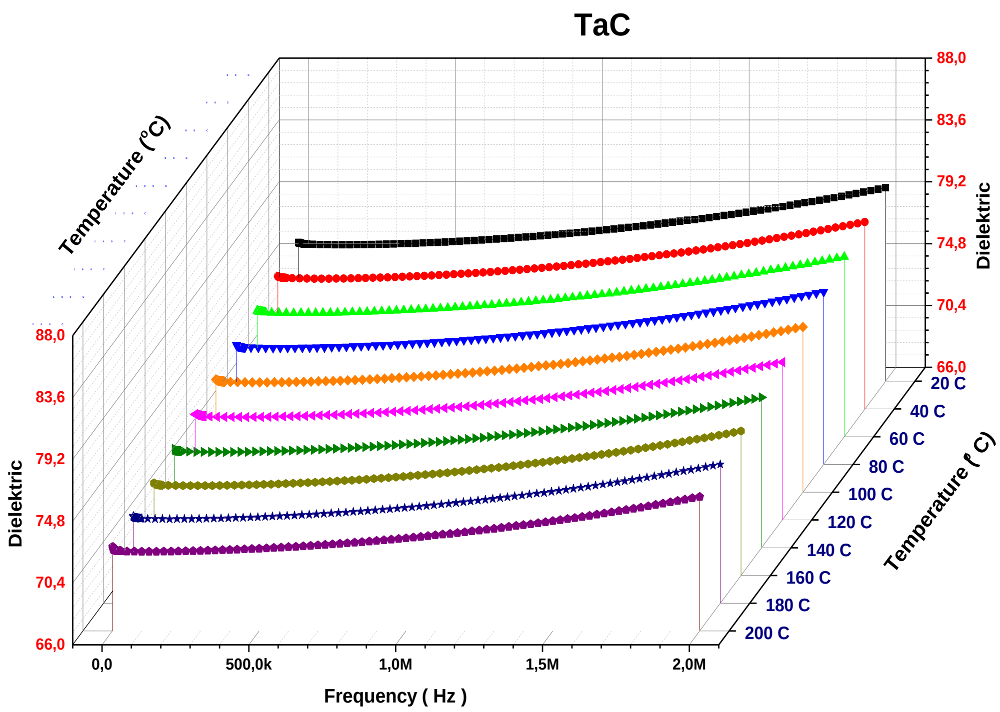

Figure IV.7c Variation of dielectric constant of Ta doped BZN irradiated with 10^{12} +6C (Ta C) with frequency and temperature

Dielectric measurements of Ta doped BZN samples indicated that although the dielectric constant values of Ta 03 A, Ta 03 B, and Ta 03 C samples were nearly stable with frequency at low frequency region between 1 kHz and 125 kHz for the temperature range of 20-200°C, the values increased with frequency above 125 kHz until 2 MHz**)** (Figure IV.7d and Table IV.7).

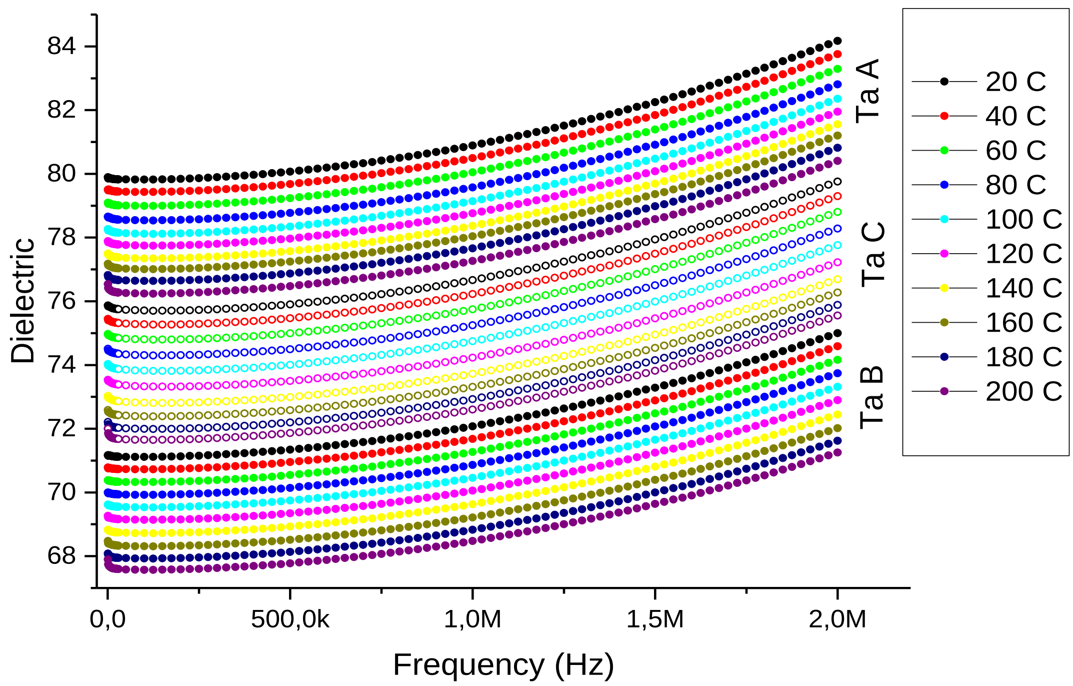

Figure IV.7d Variation of dielectric constant with frequency and temperature of Ta doped BZN (x=1.0) irradiated with 10^{11} +6C, 10^{13} +6C and 10^{12} +6C (Ta A, Ta B and Ta C).

Dielectric changes Ta(x=1) dopet BZN after C^{+6} irradiation			
	1 KHz – 125 KHz		
	40 ^{o}C	120 ^{o}C	200 ^{o}C
Ta A	79.51 – 79.43	77.89 – 77.74	76.54 – 79.24
Ta B	70.78 – 70.73	69.27 – 69.14	67.90 – 67.57
Ta C	75.45 – 75.27	73.53 – 73.32	72.00 – 71.65
	125 KHz – 2 MHz		
	40 ^{o}C	120 ^{o}C	200 ^{o}C
Ta A	79.43 – 83.76	77.74 – 81.95	79.24 – 80.40
Ta B	70.73 – 74.59	69.14 – 72.90	67.57 – 71.25
Ta C	75.27 – 79.30	73.32 – 77.22	71.65 – 75.55

Table IV.8 Dielectric constant values of Ta doped BZN (x=1.0) irradiated with 10^{11} +6C (Ta A), 10^{13} +6C (Ta B) and 10^{12} +6C (Ta C) fluences at different frequencies and temperatures.

IV.7.4.2 Dielectric Loss Results

Dielectric loss values of Ta A increased from 5.26 to 59.25 (x 10^{-4}) with respect to temperature and frequency. While at room temperature, dielectric loss values increased from 5.26 to 60.29 (x 10^{-4}), at 200°C dielectric loss values decreased from 43.65 to 59.25 (x 10^{-4}) when frequency increased from 1 kHz to 2 MHz. However, when the loss values were examined in detail it can be seen that the dielectric loss values decreased from 5.26 to 3.53 (x 10^{-4}) at lower frequency range between 1 kHz-100 kHz at room temperature but loss values increased with frequency above 100 kHz until 2 MHz from 3.53 to 60.29 (x 10^{-4}). Identical behavior was also observed above room temperature up to 200°C (Figure IV.8a and Table IV.9).

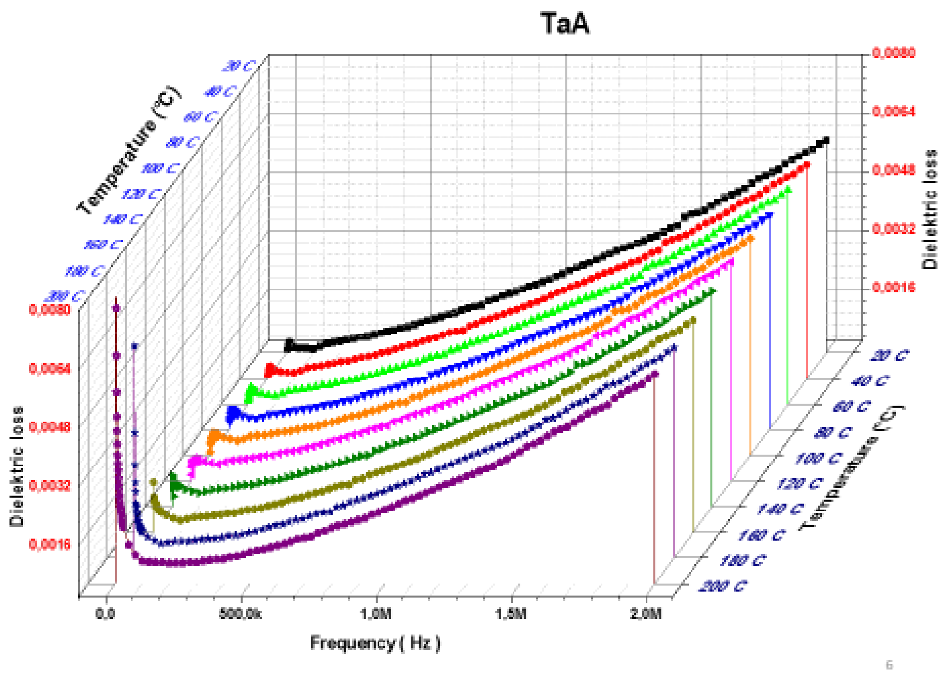

Figure IV.8a Variation of dielectric loss of Ta doped BZN (x=1.0) irradiated with 10^{11} +6C (Ta A) with frequency and temperature

Dielectric loss values of Ta B increased from 3.48 to 59.68 (x 10^{-4}) with respect to temperature and frequency. While at room temperature, dielectric loss values increased from 3.48 to 58.23 (x 10^{-4}), at 200°C dielectric loss values decreased from 24.15 to 59.68 (x 10^{-4}) when frequency increased from 1 kHz to 2 MHz. However, when the loss values were examined in detail it can be seen that the dielectric loss values decreased from 3.48 to 2.66 (x 10^{-4}) at lower frequency range between 1 kHz-100 kHz at room temperature but loss values increased with frequency above 100 kHz until 2 MHz from 2.66 to 58.33 (x 10^{-4}). Identical behavior was also observed above room temperature up to 200°C (Figure IV.8b and Table IV.9).

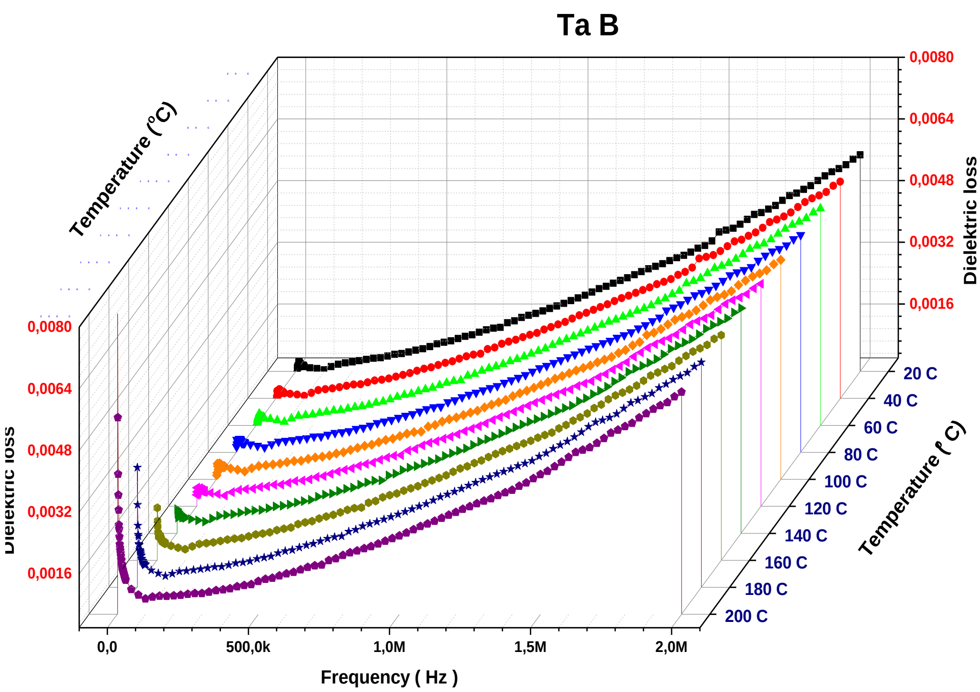

Figure IV.8b Variation of dielectric loss of Ta doped BZN (x=1.0) irradiated with 10^{13} +6C (Ta B) with frequency and temperature

Dielectric loss values of Ta C increased from 7.99 to 60.47 (x 10^{-4}) with respect to temperature and frequency. While at room temperature, dielectric loss values increased from 7.99 to 63.28 (x 10^{-4}), at 200°C dielectric loss values decreased from 38.7 to 60.47 (x 10^{-4}) when frequency increased from 1 kHz to 2 MHz. However, although below 120°C, dielectric loss values increased gradually with frequency between 1 kHz-2 MHz, above 120°C the loss values decreased between 1 kHz-100kHz but increased above 100 kHz up to 2 MHz with frequency (Figure IV.8c and Table IV.9).

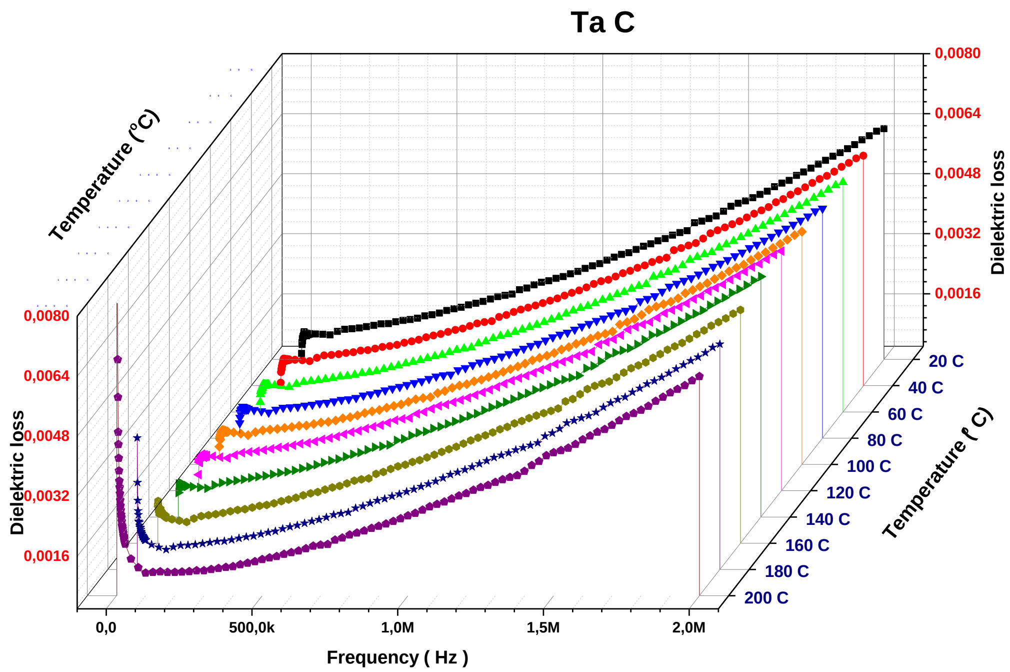

Figure IV.8c Variation of dielectric loss of Ta doped BZN (x=1.0) irradiated with 10^{12} +6C (Ta C) with frequency and temperature

Dielectric measurements of Ta doped BZN samples indicated that although the dielectric loss values of Ta A and Ta B decreased with frequency at low frequency region of 8 kHz -100 kHz between 20-200°C, dielectric loss value of Ta C sample increased with frequency at the same frequency and temperature ranges. However, above 100 kHz, all the samples of Ta A, Ta B and Ta C indicated same behavior that the loss values increased with frequency between 20-200°C (Figure IV.8d and Table IV.9).

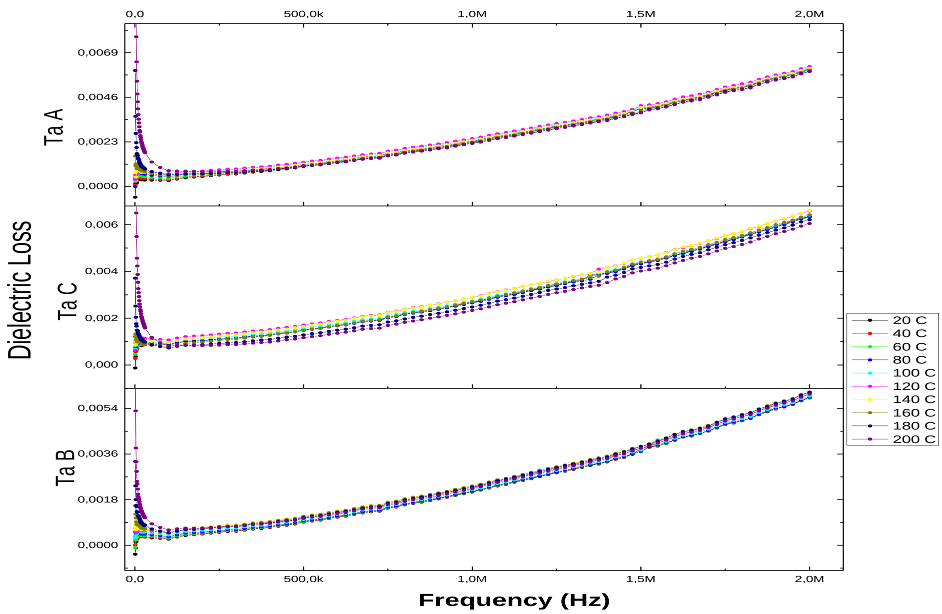

Figure IV.8d Variation of dielectric loss with frequency and temperature of Ta doped BZN (x=1.0) irradiated with 10^{11} +6C, 10^{13} +6C and 10^{12} +6C (Ta A, Ta B and Ta C).

Dielectric loss changes Ta(x=1) dopet BZN after C^{+6} irradiation			
	8 KHz – 100 KHz (X 10^{-4})		
	40 °C	120 °C	200 °C
Ta A	5.26 - - 3.53	7.46 – 6.58	43.65 – 8.15
Ta B	3.48 – 2.66	5.69 – 4.8	24.15 -6.04
Ta C	7.99 -8.54	11.21 – 10.68	38.7 -8.09
	100 KHz – 2 MHz (X 10^{-4})		
	40 °C	120 °C	200 °C
Ta A	3.53 – 60.29	6.58 – 61.83	8.15 – 59.25
Ta B	2.66 – 58.23	4.8 – 59.73	6.04 – 59.68
Ta C	8.54 – 63.28	10.68 – 65.85	8.09 – 60.47

Table IV.9 Dielectric loss values of Ta doped BZN (x=1.0) irradiated with 10^{11} +6C (Ta A), 10^{13} +6C (Ta B) and 10^{12} +6C (Ta C) fluences at different frequencies and temperatures.

IV.7.5 IRRADIATED Yb DOPED BZN

IV.7.5.1 Dielectric Results

Dielectric constant values of Yb A decreased from 118 to 112 with respect to temperature and frequency. When frequency increased from 1 kHz to 2 MHz, dielectric constants increased from 118 to 124 at room temperature and increased from 107 to 112 at 200°C. However, the detailed examination of dielectric constant changes with frequency indicated that while dielectric values decreased from 118 to 117 at frequency range of 1 kHz and 125 kHz, they increased from 117 to 124 above 125 kHz until 2 MHz. Same kind of behavior was also observed at high temperatures that dielectric constants decreased from 107 to 106 between 1 kHz-125 kHz but they started to increase above 125 kHz, from 106 to 112 at 2 MHz (Figure IV.9a and Table IV.10).

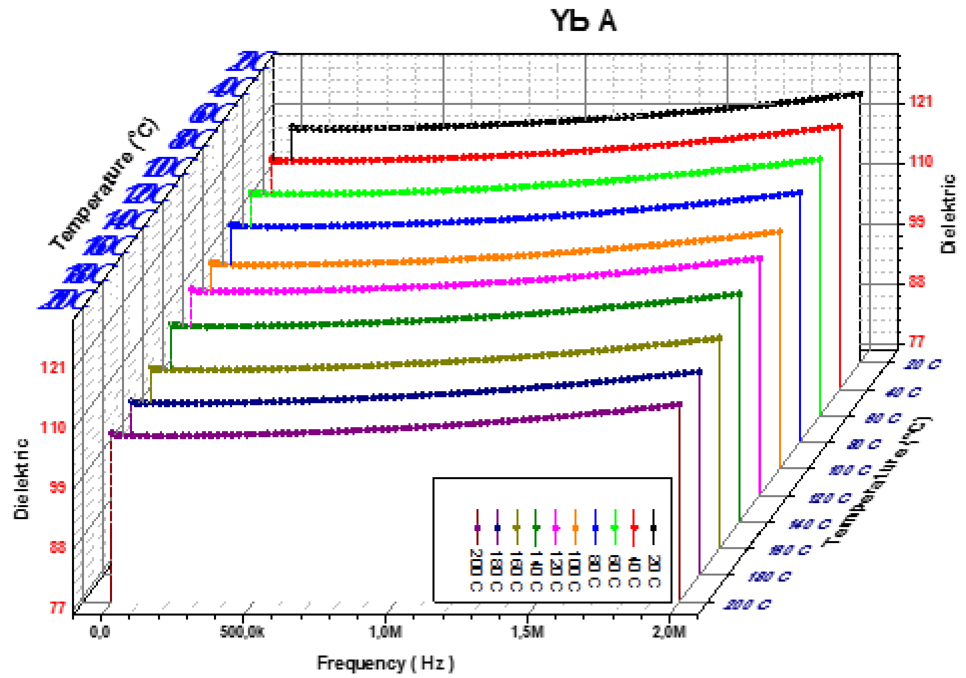

Figure IV.9a Variation of dielectric constant with frequency and temperature of Yb doped BZN irradiated with 10^{11} +6C (Yb A).

Dielectric constant values of Yb B decreased from 82 to 80 with respect to temperature and frequency. When frequency increased from 1 kHz to 2 MHz, dielectric constants increased from 82 to 87 at room temperature and increased from 77 to 80 at 200°C. However, the detailed examination of dielectric constant changes with frequency indicated that while dielectric values decreased from 82 to 81 at frequency range of 1 kHz and 175 kHz, they increased from 81 to 87 above 125 kHz until 2 MHz. Same kind of behavior was also observed at high temperatures that dielectric constants decreased from 77 to 76 between 1 kHz-175 kHz but they started to increase above 125 kHz, from 76 to 80 at 2 MHz (Figure IV.9b and Table IV.10).

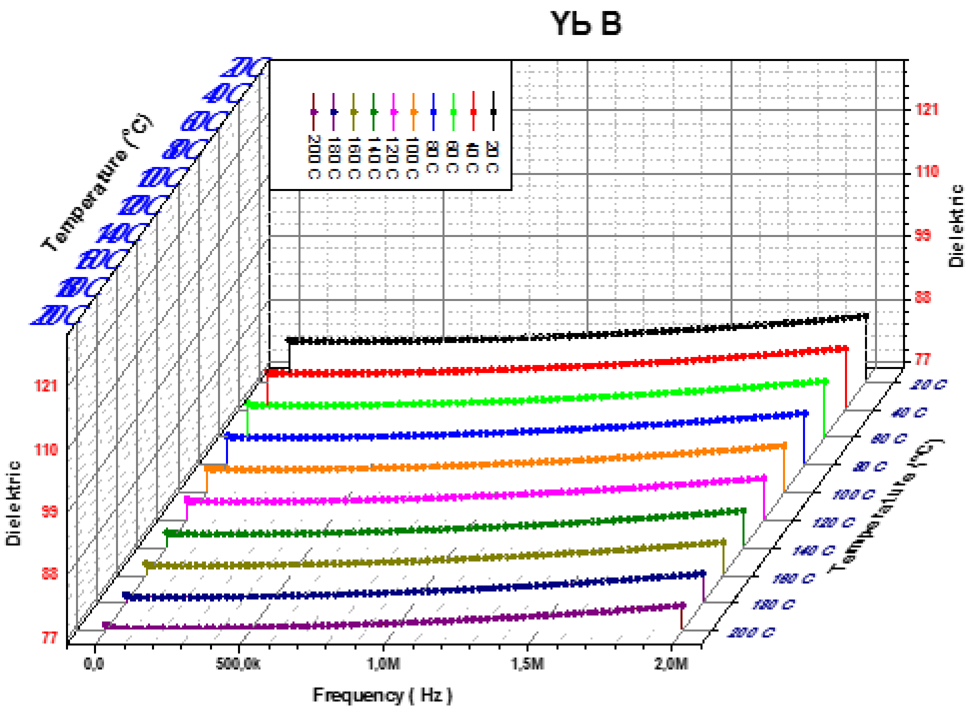

Figure IV.9b Variation of dielectric constant with frequency and temperature of Yb doped BZN irradiated with 10^{13} +6C (Yb B).

Dielectric measurements of Yb doped BZN samples indicated that although the dielectric constant values of Yb A and Yb B samples decreased with frequency at low frequency region between 1 kHz and 125 kHz and 1 kHz and 175 kHz for the temperature range of 20-200°C, the values increased with frequency above 125 and 175 kHz until 2 MHz (Figure IV.9c and Table IV.10).

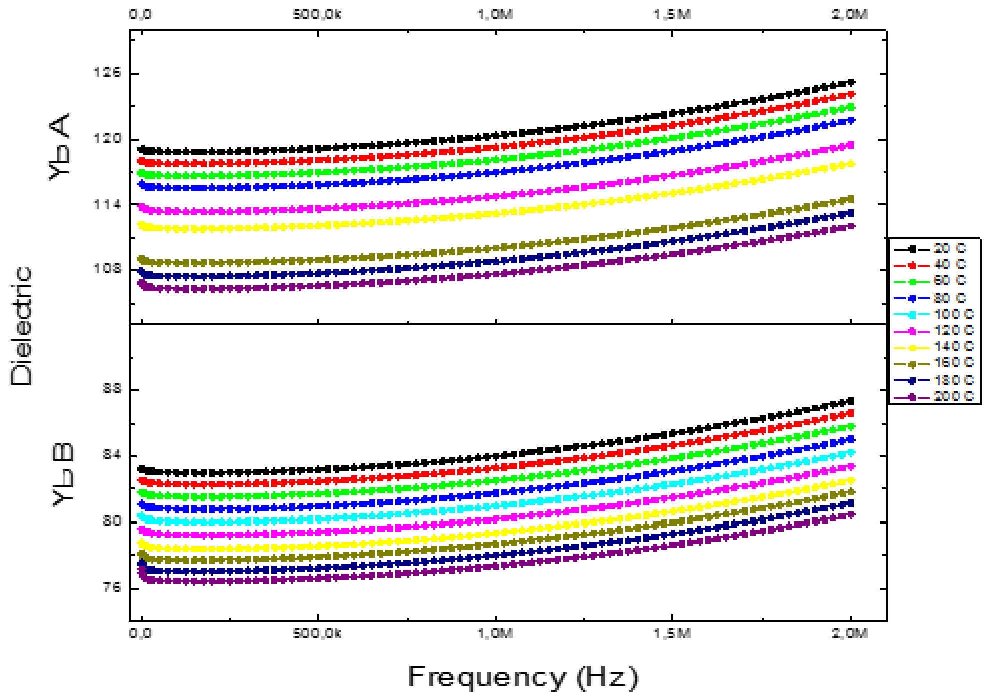

Figure IV.9c Variation of dielectric constant with frequency and temperature of Yb doped BZN irradiated with 10^{11} +6C and 10^{13} +6C (Ta A and Ta B).

Dielectric changes Yb(x=0.04) dopet BZN after C^{+6} irradiation			
	1 KHz – 125 KHz Yb A 1 KHz – 175 KHz Yb B		
	40 ^{o}C	120 ^{o}C	200 ^{o}C
Yb A	118.02 – 117.76	113.84 - 113.37	106.92 -106.30
Yb B	81.82 – 81.53	79.62 – 79.24	77.17 – 76.43
	125 KHz – 2 MHz Yb A 175 KHz – 2 MHz Yb B		
	40 ^{o}C	120 ^{o}C	200 ^{o}C
Yb A	117.76 – 124.09	113.37 – 119.45	106.30 – 112.04
Yb B	81.53 – 86.63	79.24 – 83.39	76.43 – 80.46

Table IV.10 Dielectric constant values of Yb doped BZN irradiated with 10^{11} +6C (Ta A) fluence at different frequencies and temperatures.

IV.7.5.2 Dielectric Loss Results

Dielectric loss values of Yb A increased from 4.99 to 66.52 (x 10^{-4}) with respect to temperature and frequency. While at room temperature, dielectric loss values increased from 4.99 to 68.08 (x 10^{-4}), at 200°C dielectric loss values decreased from 79.63 to 66.52 (x 10^{-4}) when frequency increased from 1 kHz to 2 MHz. However, although at and below 120°C, dielectric loss values increased with frequency between 1 kHz-2 MHz, above 120°C the loss values decreased between 1 kHz-2 MHz (Figure IV.10a and Table IV.11).

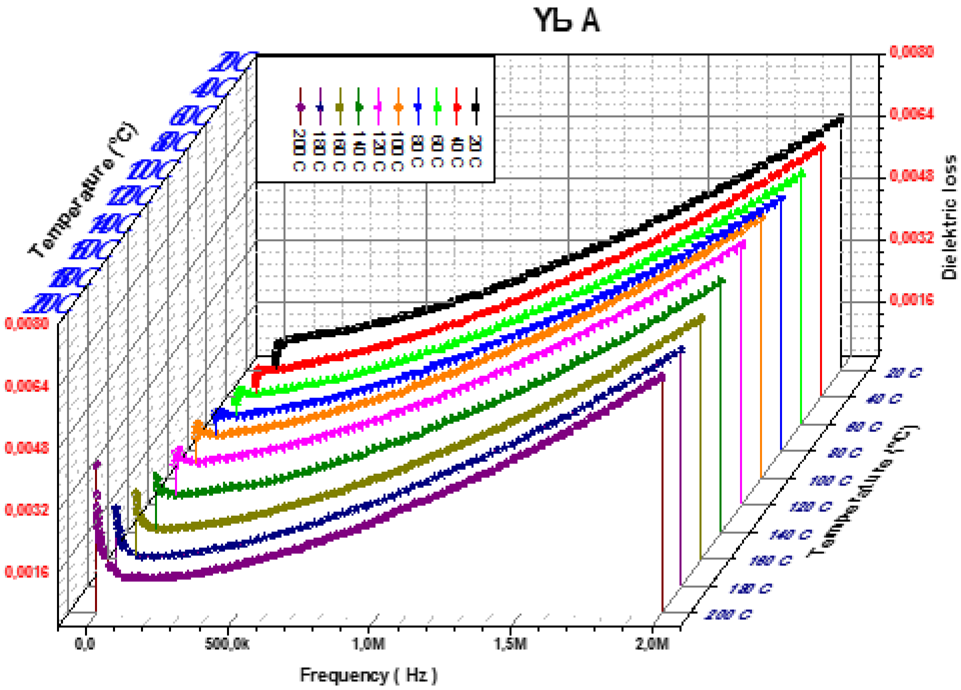

Figure IV.10a Variation of dielectric loss of Yb doped BZN irradiated with 10^{11} +6C (Yb A) with frequency and temperature

Dielectric loss values of Yb B increased from 5.21 to 63.28 (x 10^{-4}) with respect to temperature and frequency. While at room temperature, dielectric loss values increased from 5.21 to 66.51 (x 10^{-4}), at 200°C dielectric loss values increased from 40.42 to 63.28 (x 10^{-4}) when frequency increased from 1 kHz to 2 MHz. In addition, although dielectric loss values decreased from 40.42 to 11.44 (x 10^{-4}) at low frequency region of 1-250 kHz, they started to increase with frequency above 250 kHz up to 2 MHz reaching a value of 63.28 (x 10^{-4}) (Figure IV.10b and Table IV.11).

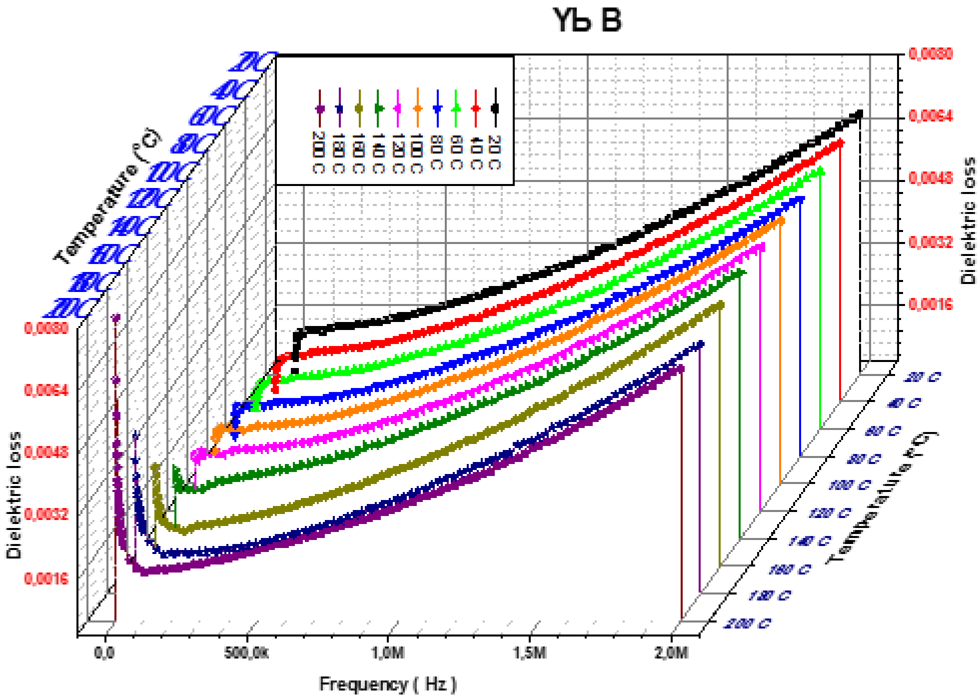

Figure IV.10b Variation of dielectric loss of Yb doped BZN irradiated with 10^{13} +6C (Yb B) with frequency and temperature

Dielectric measurements of Yb doped BZN samples indicated that dielectric loss values of Yb A increased with frequency between 1 kHz-2 MHz. However, dielectric loss of Yb B sample decreased at low frequency range of 1 kHz - 250 K Hz but then it started to increase with frequency above 250 kHz until 2 MHz reaching a value of 63.28 (x 10^{-4}) (Figure IV.10c and Table IV.11).

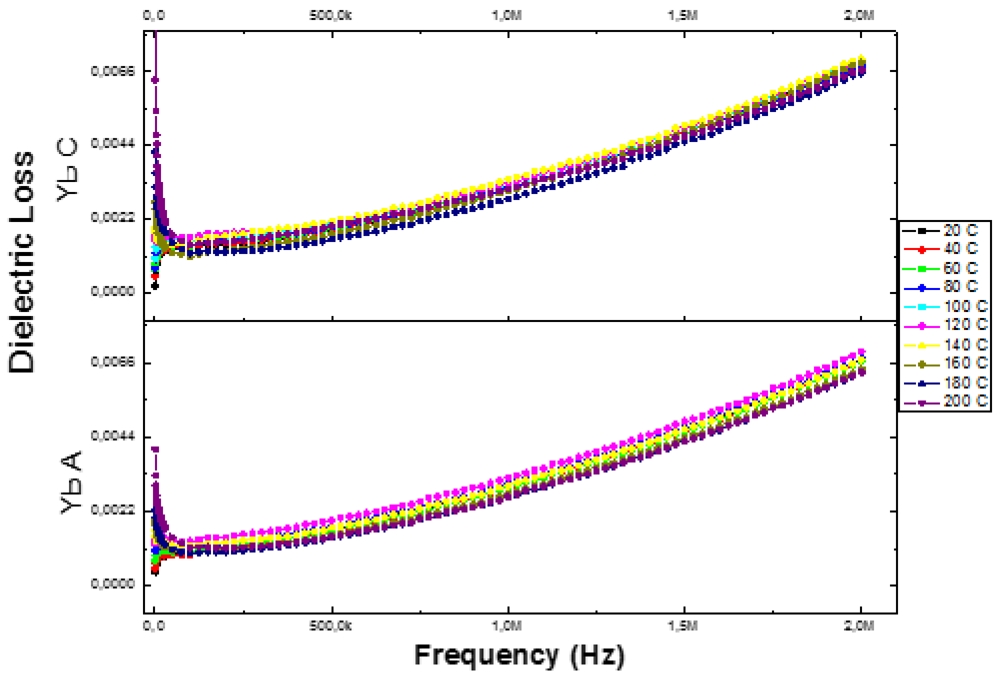

Figure IV.10c Variation of dielectric loss with frequency and temperature of Yb doped BZN irradiated with 10^{11} +6C and 10^{13} +6C (Ta A and Ta B).

Dielectric Loss changes Yb(x=0.04) dopet BZN after C^{+6} irradiation			
	1 KHz – 2 MHz (X 10^{-4})		
	40 °C	120 °C	200 °C
Yb A	4.99 – 68.08	16.78 – 69.63	79.63 – 66.52
Yb B	5.21 – 66.51	12.51 – 69.44	40.42 – 11.44 (1-250 khz)
			11.44 – 63.28 (0.25-2 Mhz

Table IV.11 Dielectric loss values of Yb doped BZN irradiated with 10^{11} +6C (Yb A) and 10^{13} +6C (Yb B) fluences at different frequencies and temperatures.

CHAPTER V

CONCLUDING REMARKS AND RECOMMENDATIONS

In the content of this study, effect of irradiation on the dielectric properties of Eu, Dy, Ta and Yb doped $Bi_{1.5}Zn_{0.92}Nb_{1.5}O_{6.92}$ (BZN) composition was studied. Eu, Dy, Ta and Yb doped $Bi_{1.5}Zn_{0.92}Nb_{1.5}O_{6.92}$ pyrochlore put under three different dose of C^{6+} irradiation (1 x 10^{11}, 1 x 10^{12} and 1 x 10^{13}). The conclusions are given below:

- Eu (x=0.12), Dy (x=0.04), Ta (x=0.3 and x=1) and Yb (x=0.04) doped compositions were produced using mixed oxide technique using the chemical compositions of $Bi_{1.5-x}Eu_xZn_{0.92}Nb_{1.5}O_{6.92}$, $Bi_{1.5-x}Dy_xZn_{0.92}Nb_{1.5}O_{6.92}$, $Bi_{1.5}Zn_{0.92}Ta_xNb_{1.5-x}O_{6.92}$,and $(Bi_{1.5-x/3}Zn_{0.46-x}Yb_x)(Zn_{0.46}Nb_{1.5})O_{6.92}$.
- XRD and SEM results indicated that Eu (x=0.12), Dy (x=0.04), Ta (x=0.3 and x=1) and Yb (x=0.04) doped compositions gave only single phase pyrochlore ($Bi_{1.38}Eu_{0.12}Zn_{0.92}Nb_{1.5}O_{6.92}$, $Bi_{1.46}Dy_{0.46}Zn_{0.92}Nb_{1.5}O_{6.92}$, $Bi_{1.5}Zn_{0.92}Ta_{0.3}Nb_{1.2}O_{6.92}$, $Bi_{1.5}Zn_{0.92}Ta_{1.0}Nb_{0.5}O_{6.92}$ and $(Bi_{1.487}Zn_{0.42}Yb_{0.04})(Zn_{0.46}Nb_{1.5})O_{6.92}$.
- Eu, Dy, Ta and Yb doped BZN pyrochlores sintered between 1025-1050°C for 4 hours had a relative density above 99%.
- Dielectric results indicated that irradiation effected significantly dielectric constant and loss values of doped BZN pyrochlores.
- Irradiation of Yb doped BZN showed that dielectric constants at low and high frequencies (1 kHz-125 kHz and 125 kHz- 2 MHz) increased at a dose of 10^{11} +6C influence (called as Yb A) but then decreased at a dose of 10^{13} +6C influence (called as Yb B).
- Irradiation of Ta doped BZN indicated that dielectric constants between 1 kHz- 2 MHz were generally decreased with irradiation dose (from 10^{11} +6C influence to doze of 10^{13} +6C).

- Irradiation of Dy doped BZN showed that dielectric constants at low and high frequencies (1 kHz-125 kHz and 125 kHz- 2 MHz decreased at a doze of 10^{12} +6C influence (called as Dy C) but then increased at a doze of 10^{13} +6C influence (called as Dy B).
- Irradiation of Eu doped BZN showed that dielectric constants between 1 kHz-2 MHz decreased at a doze of 10^{11} +6C influence (called as Eu A) but then increased at a doze of 10^{13} +6C influence (called as Eu B).
- In all samples and at every irradiations dozes, dielectric constant values decreased with temperature, as expected.

RECOMMENDATIONS

1. TEM investigation of irradiated samples should be made to reveal dielectric change with irradiation dose.
2. The optical properties of irradiated doped BZN ceramics should be investigated.

REFERENCES

1. Cann, D.P., C.A. Randall, and T.R. Shrout, *Investigation of the dielectric properties of bismuth pyrochlores.* Solid State Communications, 1996. **100**(7): p. 529-534.
2. Wuensch, B.J., et al., *Connection between oxygen-ion conductivity of pyrochlore fuel-cell materials and structural change with composition and temperature.* Solid State Ionics, 2000. **129**(1-4): p. 111-133.
3. Ewing, R.C., W.J. Weber, and J. Lian, *Nuclear waste disposal-pyrochlore (A(2)B(2)O(7)): Nuclear waste form for the immobilization of plutonium and "minor" actinides.* Journal of Applied Physics, 2004. **95**(11): p. 5949-5971.
4. Cleave, A., R.W. Grimes, and K. Sickafus, *Plutonium and uranium accommodation in pyrochlore oxides.* Philosophical Magazine, 2005. **85**(9): p. 967-980.
5. Kennedy, B.J., *Oxygen vacancies in pyrochlore oxides: Powder neutron diffraction study of Pb2Ir2O6.5 and Bi2Ir2O7-y.* Journal of Solid State Chemistry, 1996. **123**(1): p. 14-20.
6. Vassen, R., et al., *Zirconates as new materials for thermal barrier coatings.* Journal of the American Ceramic Society, 2000. **83**(8): p. 2023-2028.
7. Suresh, G., et al., *Investigation of the thermal conductivity of selected compounds of gadolinium and lanthanum.* Journal of Nuclear Materials, 1997. **249**(2-3): p. 259-261.
8. Schelling, P.K., S.R. Phillpot, and R.W. Grimes, *Optimum pyrochlore compositions for low thermal conductivity.* Philosophical Magazine Letters, 2004. **84**(2): p. 127-137.
9. McCauley, R.A. and F.A. Hummel, *Luminescence as an indication of distortion in A3+ 2 B4+ 2 O7 type pyrochlores.* Journal of Luminescence, 1973. **6**(2): p. 105-115.
10. Subramanian, M.A., G. Aravamudan, and G.V.S. Rao, *Oxide Pyrochlores - a Review.* Progress in Solid State Chemistry, 1983. **15**(2): p. 55-143.
11. Withers, R.L., et al., *Local crystal chemistry, induced strain and short range order in the cubic pyrochlore (Bi1.5-alpha Zn0.5-beta)(Zn0.5-gamma Nb1.5-delta)O(7-1.5 alpha-beta-gamma-2.5-delta) (BZN).* Journal of Solid State Chemistry, 2004. **177**(1): p. 231-244.
12. Vanderah, T.A., I. Levin, and M.W. Lufaso, *An unexpected crystal-chemical principle for the pyrochlore structure.* European Journal of Inorganic Chemistry, 2005(14): p. 2895-2901.
13. Levin, I., et al., *Crystal structure of the compound Bi2Zn2/3Nb4/3O7.* Journal of Solid State Chemistry, 2002. **168**(1): p. 69.
14. Lian, J., et al., *Ion-beam implantation and cross-sectional TEM characterization of Gd2Ti2O7 pyrochlore.* Nuclear Instruments & Methods in

Physics Research Section B-Beam Interactions with Materials and Atoms, 2006. **242**(1-2): p. 448-451.

15. Toulemonde, M., *Nanometric phase transformation of oxide materials under GeV energy heavy ion irradiation.* Nuclear Instruments & Methods in Physics Research Section B-Beam Interactions with Materials and Atoms, 1999. **156**(1): p. 1-11.

16. Szenes, G., *General Features of Latent Track Formation in Magnetic Insulators Irradiated with Swift Heavy-Ions.* Physical Review B, 1995. **51**(13): p. 8026-8029.

17. Shinde, S.R., et al., *Influence of 85 MeV oxygen ion irradiation on magnetization behavior of micron-sized and nano-sized powders of strontium ferrite (SrFe12O19).* Journal of Magnetism and Magnetic Materials, 1998. **186**(3): p. 342-348.

18. Kumar, R., et al., *Swift heavy ion irradiation effects on transport properties of epitaxial thin films of La1-xCaxMnO3.* Radiation Effects and Defects in Solids, 1999. **147**(3): p. 187-197.

19. Meldrum, A., L.A. Boatner, and R.C. Ewing, *Effects of ionizing and displacive irradiation on several perovskite-structure oxides.* Nuclear Instruments & Methods in Physics Research Section B-Beam Interactions with Materials and Atoms, 1998. **141**(1-4): p. 347-352.

20. Weber, W.J., et al., *Ion-beam-induced defects and defects interactions in perovskite-structure titanates.* Defects and Surface-Induced Effects in Advanced Perovskites, 2000. **77**: p. 317-328.

21. Jiang, W., W.J. Weber, and S. Thevuthasan, *Ion implantation and thermal annealing in silicon carbide and gallium nitride.* Nuclear Instruments & Methods in Physics Research Section B-Beam Interactions with Materials and Atoms, 2001. **175-177**: p. 610-614.

22. Patel, M.K., et al., *Effect of swift heavy ion irradiation in pyrochlores.* Nuclear Instruments & Methods in Physics Research Section B-Beam Interactions with Materials and Atoms, 2008. **266**(12-13): p. 2898-2901.

23. Barsoum, M.W., *Fundamentals of Ceramics", 2nd Ed*. 2003. 492-497.

24. Callister, W.D., *Materials Science and Engineering: An Introduction*. 7 ed. 2007: John Wiley and Sons.

25. www.engineershandbook.com. *Engineering Materials - Ceramics*. Available from: http://www.engineershandbook.com/Materials/ceramics.htm.

26. Gaertner, R.R. and B.R. Hollebone, *Formation conditions for a pyrochlore structure with two different cations at the A site.* Mineral. Geol. Palaeontol. Ref, 1930. **61**(1).

27. Choi, J.H., et al., *Microwave dielectric properties of Ba–Nd–Ti–O system doped with metal oxides.* Materials Letters, 2000. **44**(1): p. 29-34.

28. Stanek, C.R., *Atomic Scale Disorder in Fluorite and Fluorite Related Oxides.* 2003: p. 16-21.

29. Wang, X.L., H. Wang, and X. Yao, *Structure, phase transformations, and dielectric properties of pyrochlore containing bismuth" J. Am. Ceram. Soc.* J. Am. Ceram. Soc., 1997. **80**(10): p. 2745-2748.

30. Sleight, A.W., et al., *Semiconductor-Metal Transistion in Novel Cd2os2o7.* Solid State Communications, 1974. **14**(4): p. 357-359.

31. J. Nair, P.N., E.B.M. Doesburg, J.G. van Ommen, J.R.H. Ross, A.J. Burggraaf and F. Mizukami, *Combustion synthesis and photoluminescence of Eu3+, Dy3+-doped La2Zr2O7 nanocrystals.* Mater. Sci., 1998. **33**: p. 4517.

32. www.SiliconFarEast.com. *Permititivity and Dielectric Constant*. 2005; Available from: http://www.siliconfareast.com/dielectric-constant.htm.

33. Richerson, D.W. and E. Marcel, *Modern Ceramic Engineering Properties, Processing, and Use in Design", 2nd*. 1993. 252-261.

34. Johnson, G., *Lossy Capacitors", http://eece.ksu.edu/~gjohnson/tcchap3.pdf (22.03*. 2010.

35. Moulson, A.J. and J.M. Herbert, *Electroceramics: Materials, Properties, Applications", 2nd Ed*. 2003. 243-256

SRC - GoogleScholar.

36. Sebastian, M.T., *Dielectric Materials for Wireless Communication", 1stEd.* Elsevier, 2008: p. 1-37.

37. W.E., M.A.L., *Crystal chemistry, thermal expansion and dielectric properties of (Bi1.5Zn0.5)(Sb1.5Zn0.5) O7 pyrochlore.* Mater. Res. Bull. , 1997. **32**: p. 175.

38. Wang H.; Zhang D.; Wang .; Yao X, J., *Effect of La2O3 substitutions on structure and dielectric properties of Bi2O3–ZnO–Nb2O5-based pyrochlore ceramics.* Mater. Res. Bull., 1999. **14**: p. 546.

39. Thomson, J.B., A.R. Armstrong, and P.G. Bruce, *An oxygen-rich pyrochlore with fluorite composition.* Journal of Solid State Chemistry, 1999. **148**(1): p. 56-62.

40. Aleshin, E. and R. Roy, *On the crystal structure and properties of Ca 2 Nb 2 O 7" J. Am. Ceram. Soc. 18.* J. Solid State Chem. , 1965. **45**(18).

41. Ismunandar, A., J. Kennedy, and B. Hunter, *Structural and magnetic studies of manganese-containing pyrochlore oxides" Mater. Res. Bull. 1263.* Mater. Res. Bull. , 1999. **34**: p. 1263.

42. A.M, L.M.E.G., *Principles and Application of Ferroelectrics and Related Materials.* Clarendon Press, Oxford, 1977: p. 291.

43. P.K., V.M.D., *Synthesis and dielectric properties of pyrochlore solid solutions in the Bi2O3-ZnO-Nb2O5-TiO2 system.* J. Am. Ceram. Soc., 2000. **83**: p. 147.

44. Nino, J., C.A. Randall, and L.a. M.T, *C, Lanagan and M.* J. Appl. Phys., 2001. **89**: p. 4512.

45. K., S., R. K.C., and J. Eur., *Temperature-dependent dielectric, impedance and tunability studies on bismuth zinc niobate ((Bi1.5Zn0.5)(Nb1.5Zn0.5)O7) ceramics.* Elsevier 2007: p. 1.

46. Wang, H., X. Wang, and X. Yao, *Structures Phase Transformations, and Dielectric Properties of Pyrochlores Containing Bismuth.* J. Chin. Ceram., 1995. **23** p. 241.

47. M.C., W., et al., *Comparison of microwave dielectric behavior between Bi1.5Zn0.92Nb1.5O6.92 and Bi1.5ZnNb1.5O7.* J. Eur. Ceram. Soc., 2006. **26**: p. 1889.

48. N.Bakır , A.M., S.Keskin *Fabrication of Bi1.5Zn0.92Nb1.5O6.92 Dielectric Pyrochlore Ceramics with La, Gd and Eu Additives,* in *International Ceramic Congress, Afyonkarahisar, Turkey*. November 2008. p. 26-28

49. Qasrawi, A.F. and A. Mergen, *Structural, electrical and dielectric properties of Bi1.5Zn0.92Nb1.5-xTaxO6.92 pyrochlore ceramics.* Ceramics International, 2012. **38**(1): p. 581-587.

50. Bakır, N., *Effect of Additives on Dielectric Properties of Bi1.5Zn0.92Nb1.5O6.92 Pyrochlore,* . 2010, Marmara University.

51. Su, W.F. and S.C. Lin, *Interfacial behaviour between Bi1.5ZnNb1.5O7 center dot 0.02V(2)O(5) and Ag.* Journal of the European Ceramic Society, 2003. **23**(14): p. 2593-2596.

52. Mergen, A. and O. Ozyoldas, *PREPARATION AND DIELECTRIC PROPERTIES OF Bi1.5Zn1.0Nb1.5O7 AND Bi1.5Zn0.92Nb1.5O6.92 PYROCHLORE CERAMICS.* Ceramics-Silikaty, 2010. **54**(1): p. 31-37.

53. A.M, L.M.E.G., *Principles and Application of Ferroelectrics and Related Materials*. 1977, Oxford: Clarendon Press.

54. Wang, H., et al., *Mn4+ and W6+ substitution on Bi2O3-ZnO-Nb2O5-based low firing ceramics.* Ceramics International, 2004. **30**(7): p. 1219-1223.